Eco Charging System Design for Plug-in Electric Buses

Syed Muhammad Arif

A Thesis submitted to

Auckland University of Technology

In fulfillment of the requirements for the degree of

Doctor of Philosophy (Ph.D.)

2021

School of Engineering, Computer and Mathematical Sciences

Abstract

The Energy Management System (EMS) applied in Plug-in Electric Bus Depot Charging (PEBDC) ecosystem performs the pivotal role to monitor, control, serve the electric power, and also performs the energy trading among depot entities i.e., commercial building, Plug-in Electric Bus (PEB) and Photovoltaic (PV) integrated with Energy Storage System (ESS). The uptake of PEBs in the market is dependent on the advancement in the state-of-the-art of EMS technique for PEB charging infrastructure and charge scheduling algorithms for PEBs. Thus, this thesis aims to provide i) an EMS for the PEBDC ecosystem integrated with the distribution grid and ii) a PEB charge scheduling algorithm for pantograph and depot. Moreover, the discharging model for PEBs is also proposed for the State of Charge (SOC) estimation.

The proposed EMS which is based on double-sided auctioning firstly determines the total available power and load of each entity in the PEBDC ecosystem. Then the proposed EMS maximises the daily profit of the depot owner by performing energy trading among depot entities. On the other hand, the charge scheduling algorithms firstly take the real arrival and departure schedule of the bus fleet to estimate the SOC of the PEBs over every 10-minute interval and then charge the PEBs using the available power from PV, ESS, and grid (when the price is low).

The main advantage of the PEBDC ecosystem is the usage of PV and ESS which ultimately reduce the i) carbon emission and, ii) charging impact on the low voltage (LV) feeder. Particle Swarm Optimization (PSO) is used for the sizing and allocation of the PV system in a practical distribution system (KEPCO (Korea Electric Power Corporation)) and three IEEE bus systems (14-bus, 33-bus, and 69-bus) and analysed the charging impact of PEBs on the LV feeder using Matlab.

Finally, the proposed EMS and the charge scheduling algorithms for all four seasons (summer, autumn, winter, and spring) and a fleet of busses (during peak, normal and off-peak period) respectively, have been modeled as a Mixed Integer Linear Programming (MILP) and tested using the IBM ILOG studio with CPLEX solver to see the effectiveness of the proposed algorithms.

Attestation of Authorship

I hereby declare that the content of this work is original and has been carried out by myself at the Auckland University of Technology. I also declared that the information obtained from the literature has been duly acknowledged. To the best of my knowledge, no part of this thesis was previously submitted for another degree or diploma at any other institution of higher learning.

Syed Muhammad Arif

January 2021

Acknowledgment

Throughout the Ph. D journey, I have received a great deal of encouragement and assistance from academia and industry.

Firstly, I would like to thank, Professor Tek Tjing Lie (primary supervisor) and Professor Boon-Chong Seet (secondary supervisor) for enormous guidance in the formulation of research questions, methodology, and scientific writing despite their busy schedule. Your expertise and insightful feedback pushed me to sharpen my thinking and brought the research work to a higher level.

Secondly, I would like to acknowledge the Auckland University of Technology for offering me the Vice-Chancellor's Doctoral Scholarship throughout my Ph.D. studies. Also grateful to the Lahore University of Management Science (LUMS) research group for their wonderful research collaboration and for providing outstanding hospitality during my visit to LUMS Pakistan.

Thirdly, I would like to thank Auckland Transport (AT) for involving me in the low emission bus trial study in Auckland also provided me a chance to work with AT Low Emission Bus Working Group where I learned the insight challenges related to the electrification of public transportation including charging infrastructure, financing, and technology adoption. Also, thanks to the Yutong bus company for providing the real electric bus data on the Auckland route and Vector New Zealand for providing the opportunity to test the proposed algorithm on the Go bus route in Auckland New Zealand.

Furthermore, I would like to thank my family specially my father, sisters, and brothers for their wise counsel, a sympathetic ear, and continuous moral support. Finally, I could not have completed my thesis without the encouragement of my buddies, Dr. Soumia Ayyadi, Dr. Akhtar, and Dr. Raza who offered stimulating discussion to rest my brain outside of my research.

Table of Contents

List of Figures

List of Tables

List of Symbols and Abbivations

PEB	Plug-In Electric Bus
PEBDC	Plug-In Electric Bus Depot Charging
ICE	Internal Combustion Engine
EV	Electric Vehicle
HEV	Hybrid Electric Vehicle
FCEV	Fuel Cell Electric Vehicle
FCHEV	Fuel Cell Hybrid Electric Vehicle
BSS	Battery Swap Station
WPT	Wireless Power Transfer
CC	Conductive Charging
V2V	Vehicle-to-Vehicle
V2G	Vehicle-to-Grid
G2V	Grid-to-Vehicle
V2B	Vehicle-to-Building
DGs	Distributed Generators
RESs	Renewable Energy Resources
WTGs	Wind Turbine Generators
PVs	Photovoltaics
BESSs	Battery Energy Storage Systems
POC	Point of Common Coupling
GHG	Greenhouse Emission
DC	Direct Current
LVDC	Low Voltage Direct Current
SOC	State of charge
IEC	International Electrotechnical Commission
SAE	Society of Automotive Engineers
SAC	Standards Administration of China

UNFCCC	United Nations Framework Convention on Climate Change
FITs	Feed-in Tariffs
k	Iteration
i, j	Number of Buses
d	DG types
N	Total distance of feeder
C_1, C_2	Cognitive factor and Social factor [0; 1]
$\alpha_{i,j}, \beta_{i,j}$	Sensitivity factor of exact loss formula.
r_{ij}	Resistance of line connecting buses i and j
x_{ij}	Reactance of line connecting buses i and j
u_d^{DG}	D-type DG indicator
V_i^{min}	Minimum voltage at bus i.
V_i^{max}	Maximum voltage at bus i.
P_{best}	Personal Best
g_{best}	Global Best
P_{DG_i}	Active power injected by DG units at bus i
Q_{DG_i}	Reactive power injected by DG at bus i
P_{Load_i}	Active loads at bus i
Q_{Load_i}	Reactive loads at bus i
V_i, V_j	Voltage magnitude at bus i and j
δ_i, δ_j	Phase angle at bus i and j
P_i, P_j	Active power at bus i and j
Q_i, Q_j	Reactive power at bus i and j
${V_i}^k$	Velocity of particle i at iteration k
${x_i}^{k+1}$	Current velocity of particle i at iteration k
${x_i}^k$	Position of particle i at iteration k
${P_{best}}^k$	Personal best of agent i at iteration k
${g_{best}}^k$	Best among all in the group
r_1, r_2	Random number between [0, 1]
$P_{\overrightarrow{loss}}(x_0)$	Total value of power losses at node x0
$I_d(x, T_i)dx$	Phasor current density DG i at time T
$I_{DG}(T_i)$	Injected current of DG i at time period T
C_d^{DG}	Cost for deployment of a d-type DG
u_i^{voil}	Penalty cost for voltage violation at bus i
$P^{s/s}$	Power injected by the substation

P_d^{DG}	Power generated by the d-type DG
P_d^{min}	Minimum power generated by d-type DG
P_d^{max}	Maximum power generated by d-type DG
δ^{min}	Minimum allowable _ for voltage at bus j
δ^{max}	Maximum allowable _ for voltage at bus j
δ_j	Angle at node j
I_i	Current at node i
I_i^{rated}	Rated current at node i
V_i	Voltage at bus i.
AT	Auckland Transport
PSO	Particle Swarm Optimization
GA	Genetic Algorithm
SA	Simulated Annealing
KEPCO	Korea Electric Power Cooperation
GXP	Grid Exit Point
EMS	Energy Management System
BDO	Bus Depot Owner
PWF	Present Worth Factor
MILP	Mixed-Integer Linear Problem
LTO	Lithium Titanite Oxide
CBD	Central Business District
t	Hours (1-24)
i	Number of PEBs
η_{char},η_{dis}	ESS and PEB batteries charging/discharging efficiency (90%)
$E_{\min}^{ESS}(t)$, $E_{\max}^{ESS}(t)$	Minimum and maximum energy level of ESS at any time interval ‘t’ (kWh)
$P_{\min}^{ESS}(t)$, $P_{\max}^{ESS}(t)$	Minimum and maximum ESS power limit at any time interval ‘t’ (kW)
$E_{\min}^{PEB(i)}(t)$, $E_{\max}^{PEB(i)}(t)$	Minimum and maximum energy level of PEB i at any time interval ‘t’ (kWh)
$C_{Sell}^{2G}(t)$, $C_{Sell}^{2B}(t)$	Selling cost to grid and building at any time interval ‘t’ ($/kWh)
$C_{Sell}^{2PEB(i)}(t)$	Selling cost to PEB i at any time interval ‘t’ ($/kWh)
$C_{Pur}^{fromG}(t)$	Purchasing cost from grid at any time interval ‘t’ ($/kWh)
$P_{\max}^{Grid}(t)$	Maximum power grid can deliver at any time interval ‘t’ (kW)
$x(t), y(t)$	Binary variable associated with charging/discharging the ESS
$P^{PV2ESS}(t)$, $P^{PV2B}(t)$	PV to ESS and building power flow (kW) at any time interval ‘t’

$P^{PV2G}(t)$, $P^{PV2C}(t)$	PV to grid and charger power flow (kW) at any time interval ‘t’
$P^{G2B}(t)$, $P^{ESS2B}(t)$	Grid and ESS to building B power flow (kW) at any time interval ‘t’
$E^{ESS}(t)$, $E^{PEB(i)}(t)$	Energy level of ESS and PEB i (kWh) at any time interval ‘t’
$P^{G2C}(t)$, $P^{G2PEB(i)}(t)$	Grid to charger and PEB i power flow (kW)at any time interval ‘t’
$P^{PV}(t)$, $P_{\max}^{PV}(t)$	PV power production (kW) and its maximum limit at any time interval ‘t’
$P^{PV2PEB_i}(t)$	PV to PEB i power flow (kW) at any time interval ‘t’
$P^{C2PEB(i)}(t)$	Charger to PEB i power flow (kW) at any time interval ‘t’
$P^{G2ESS}(t)$	Grid to ESS power flow (kW) at any time interval ‘t’
$P^{ESS2G}(t)$	ESS to grid power flow (kW) at any time interval ‘t’
$P^{ESS2C}(t)$	ESS to charger power flow (kW) at any time interval ‘t’
$P^{PV2ESS}(t)$, $P^{PV2B}(t)$	PV to ESS and building power flow (kW) at any time interval ‘t’
$P^{PV2G}(t)$, $P^{PV2C}(t)$	PV to grid and charger power flow (kW) at any time interval ‘t’
$P^{G2B}(t)$, $P^{ESS2B}(t)$	Grid and ESS to building B power flow (kW) at any time interval ‘t’
$E^{ESS}(t)$, $E^{PEB(i)}(t)$	Energy level of ESS and PEB i (kWh) at any time interval ‘t’
V,P	Vehicle and passenger weight
r, S	Route and stop
A	Air-condition unit

Chapter 1 Introduction

This chapter introduces the background, feasibility study for the green and resilient transportation infrastructure, challenges, and issues of PEB Depot Charging (PEBDC) ecosystem allocation, the motivation, and the objectives of the thesis.

1.1 Background

Urbanisation refers to the migration of the population from rural to urban areas due to economic growth and job opportunities [1] and industrialisation is the transition from an agrarian society into an industrial society [2]. Both urbanisation and industrialisation cause population growth in the cities and therefore, the development of the urban transport system is very important in terms of capacity and fuel efficiency. Before urbanisation and industrialisation, the movement of the people in cities tended to be restricted to walking; this makes urban mobility less efficient and time-consuming. Due to transportation innovation and technological improvement, city commuters have more options e.g. city buses, rails, ferries, cars, motorbikes, and micro-mobility to travel in the urban area; these offer less traveling time and less fuel consumption.

However, transportation with fossil fuel dependency is the main threat to the earth's environment as it contributes to most CO_2 emissions. Figure 1. 1 shows the percentage contribution of CO_2 emissions by the (i) electricity and heat sector, (ii) transportation sector, (iii) industry sector, (iv) residential sector, and (v) other areas, according to the International Energy Agency [3]. Transportation is one of the significant emission sectors, contributing 22% of the total CO_2 emissions in 2011. Most public and personal vehicles run on an internal combustion engine (ICE) which can be considered as one of the major causes of climate change. On the other hand, Electric Vehicles (EVs) do not directly emit CO_2 and are not susceptible to high oil prices.

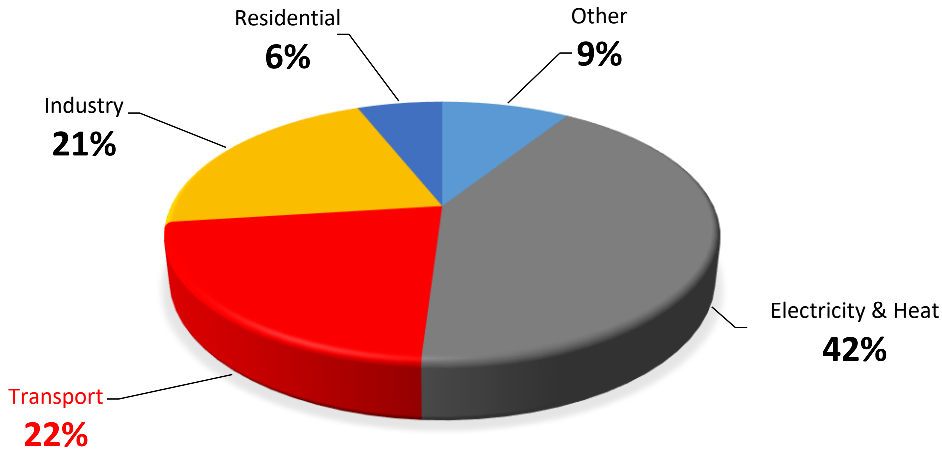

Figure 1. 1 CO_2 Emission by different sectors [3].

The world is facing a deficiency of fossil fuels, so most countries are moving towards sustainable, reliable, efficient, economical, and green resources of energy. Thus, Plug-in Electric Buses (PEBs) are experiencing rapid growth because of five key global trends:

(i) Fossil fuel depletion, and subsequent increases in fuel cost.

(ii) Growing public awareness of EVs and a desire to combat climate change.

(iii) Advances in renewable energy technologies.

(iv) Development of electric motors that generate rotational motion for EVs directly.

(v) Advances in EV supporting technologies such as Grid-to-Vehicle (G2V), Vehicle-to-Grid (V2G), Vehicle-to-Vehicle (V2V), and Vehicle-to-Building (V2B).

In addition, two-way power transfer capability between EVs and Battery Energy Storage System (BESS) offers a new economic paradigm. Businesses, institutions, and individuals will be able to leverage their premises to access: (i) Cleaner and cheaper electricity; (ii) Electricity revenue by selling excess supply back to the grid or to other buyers.

In essence, some consumers will become competitors to the current power companies and offer new opportunities in resolving issues such as intermittency of renewable energy resources (RESs) such as Wind Turbine Generators (WTGs) and Photovoltaics (PVs) [4], energy loss reduction [5], and reliability to distribution systems [6]. There is existing research on designing efficient charging stations for private EVs [7]. However, from the literature survey conducted so far, very little research exists on the integration challenges and benefits for the use of Battery Energy Storage System (BESS), PVs for EVs charging stations in the public sector; more specifically, with regard to transport service providers such as bus and taxis operators.

1.2 Feasibility Study for Green and Resilient Transportation Infrastructure

The future of public transportation will be very different from today's in many ways due to climate change and increasing urbanisation. Communities are migrating from rural to urban areas because of urbanisation, thus cities require more public transportation. However, dependency on fossil-fuel-based transportation causes Greenhouse Gas Emissions (GHG). Therefore, building a green and resilient transportation infrastructure is important for the environment and society.

Here the Plug-in Electric Buses (PEBs) with zero carbon emissions play a vital role in urban mobility. The convenience, availability, and resilient charging infrastructure are one of the key factors favoring the adoption of PEBs. The use of an Energy Storage System (ESS) to store i) the surplus power generated by the Solar PV, and ii) electricity from the grid (at low tariff) and charging the PEBs using smart charging strategies makes the PEB Depot Charging (PEBDC) Ecosystem more cost-effective, resilient and intelligent. The following factors need to be considered for the transition to green, resilient, and future-ready transportation.

1.2.1. International Policy Framework

The study shows that the governments' policies around the globe have played an instrumental role in reducing the impact of abrupt climate change [8] e.g.,

1. Setting vehicle emission targets and commitment to phase out the Internal Combustion Engine (ICE) technology at the government and industry level.
2. Introducing subsidies and grants for EV owners
3. Funding allocation for the new technology trial

For example, China, Europe, US, and Canada provide funding to support the electric bus uptake target and their charging infrastructure in the market. For example, the UK granted a $197.5m subsidy for the electric bus for the year 2017/18 and 2020/21 [9].

1.2.2. National and Regional Policy Framework

New Zealand is a part of the Paris Agreement, the Kyoto Protocol, and the United Nations Framework Convention on Climate Change (UNFCCC). Thus, the government introduced the following policies to uplift the intake of electric buses in the public transportation sector.

i) **Incentives:** New Zealand government has introduced incentives such as the Road User Charge (RUC) exemption for light and heavy vehicles until June 2021 and December 2025, respectively [10].

ii) **New technology trial demonstration funding allocation:** Government has allocated a Low-Emission Vehicle, Contestable Fund up to $7 million per year to encourage low-emission vehicle projects which are controlled by Energy Efficiency and Conservation Authority [11].

iii) **Setting GHG and vehicle emission targets**: The government has set net-zero emission for all GHG sectors by 2050 and set a target to make the bus fleet 100% electric by 2040 [12].

1.2.3. Sustainable Transportation: International context

The uptake of battery-electric buses country wise are i) China 421,000 ii) Europe 2,250 iii) USA 300, iv) Other countries 1450 shown in Figure 1.2 [13].

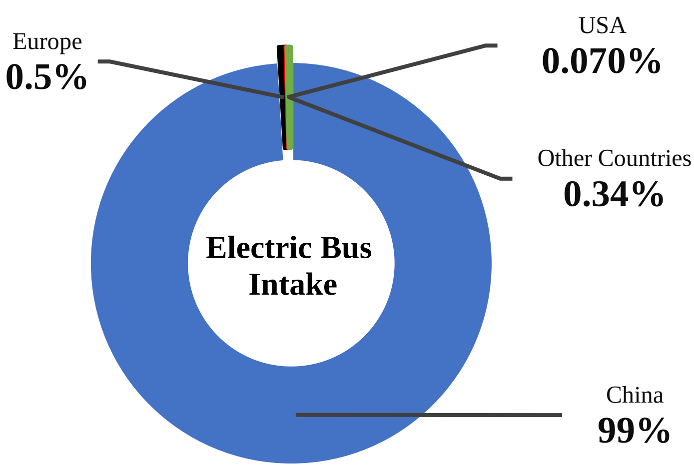

Figure 1.2 Battery Electric Buses uptake Country wise.

The different kinds of low emission bus markets around the globe include i) Battery Electric 229,593, ii) Plug-in Hybrid 63,703, iii) Hybrid 42,041 iv) Biodiesel B20:9,300 v) Biomethane 6,472, and vi) Hydrogen fuel cell 131 as shown in Figure 1.3.

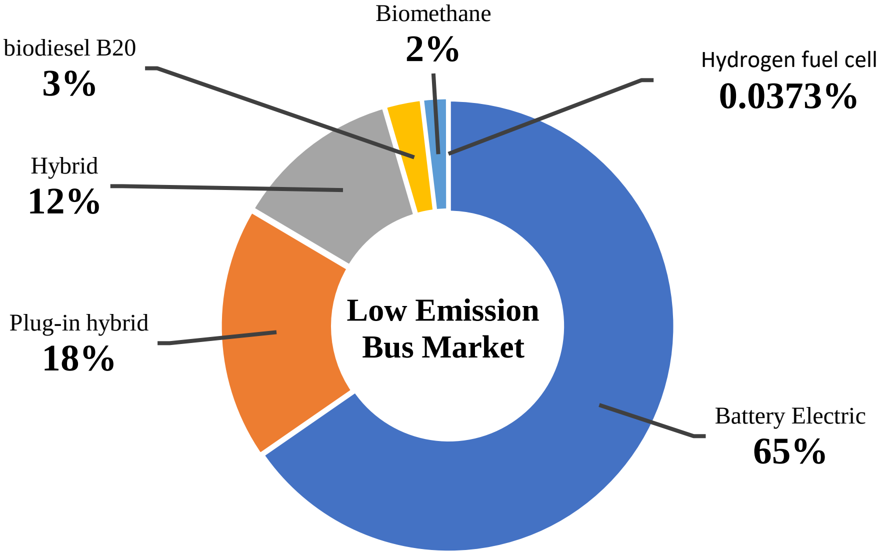

Figure 1.3 Global Low Emission Bus Market.

1.2.4. Sustainable Transportation: New Zealand context

The Mayor of Auckland joined 11 other cities in signing the C40 Fossil-Fuel-Free Streets Declaration in 2017 and set a target of having a net zero-emission bus fleet in Auckland city by 2040. Thus, Auckland Transport set the pathway to phase out the diesel buses from the city's road as shown in Figure 1.4.

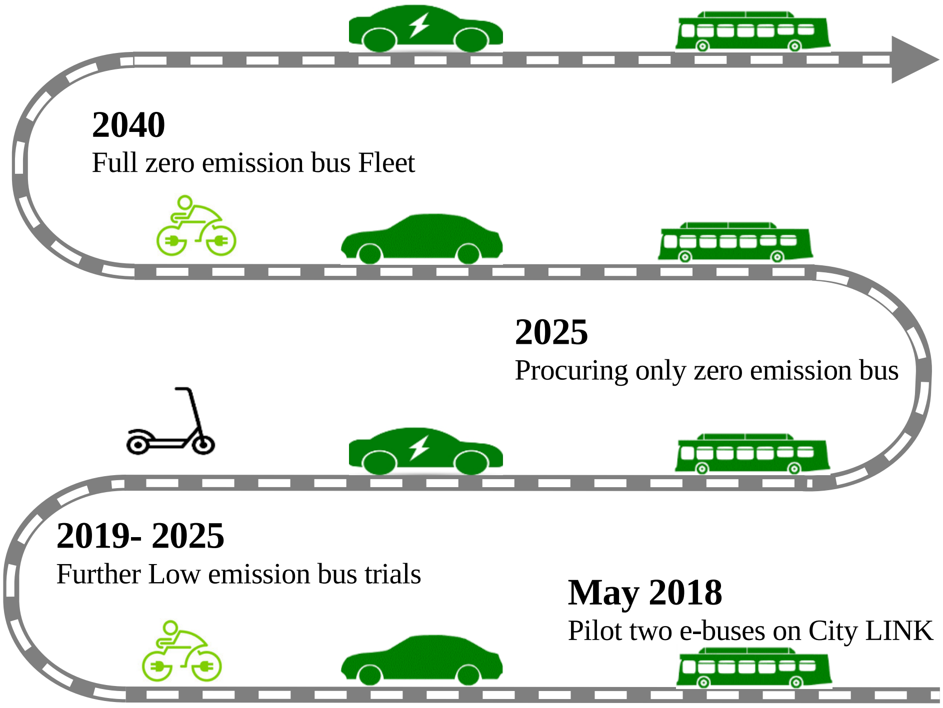

Figure 1.4 Auckland Transport Low Emission Bus roadmap: 2018 to 2040 [9].

The following major cities in New Zealand have included electric buses in their public transportation to achieve the carbon emission target set by the government.

i) **Auckland:** Airportlink one of the Auckland bus routes recently announced to introduce 9 fully battery-electric buses which are run by Go bus between Onehunga and Auckland airport by 2021. Furthermore, the Waiheke bus company (Fuller) announced it is replacing its 5 diesel buses with electric early in November 2020 [14]. After the successful trial of two e-bus on the City LINK, the whole fleet (12) became electric in May 2021.

ii) **Wellington**: Tranzit coachlines is one of the largest coach companies in Wellington. The Tranzit group introduced the first fully electric bus in New Zealand in 2017 in conjunction with the Auckland University of Technology (AUT). After the successful trial in July 2018, 10 fully electric double-deckers were rolled out in Wellington with another 98 to be added by 2023 [15].

iii) **Christchurch**: In 2017, 53% of Christchurch's emissions were due to transportation. To reduce carbon emissions due to public transportation, the Red bus in 2019 commissioned 3 fully electric buses having a 250 km range in single charge [16]. Go bus introduced 25 fully electric buses in October 2020.

1.2.5. Plug-in Electric Bus and Charging Infrastructure Economic

The bus capital and infrastructure development costs are the two main costs that must be considered for the successful implementation of the zero-emission bus fleet as discussed below:

i) **Bus capital costs**: 50% of the capital cost of an electric vehicle is due to the batteries [17]. However, the price of batteries is decreasing every year. Bloomberg New Energy Finance forecasts the lithium-ion battery cost for a decade as shown in Figure 1.5.

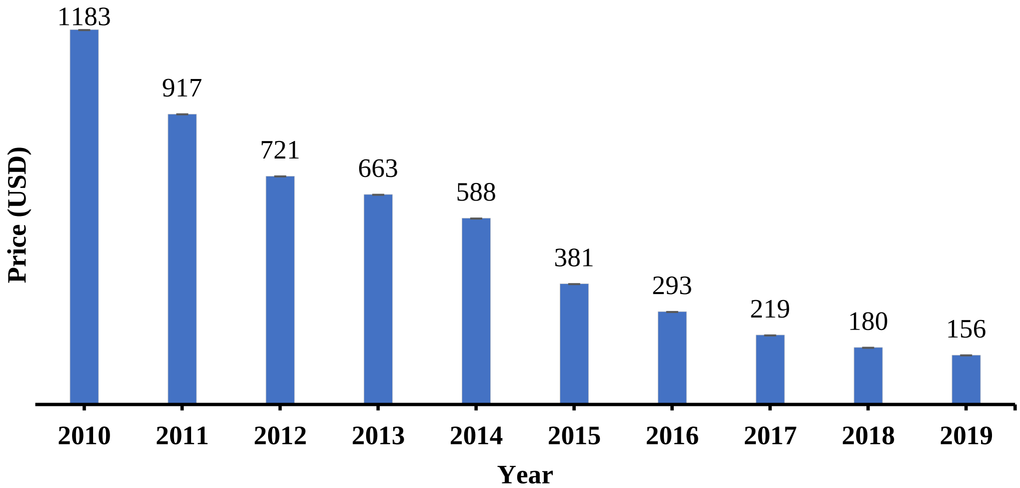

Figure 1.5 Lithium-ion Battery Price USD/kWh [18].

ii) **Infrastructure development cost**: Another main cost related to the electric bus is the development cost of electric bus charging infrastructure. Auckland Transport (AT) has done an initial six-month trial on the City link route using 2 Yutong electric buses. Each bus and charger cost $840,000 and were purchased with a $500,000 contribution from EECA's contestable fund [9]. The main two types of electric bus charging infrastructure considered in this study are i) Overnight depot charging (PV integrated with ESS) and ii) Pantograph (grid only) charging. A detailed comparison of the depot vs pantograph charging infrastructure has been done in Chapter 3.

1.2.6. Auckland's Greenhouse Gas (GHG) Emissions

In 2016, Auckland's total GHG emissions were 11,326 Kilo tonnes which caused the premature death of 130 Aucklanders every year [19]. The emission due to different business sectors is shown in Figure1.6.

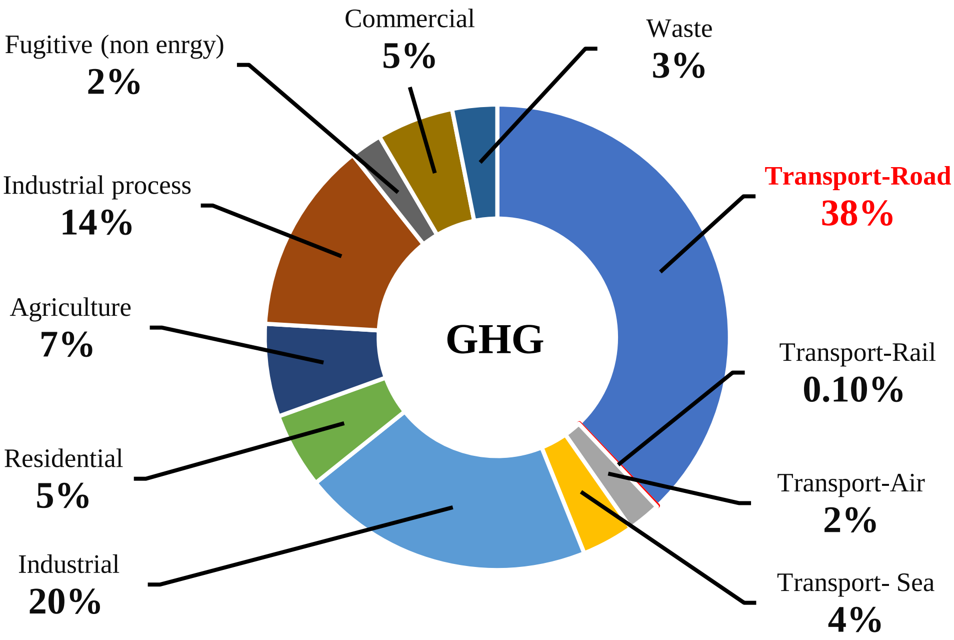

Figure 1.6 Auckland's Greenhouse Gas Emission profile 2016 [19].

1.2.7. New Zealand Current and Future Power Generation

New Zealand's net power generation was 5,126 MW of which 2,855 MW and 2,271 MW came from North Island and South Island, respectively[20]. Currently, 85% of power generation is renewable. The major electricity generation in New Zealand is shown in Figure 1.7 [21] accessed on 21 July 2020 at 4: 00 pm. However, the government set a target to make it 100% renewable by 2035.

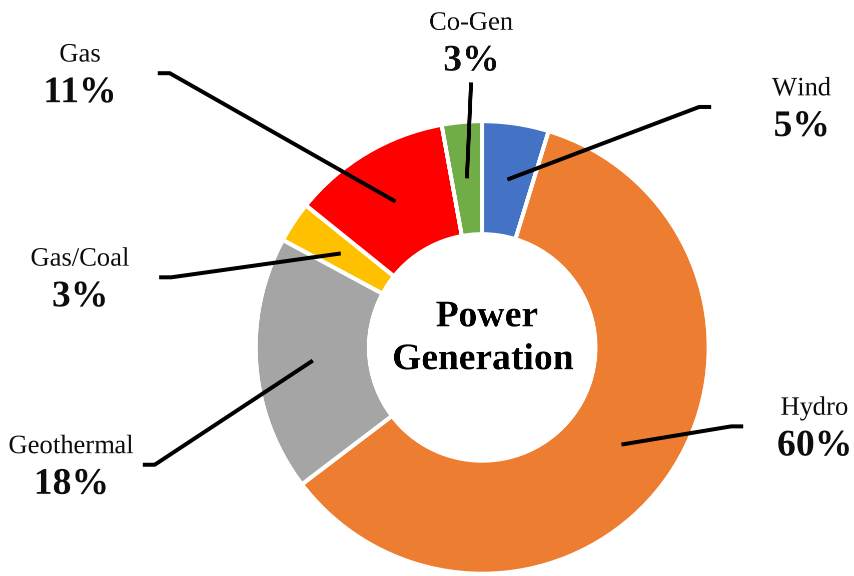

Figure 1.7 New Zealand Power Generation [20].

1.3 Challenges and Issues of PEBDC Ecosystem Allocation

The appropriate capacity determination and site location of the charging station can be beneficial for both the depot owner and grid operator thus promote sustainable transportation. The influencing factors are i) charging demand, ii) operating economy, iii) power grid security and iv) geographical and social ecology [22] as detailed below:

1.3.1. Charging Demand

The depot location must meet the charging demand for a new charging station installation. If the charging demand of the PEB fleet is higher than the maximum charging capacity of the charging station, this ultimately overloads the distribution transformer. The charging demand should be considered in the following two aspects.

i) **PEBs Purchasing Intention:** Future growth of charging demands of the bus companies depends on the PEB's purchasing intention. Districts having greater purchase objectives will likely have more charging demand.

ii) **Sales of PEBs:** The sales of PEBs also indicate the electricity demand in a district.

1.3.2. Operating Economy

Building a depot charging infrastructure needs a huge amount of investment which is as follows:

i) **Infrastructure construction cost:** This includes demolition cost, equipment purchasing cost, and land cost.

ii) **Operation and maintenance cost:** The operation cost includes staff salaries, tax, and EV charging costs, etc., and the maintenance cost includes maintaining equipment in the charging station. As a general rule, the operation and maintenance cost is assumed to be 10% of the total investment cost [23].

1.3.3. Grid security

Fast charging of PEBs having a big battery requires a high current and has a harmful impact on the electrical grid. The impact of charging PEBs on the electrical grid is described as follows:

i) **Impact on the distribution network and transformer:** Charging a large fleet of PEBs at the same time from the grid has a negative impact on the distribution transformer. Thus, an optimal charge scheduling of electric buses can minimise the peak load on the grid and ultimately reduce the transformer overloading issue [24]. The authors proposed two charge scheduling algorithms, one for depot charging and another for pantograph charging, and compared the impacts on one of the Auckland LV feeder networks [25].

ii) **Grid Harmonic pollution:** Charging the PEBs required a charger which is a non-linear device. These non-linear loads produce harmonics in the electrical grid which needs to be handled quickly and effectively otherwise the power quality is affected. A harmonic controller is used to overcome this problem which increases the construction and operation cost of the depot charging station.

1.3.4. Geographical and Social Ecology

The charging pile is an electrical equipment which is hooked up to higher voltage and higher current electrical system whose operation is greatly influenced by humidity (caused corrosion), temperature, and other environmental factors described as follows:

i) **Geographical ecology:** One of the most important factors for choosing the location is the geographical ecology near of charging station which directly affects the construction feasibility. Choosing the right charging location can reduce the corrosion in the equipment which ultimately reduces the maintenance cost.

ii) **Social ecology:** Social ecology is another charging station construction feasibility factor need to be considered. The social ecology needs to be considered while determining the location of the station due to i) impact on residents, ii) city construction department support required, iii) environmental damage, and iv) regional security situations.

1.4 **Motivation**

In recent years, the zero-emission electric buses have attracted significant attention, such as in 2020 the total number of zero-emission buses around the globe reached 500,000 including 4,000 in Europe with 98% being deployed in China [26, 27]. However, the zero-emission bus uptake in 2017 in China, Europe, and USA was 343,500, 1,273, and 200 buses, respectively [4]. In Auckland, 81% of air pollution-related health costs are due to emissions by diesel vehicles. Thus, AT has committed to using only zero-emission buses starting in 2025 [9] to achieve the decarbonisation target of the public transport sector set by the New Zealand government. Thus, it will require a huge amount of power to charge these zero-emission buses.

The early concept of power flow in the power system was unidirectional i.e., electricity is generated at the main power station and then transmitted through overhead power lines to the consumers. The central power plant is operated to generate necessary electricity based on the total load requirement. However, due to advancements in digital technologies and communication technologies, the integration of renewable energy resources e.g., solar PV, wind energy, and EVs into the grid is becoming easier thus power flow in the power system is becoming bidirectional i.e., power generation is not centralised. In this way, the consumers can participate in the energy market, having incentives and choices which modify their electricity buying behavior and pattern [28].

Moreover, off-peak hours charging of all PEBs increases the load curve of the utilities, therefore the charging of the fleet of PEBs must be accurately optimised for various charging technologies and setups. Demand response is another advantage for bus depot charging station owners by reducing the PEBs charging demand during the peak hour. In parked condition, the stored power in the PEB's battery can be exported back to the grid [29] or sold to a building [30] or sold to another PEBs [31], this is known as V2G, V2B, or V2V, respectively. The PEBs batteries plugged into the bus depot charging ecosystem can act as a distributed energy storage system for the power grid which provides a "spinning reserve" for the power grid thus makes the grid more resilient and secured. Also, the use of the Battery Energy Storage System (BESS) and V2G concept in the bus depot charging ecosystem can mitigate the transformer overloading problem and reduce the electricity purchasing cost [32]. However, frequent charging and discharging of PEBs can reduce the battery's life cycle, and therefore the energy delivering back to the grid must be at a price such that the additional cost (battery degradation) incurred due to V2G is recovered.

The rollout of PEBs technologies is becoming popular in the government and private sectors i.e., public transport companies and EV industries. Despite such positive evidence, some of the downsides must be addressed to accelerate EV adoption. For example, i) unavailability of a recharging station on the bus route, ii) longer recharging time, iii) range anxiety syndrome which is common to EV users [33]. To eliminate the bus driver range anxiety syndrome following two conductive charging solutions for PEBs are proposed in this thesis and the details are given in Chapter 4.

1.5 PEBDC Ecosystem Deployment

The objective of the PEB depot charging ecosystem deployment is to provide:

1. **A proper charge scheduling for PEBs** considering i) Bus arrival/departure schedule, ii) Grid load, iii) Available power from the solar PV system, iv) ESS SOC, and v) Building load demand.
2. **Minimise the PEB charging cost** by i) Charging the PEBs when the price on the grid is low, and ii) Utilising the penetration of the solar PV system.

The detailed procedure of PEB depot charging ecosystem deployment is given in Figure 1.8

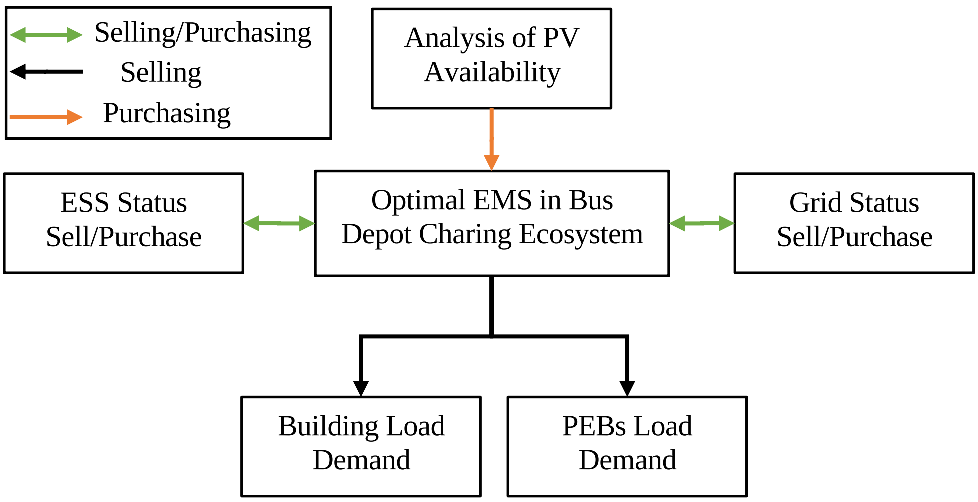

Figure 1.8 A Comprehensive Model for the deployment of the PEBDC Ecosystem.

The PEBs are charged if the power is available in the i) ESS, ii) solar PV, and/ or iii) when the price on the grid is low. Thus, the depot owner minimises the PEBs charging cost. In the case of no PV/ESS power being available or the price on the grid is high, all PEBs should be charged from the grid.

1.5.1. Mathematical Modeling of PEBDC Ecosystem

The mathematical modeling of components including solar Photovoltaic, ESS, charge controller, and inverter used in the proposed PEBDC ecosystem are described as follows:

Solar PV for PEBDC Ecosystem: The solar radiation reaching the PV module surface depends upon i) declination angle of sunlight on earth (δ), ii) inclination angle of the PV module (β) with the horizon as can be seen in Figure1.9, and iii) latitude of the location (ϕ) in degrees [34]. The declination angle varies through the year between - 23.45^o to + 23.45^o which can be calculated using equation (1.1).

$$\delta = 23.45 * sin\left[\frac{360}{365}(284 + n)\right] \tag{1.1}$$

where, *n* shows the nth day of the year, which is 1 for 1st January and 365 for 31st December.

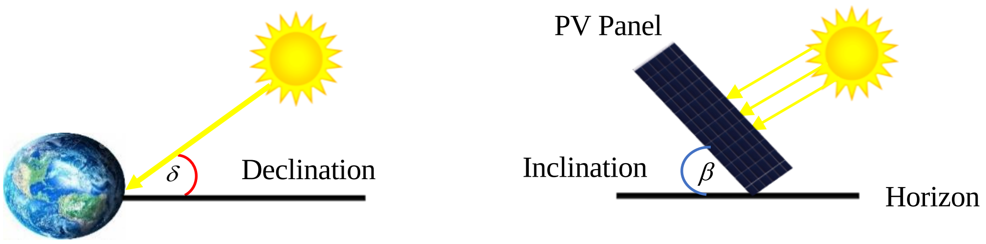

Figure 1.9 Declination and Inclination Angle.

A solar tracking system is required to adjust the optimal inclination angle of the solar panel throughout the day for maximum energy harnessing. For better performance, the two-axis tracking system can be used. However, this increases both the installation and maintenance costs [34]. Due to the changing of the declination angle of sunlight on earth each year, it becomes very difficult to change the inclination angle of the PV module thus, the fixed angle module is chosen. The PV inclination angle should be carefully evaluated depending upon the latitude of the location [35]. The inclination angle of the PV module β can be calculated using equation (1.2).

$$\beta = \phi \pm \delta \tag{1.2}$$

where, $\beta = \phi + \delta$ and $\beta = \phi - \delta$ are used for the winter and summer, respectively. As a rule, the average value $\delta = \delta_{Avg} = 15^0$is selected for a fixed angle module. Thus, the optimum value β for winter and summer is shown in equation (1.3) and equation (1.4) respectively.

$$\beta = \phi + 15 \tag{1.3}$$

$$\beta = \phi - 15 \tag{1.4}$$

The PV power generation depends on the sunshine hour thus during summer the PV system harnesses more power. Therefore, it is economical for selecting the inclination angle. However, selecting equation (2.3) for tropical countries will reduce the PV power generation. Therefore, for reliable and better PV power harnessing, equation (1.4) is preferred. In this work to harnesses more power from the PV system, the inclination angle is selected as shown in equation (1.5)

$$\beta = \phi - 15 = 35 - 15 = 20^0 \tag{1.5}$$

The output power of the PV panel $PV_{pv(t)}$at any time *t* can be calculated using equation (1.6).

$$P_{pv,t} = C_{i,t} * I_{SC}\left(1 + \frac{33}{100} cos\left(\frac{360d}{365}\right)\right) * (sin\,\phi\, sin\,\delta + cos\,\phi\, cos\,\delta\, cos(\omega t)) \tag{1.6}$$

where, $C_{i,t}$and I_{SC}represent the clearing index at time *t* and solar constant respectively. ω is the hour angle (varies from 15^0 to -15^0 morning to afternoon respectively) and ϕ is the geographical latitude [36]. The system information used in the simulation is given in Table 1.1.

Table 1. 1 Solar PV System Information

System Components	**Information**
System Size	$100\ kW$
Module Type	Standard
Array Type	Fixed (Open rack)
Declination angle	15^0
Inclination angle	20^0
Inverter Efficiency	96%

Energy Storage System for PEBDC Ecosystem: The factors influencing the output power of an ESS are i) ESS capacity, ii) Charging rate and iii) discharging rate of ESS. In the PEBDC Ecosystem, the ESS (Lithium-ion battery) is important to store the excess power generated by the PV system and sell it to a grid or building depending upon the applications. The battery State-of-Health (SOH) is one of the key parameters which is the ratio of full charge capacity to designed capacity [37], given by:

$$SOH = \frac{C_{Fullcharge}}{C_{Design}} \times 100\% \tag{1.7}$$

The C_{Design} is the design capacity of the battery shown in Figure 1.10. The SOH is important for the real-time battery State of Charge (SOC) estimation. The SOC is as below.

$$SOC = \frac{C_{Remaining}}{SOH \times C_{Design}} \times 100\% \tag{1.8}$$

Whereas $C_{Remaining}$ is the real-time battery remaining capacity. The mathematical expression for the current SOC is described in equation (1.9).

$$SOC_t = (1 - Q)SOC_{t-1} + \frac{P_{char}\,\Delta(t)}{E}\eta_{char/dis} \tag{1.9}$$

where, SOC_t and SOC_{t-1} represent the battery state of charge at a time interval (t) and $(t-1)$. E, Q, and $\eta_{char/dis}$ show the total energy of the battery, hourly discharge rate and battery charge, and discharge efficiencies respectively. P_{char} is the charging power of the battery at the time interval $\Delta(t)$. The battery wear cost is described in equation (1.10) [38].

$$C_{bw} = \left(\frac{C_{\text{rep, batt}}}{N_{\text{batt}}\,Q_{\text{life time}}\sqrt{\eta_{\text{round trip}}}}\right) \tag{1.10}$$

where, $C_{rep,batt}$ and $\eta_{\text{round trip}}$ are the replacement cost of the battery bank and the round-trip efficiency, respectively. Equation (1.11) represents the battery bank life cycle (years).

$$R_{batt} = min\left(\frac{N_{\text{batt}}\,Q_{\text{life time}}}{Q_{\text{thrpt}}}\,R_{batt,f}\right) \tag{1.11}$$

The battery bank consists of different cells that are represented N_{batt}. The total expected amount of energy a battery can be store and deliver over its lifetime is called battery energy throughput. The throughput of a single battery and float life of the battery is $R_{batt,\text{f}}$ and $Q_{Life\,\text{time}}$ respectively. To increase the battery bank life, the upper and lower limit is defined as 10 % and 90% respectively which is shown in Figure 1.10.

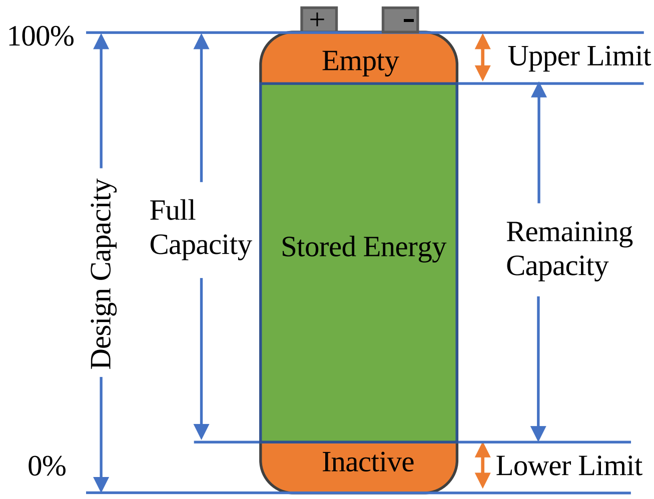

Figure 1.10 A Battery Capacity, Upper, and Lower Limit representation.

Charge Controller for PEBDC Ecosystem: A battery charge controller or regulator controls the rate of electric current drawn or added to the battery bank. Overcharging of an ESS can reduce the life span or performance of the battery and cause a safety risk. Thus, a controller is used to avoid overcharging, deep discharging (completely draining) and to protect battery life. Equations (1.12) and (1.13) define the mathematical model of the input and output for a charge controller, respectively [39].

$$E_{CC-OUT}(t) = E_{CC-IN} * \eta_{CC} \tag{1.12}$$

$$E_{CC-IN}(t) = E_{PV}(t) + E_{Grid}(t) \tag{1.13}$$

The charge controller energy output, input, and its efficiency are $E_{CC-OUT}(t)$,$E_{CC-IN}(t)$and η_{CC} respectively. The $E_{PV}(t)$and $E_{Grid}(t)$ represent the energy coming from solar PV and grid respectively. The integration of the ESS charge controller with solar PV, grid, and ESS is shown in Figure 1.11

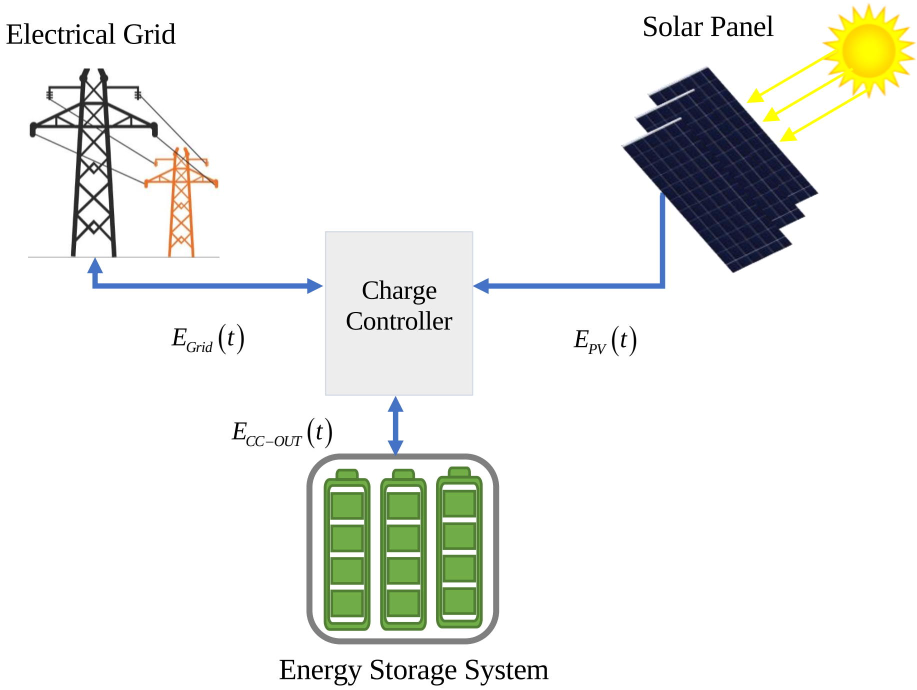

Figure 1.11 ESS and Charge Controller connected with Solar PV and Grid.

Inverter for PEBDC Ecosystem: The power generated by the solar PV system (DC), grid power (AC), and stored energy in ESS (DC). In the New Zealand scenario, most of the electrical load is AC, thus bidirectional inverters (AC/DC and DC/AC) are needed to exchange the power between these entities as shown in Figure 1.12. The mathematical model of an inverter connected with PV and ESS integrated system is described in equations (1.14) and equation (1.15).

$$E_{INV-Output}(t) = \left(E_{PV}(t) + E_{Grid}(t)\right) * \eta_{INV} \tag{1.14}$$

$$E_{batt}(t) = \left(\frac{E_{batt}(t-1) + E_{INV\_Output}(t)}{\eta_{batt}}\right) \tag{1.15}$$

Where $E_{PV}(t)$ $E_{Grid}(t)$is the energy generated by the solar PV and energy coming from the electrical grid, respectively. $E_{batt}(t)$ is the energy in the battery at a time interval(t). $E_{batt}(t)$ and $E_{batt}(t-1)$is the energy in the battery at a time interval (t) and $(t-1)$. The η_{INV} and $\eta_{batt}$are the efficiencies of the inverter and battery.

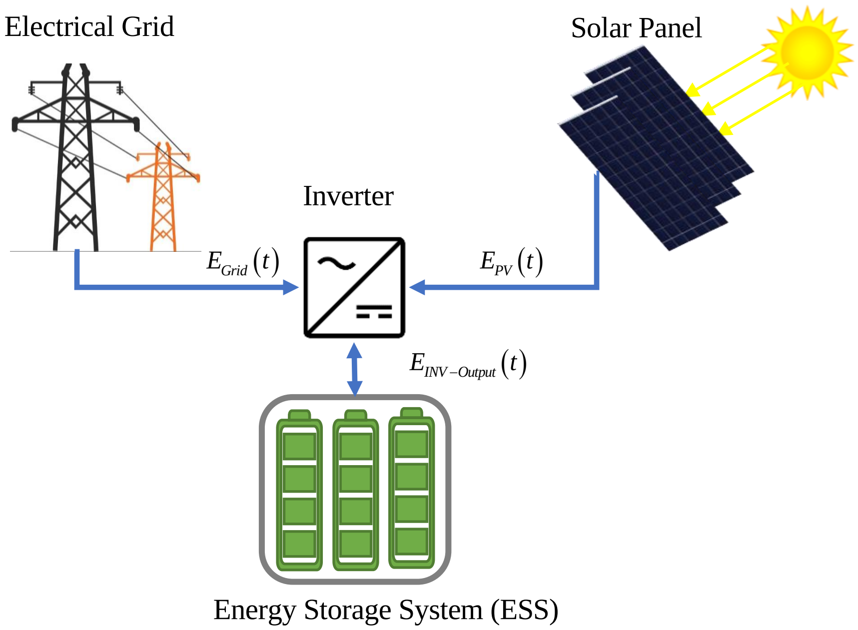

Figure 1.12 An inverter connected with Solar PV and Grid.

1.6 Simulation Data for PEBDC Ecosystem

The PEBDC Ecosystem consists of one of the campus buildings of Auckland University of Technology (AUT) equipped with a solar PV system integrated with ESS and PEB chargers. The hourly electricity consumption of the building and solar PV generation for all four seasons, FITs pricing, the Skybus arrival and departure schedule, and bus depot charging ecosystem case studies are highlighted in the following subsections.

1.6.1. Building Load

The amount of electricity being consumed by a building is called building electricity demand which is affected by mainly two factors: i) Time of the day and ii) Season (due to temperature variation). Therefore, the hourly electricity demand in a day and every four seasons are different. Figure 1.13 shows one of the AUT campus building hourly electricity demand in a single day for the following four seasons:

i) Summer- January
ii) Autumn- April
iii) Winter- July, and
iv) Spring- October

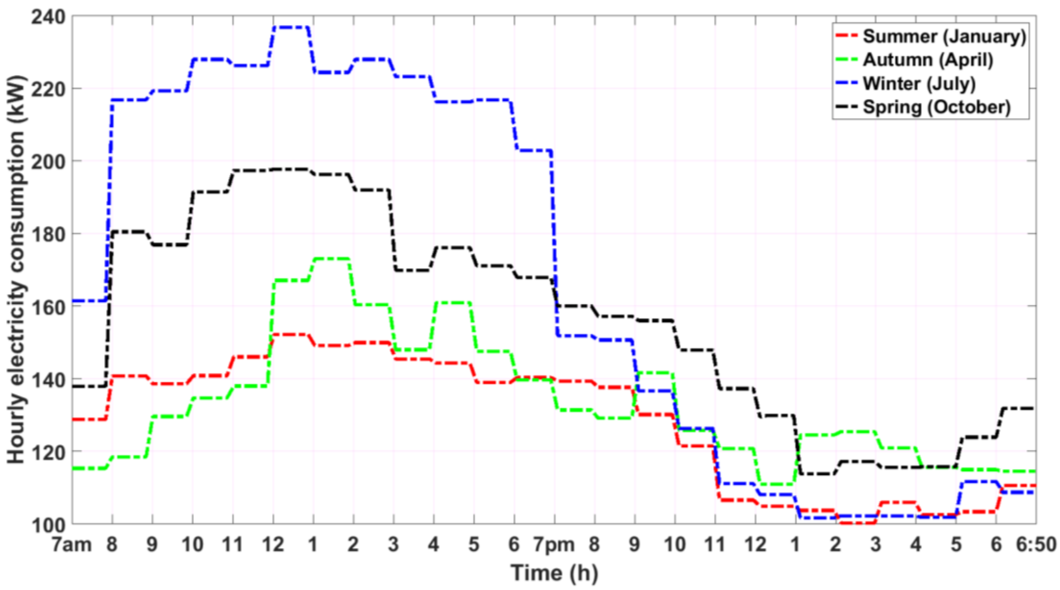

Figure 1.13 Hourly Building Electricity Demand: Summer, Autumn, Winter, and Spring.

In the winter and spring, the electricity demand is more than in summer and autumn due to more usage of i) hot water, ii) heaters, and iii) cooking. Due to such multiple actions of hundreds of people on campus, the winter and spring hourly electricity consumptions are more for the time interval from 7:00 am to 7: 00 pm. For the remainder of the time, all four seasons have almost similar electricity consumption.

In the summer, the electricity consumption (red dotted line) pattern is smaller and similar throughout the day due to the summer holidays. However the autumn electricity consumption gradually increases for the time intervals from 7:00 am to 12:00 pm then there is a sudden increase from 12:00 pm to 2:00 pm due to i) warming up the lunches and, ii) turning on the coffee maker as shown in Figure 1.14.

1.6.2. Solar PV generation

The power generation of the solar panel depends on the solar irradiation (sunlight hitting perpendicularly to the solar panel). The change of position of the sun over different seasons has a huge impact on the response of the solar panel. Figure 1.14 shows the hourly solar PV electricity generation installed at AUT campus building in a single day for the following four seasons:

i) Summer- January
ii) Autumn- April

iii) Winter- July, and

iv) Spring- October

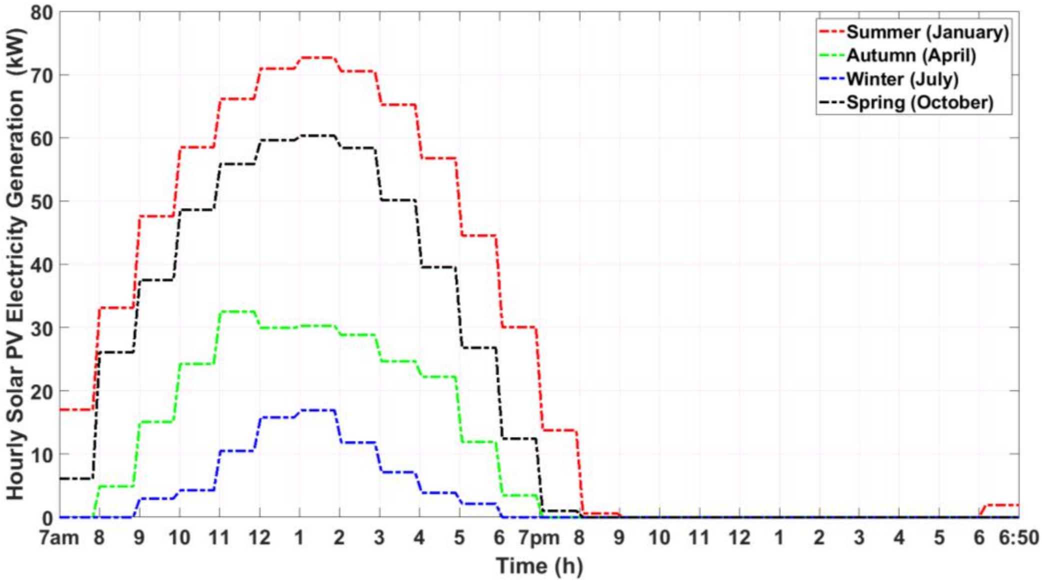

Figure 1.14 PV Power Generation: Summer, Autumn, Winter, and Spring.

In summer and spring, there is no rainy and windy weather also the solar irradiation is more and for a longer time; thus the panel produces more electricity. However, autumn and winter have more rainy and windy weather and less solar irradiation for less time interval thus, the solar PV power generation for these seasons is less.

1.6.3. Feed-in Tariffs (FITs) Price

The FITs is (also known as renewable energy payment) a policy mechanism which is designed to increase the investment in the renewable energy technologies by providing long term contract to the renewable energy producers[40]. Three different FITs pricing ($/kWh) shown in Figure 1.15 are used for charging the PEBs in a PEBDC Ecosystem are as follows:

i) BDO to PEB Energy selling price

ii) Purchasing price from Grid and

iii) BDO to the Grid selling price.

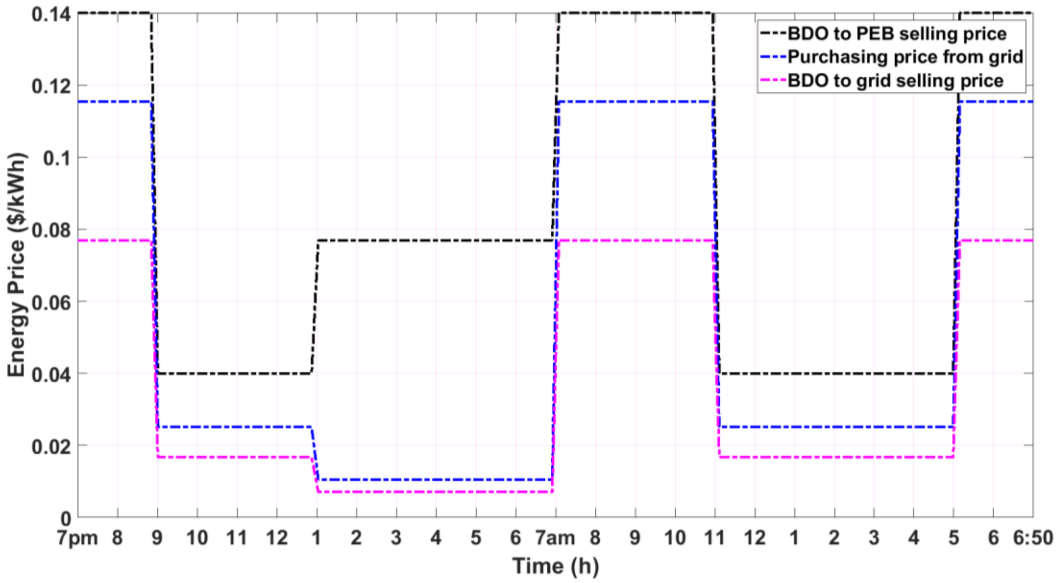

Figure 1.15 Proposed FITs Scheme for PEBDC Ecosystem.

1.6.4. Skybus Arrival and Departure Schedule

The Skybus arrival and departure schedule for three different intervals including i) peak, ii) normal and iii) off-peak time operates at 10, 20, and 30 minute intervals respectively, are used to verify the following two proposed charge scheduling algorithms:

i) Overnight Depot Charge Scheduling Algorithm

ii) Pantograph Scheduling Algorithm

The impact of charging PEBs using these two proposed charge scheduling algorithms is tested on K-9 feeder (LV distribution) in Manurewa, Auckland New Zealand, and has been presented in chapter 5, subsection 5.2.5.

1.7 Case Studies

For the PV sizing and allocation for three different test systems and to verify the proposed energy management model of the bus depot charging ecosystem, the proposed energy management model has been tested for four different test systems as highlighted below:

1.7.1. PEBDC Ecosystem Deployment

To overcome the carbon emission impact, this study utilised the solar PV system and increased the PEBs penetration from 0% to 100%. The PV sizing and allocations have been done for the following two IEEE test systems and one of the real distribution networks i.e., KEPCO.

i) IEEE-33 Bus Test System

ii) IEEE-69 Bus Test System

iii) KEPCO Distribution System

The PV sizing, allocation, and the losses for each of the above three case studies have been presented in chapter 3, section 3.

1.7.2. Energy Trading among PEBDC Ecosystem's Agents

To maximise the daily profit of PEBDC Ecosystem owner, energy trading (selling and buying) is performed among the agents (PV, ESS, Building, PEBs, and grid) for a whole day for the following four seasons:

i) Scenario 1- Summer

ii) Scenario 2 - Autumn

iii) Scenario 3 - Winter

iv) Scenario 4- Spring

The simulation results of energy trading among the PEBDC Ecosystem's agents for each of the above four cases have been presented in chapter 4, section 4.4.

1.8 Thesis Objectives

The objectives of the thesis are as follows.

Based on GHG emissions, RES's viability, ESS and EV technology development, feasibility study, design, optimisation, and implementation of green, resilient, and future-ready transportation infrastructure in a smart grid.

(i) To find the optimal DG location and size using PSO for PEB depot charging ecosystem integrated with a smart grid to reduce costs such as i) DG deployment, ii) voltage limit violation, iii) active power loss have been presented in chapter 3.

(ii) A comprehensive mathematical model is developed to maximise the BDO profit by performing the energy trading (among the participants in the bus depot charging ecosystem); this is based on the double-sided auction mechanism that has been presented in chapter 4.

(iii) To design charge scheduling algorithms for i) Depot charging (consisting of the grid and solar PV system integrated with ESS) and ii) Pantograph charging (grid only) and discharging model (based on route topography, vehicle weight, air-conditioning, and passenger weight) for PEBs and these charge scheduling algorithms are presented in chapter 5.

1.9 Thesis Organisation

In Chapter 1, the background study, feasibility study for green and resilient transportation and economic of PEB infrastructure in national and internal prospective, low emission bus road map, PEB and charging infrastructure economic, Auckland greenhouse emission, New Zealand current and future power generation are discussed. The detailed mathematical modeling for PEB depot charging ecosystem components including energy storage system, solar Photovoltaic, charge controller, and the inverter has also been discussed in this chapter. Finally, the motivation has been also presented.

Chapter 2 highlights the literature review on the State-of-the-Art Microgrid, EV technologies, charging Methods, configuration, standards, ports, and connectors, PEBDC ecosystem opportunities, and challenges. Finally, the PEB charging impact on the electrical grid has been presented.

In Chapter 3, the PSO algorithm is used to find an optimal DG location and size for the PEB depot charging ecosystem integrated with a smart grid to reduce costs such as i) DG deployment, ii) voltage limit violation and, iii) active power loss. The optimal DG size and location have been calculated for two IEEE test systems (i.e., IEEE 33 and IEEE 69) and a real distribution system (Korea Electric Power Cooperation) while increasing the PEB penetration from 0 % to 100 %.

Chapter 4 presents a comprehensive mathematical model to maximise the Bus Depot Operators' (BDO) profit by performing the energy trading among the participants such as grid, PV, ESS, and PEBs in the bus depot charging ecosystem, using real-world data. This energy trading is based on the double-sided auction mechanism which is tested for all four seasons. The simulation results and discussions are made in this chapter.

Chapter 5 presents the charge scheduling algorithms for i) Depot (consisting of the grid and solar PV system integrated with ESS) and ii) Pantograph (grid only), and the discharging model (based on route topography, vehicle weight, air-conditioning, and passenger weight) for PEB. The proposed algorithms are tested for all four seasons. In the pantograph worst case, charging all the PEBs at the same time causes the distribution transformer to be heavily overloaded. However, in depot charging the distribution transformer is not overloaded due to charging the PEBs during the low peak hours (night-time). The simulation results are discussed in this chapter.

1.10 Contributions

The research taken in this thesis has made the following contributions to enhance the utilisation of eco charging systems integrated with ESS and Solar PV systems.

1. The penetration of EV, particularly PEBs is increasing and the electricity demand will increase in near future, which can be fulfilled by integrating the renewable energy resource and ESS. In this study, the sizing and location of PV are performed for LV feeder to reduce costs such as i) DG deployment, ii) voltage limit violation and, iii) active power loss.
2. The components of the eco charging system are expensive, thus the total system cost (capital investment, operation, and maintenance) of PV, ESS, and PEB chargers per day are incorporated in the proposed double-sided auction-based EMS model and used for energy trading.

3. PEB charge scheduling has been attracted the attention of the researcher to fully charge the PEBs before it departs from the depot. However, the overnight depot charge scheduling algorithm and battery discharging model (factors such as vehicle weight, air-conditioning unit, passenger weight, route topology, and stop) which has never been considered in the previous studies.

The list of publications as part of this research work is as follows.

1. **Arif, S. M.,** Lie, T. T., Seet, B. -C., Ayyadi S, (**2021**). "A novel and cost-efficient energy management system for plug-in electric bus charging depot owners" Electric Power Systems Research doi: 10.1016/j.epsr.2021.107413
2. **Arif, S. M.,** Akhtar, H., Lie, T. T., Ahsan, S.M, and Hassan, A.K (**2020**). "Analytical Hybrid Particle Swarm Optimization Algorithm for Optimal Siting and Sizing of Distributed Generation in Smart Grid." Journal of Modern Power Systems and Clean Energy. doi: 10.35833/MPCE.2019.000143
3. **Arif, S. M.,** Lie, T. T., Seet, B. -C., Ahsan, S. M., and Khan, H. A. (**2020**). "Plug-in electric bus depot charging with PV and ESS and their impact on LV feeder". Energies, 13(9), 2139. doi:10.3390/en13092139
4. **Arif, S. M.,** Lie, T. T., and Seet, B. C. (**2018**). "A Novel Simulation Model for Analyzing the State of Charge of Electric Vehicle". In IEEE International Conference on Innovative Smart Grid Technologies (ISGT Asia) (pp. 151-155). Singapore:
5. **Arif, S. M.,** Lie, T. T., Seet, B. -C., Ayyadi S, (**2021**). "A Review of Electric Vehicle Technologies, Charging Methods, Standards and Optimization Techniques" Energies, under review).

Co-author works :

1. Ahsan, S. M., Khan, H. A., Hassan, N. U., **Arif, S. M.,** Lie, and Lie, T. T. (**2020**). "Optimized power dispatch for a solar photovoltaic storage system with multiple buildings in bilateral contracts". Applied Energy, 273. doi:10.1016/j.apenergy. 2020.115253.

2. Ayyadi S, Maaroufi. M, **Arif, S. M.,** "EVs charging and discharging model consisted of EV users behaviour" (**2020**). 5th International Conference on Renewable Energies for Developing Countries (REDEC).
3. Akhtar, H., Aslam, M., **Arif, S. M.,** "A standards-based approach for Auto-drawing single line diagram of multivendor smart distribution systems" (**2018**) International Journal of Electrical Power & Energy Systems 96, 357-367
4. Akhtar, H., Aslam, M., **Arif, S. M.,** "Optimal siting and sizing of tri-generation equipment for developing an autonomous community microgrid considering uncertainties" (**2017**) Sustainable cities and society 32, 318-330
5. Akhtar, H., Aslam, M., **Arif, S. M.,** "Emerging renewable and sustainable energy technologies: State of the art" (**2017**) International Journal of Electrical Power & Energy Systems 96, 357-367
6. Akhtar, H., Aslam, M., **Arif, S. M.,** "Optimal siting and sizing of tri-generation equipment for developing an autonomous community microgrid considering uncertainties" (**2017**) Sustainable cities and society 32, 318-330

Chapter 2 Literature Review

This chapter is based on the work from the following journal publication in which the author of this thesis is the main author ("A Review of Electric Vehicle Technologies, Charging Methods, Standards and Optimization Techniques" Energies, under review).

In recent years, the implementation of public transportation specifically, Plug-in Electric buses (PEBs) related technologies have progressed significantly, due to government policies established to achieve greenhouse gas emissions reduction targets. The Microgrid and public charging infrastructure play an important role in achieving this emission target and the successful implementation of all types of EVs specifically, PEBs.

This chapter provides an in-depth overview of the followings: i) the State-of-the-Art Microgrid ii) EV cutting-edge technologies such as Hybrid Electric Vehicle (HEV), Electric Vehicle (EV), and Fuel Cell Electric Vehicle (FCEV), iii) EV Charging Methods e.g., Battery Swap Station (BSS) Wireless Power Transfer (WPT), and Conductive Charging (CC), iv) EV Charging Configurations, Standards, Ports, and Connectors, v) PEB Depot Charging (PEBDC) Ecosystem opportunities and challenges and, vi) Finally, the PEB charging impact on the electrical grid has been presented.

2.1 The State-of-Art Microgrid: Overview and Architecture

A microgrid is a local electrical grid integrated with local renewable energy resources e.g. solar PV, wind turbine and biofuel, etc., or non-renewable resources and connected with a cluster of loads with a control capability. This means a microgrid can work in both the grid-connected and/or islanded modes. The main grid is connected to the microgrid at a point of common coupling (PCC) which has the same voltage level as the grid. In case of any problem, the PCC disconnects the microgrid from the main grid. Thus, a microgrid improves power quality, reliability, and system efficiency while providing grid independence to each connected end-user [41].

Three basic characteristics of a microgrid are: i) a master controller that regulates the cluster of loads, and distributed energy resources, ii) installed generation capacity to meet the peak load demand, and iii) well-defined electrical boundaries. Thus, the microgrid consists of i) master controller ii) group of loads, iii) distributed Generations (DGs), iv) solid-state smart switch, v) automatic protective devices, vii) inverters/ converters, control, automation, and commination systems. The basic overview of a typical microgrid is shown in Figure 2.1.

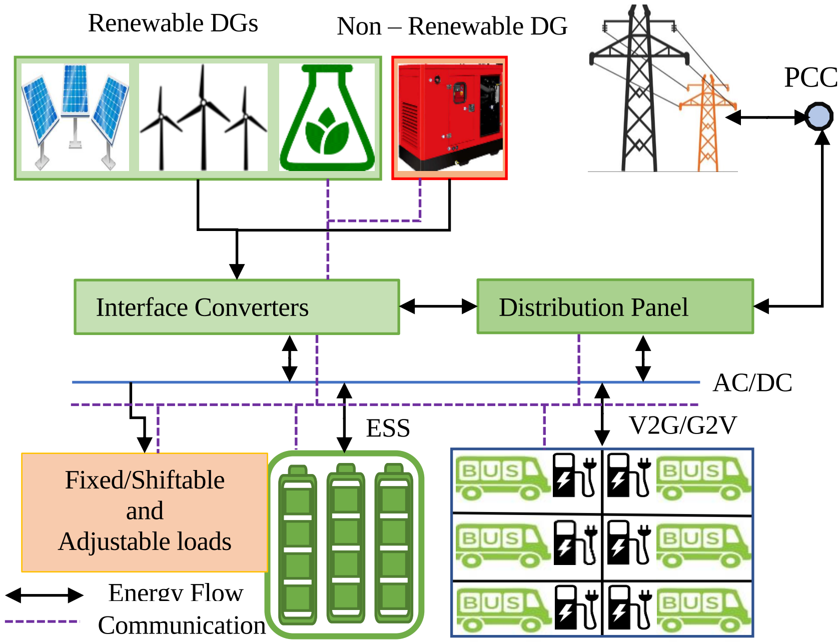

Figure 2.1 An overview of typical Microgrid.

The loading system in a microgrid is mainly divided into three parts which are as follows:

(i) **Fixed loads** are the types of load that must be satisfied during a certain period e.g., microwave, TV, and computer, etc., which cannot be changed except by the user.

(ii) **Shiftable loads** are also known as spring or deferral loads, the examples are electric vehicles, dryers, washing machines, and electrical pumps. These loads can be on/off during the grid price low/high, respectively.

(iii) **Adjustable loads** are the type of loads that can be partially increased or curtailed due to control signals for example lighting, HVAC, and refrigerator.

Distributed energy generation comprises ESS and DGs which might be installed at the user end sites and/or electric utility grid system. In a microgrid, DGs are classified into two types namely dispatchable and non-dispatchable. Dispatchable DGs are also known as conventional DGs which can be turned on or off according to load demand which means the output is controllable e.g., diesel generator [42]. However, the non-dispatchable DGs are commonly known as renewable DGs, the output of which cannot be controlled according to the load demand due to the intermittent nature e.g., solar PV, wind turbine, and biofuel [43]. The major drawback associated with the fossil-fuel-based dispatchable DGs is the greenhouse emission (GHG), which motivates the energy supply sector to move towards renewable DG systems. The sporadic and intermittent characteristic of non-dispatchable energy generation units requires the use of an energy storage device. The ESS is used as a coordinating unit with non-dispatchable DGs to assure continuous power to the main grid. During off-peak, the ESS stores the power and feeds back the stored energy to the grid at peak hours; these are more important in the stand-alone microgrids [44].

The entire connection between the DGs, ESSs, and loads in the microgrid system is managed by switches and solid-state protective devices. Wherever a fault occurs anywhere in the system, these protective devices will isolate the faulted area by disconnecting/ connecting and rerouting the power flow in the system. The master controller is used to change the mode of the microgrid from the grid-connected to the islanded or vice versa by connecting or disconnecting at the PCC. The microgrid presents various advantages For example i) high power quality, ii) it offers high energy efficiency through real-time market pricing, and iii) reduces the GHG emission by introducing renewable energy resources, and iv) reduces the transmission costs which makes it more economical. The renowned feature of a microgrid is the capability of "islanded mode" which provides energy security to the faulted or disturbance area and reconnects the microgrid with the grid after the fault clearance [45]. Based on various attributes, microgrid are classified as follows

(i) Urban Community Microgrids
(ii) University Campus Microgrids
(iii) Commercial Microgrids
(iv) Military Microgrids
(v) "Off-Grid" Microgrids for remote areas

2.1.1. PEB Depot Charging Ecosystem integrated with Microgrid

The configuration of the proposed PEBDC ecosystem connected with the Low Voltage Direct Current (LVDC) microgrid is shown in Figure 2.2. It consists of 24 PEB charging units, a Li-ion battery-based ESS, and a Solar PV system integrated with the local grid. All charging units have a rated charging power of 30 kW. Each component is tied with an 11 kV LVDC common bus through converters. The DC/DC converters at the charging unit control the charging power to each of the respective PEBs which has a battery capacity of 374 kWh.

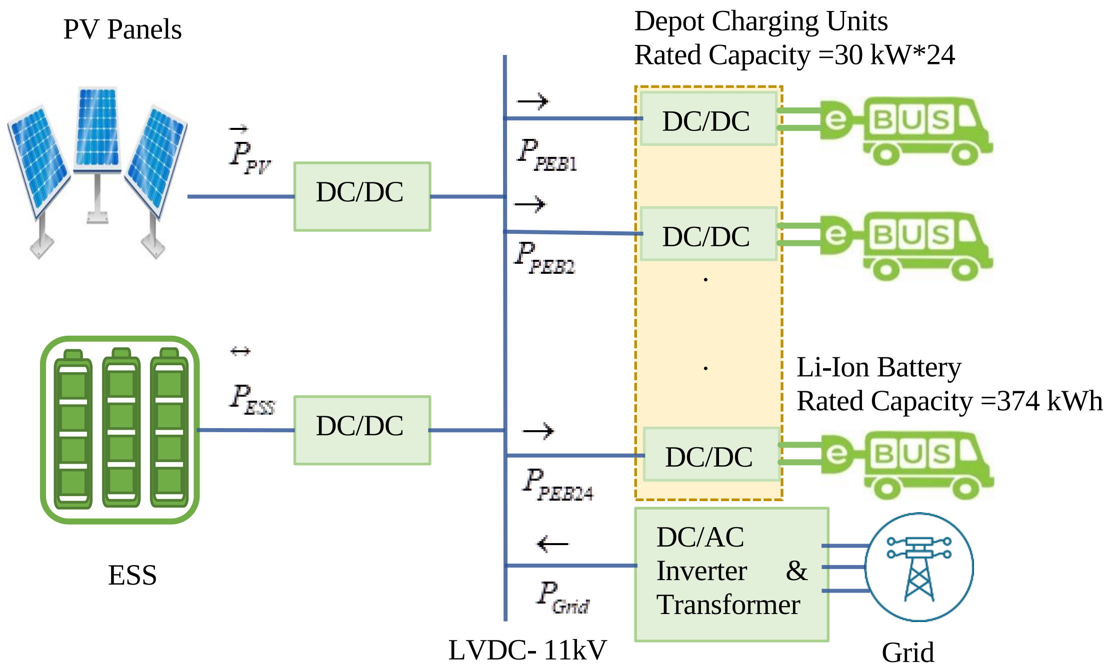

Figure 2.2 Configuration of PEBDC Ecosystem connected with LVDC Microgrid understudy.

Four possible energy trading scenarios between the PV, ESS, PEBs, and grid can occur in the PEB depot charging station which is as follows.

(i) PEBs are on the road and high tariff on the grid

(ii) PEBs are in the depot and high tariff on the grid

(iii) PEBs are on the road and a low tariff on the grid

(vi) PEBs are in the depot and a low tariff on the grid

In the 1st scenario, the energy available in the ESS is sold back to the grid to generate a profit for the depot owner, in case of the PEBs have arrived late in scenario 2, the available energy in the ESS or the solar PV power (if available) is used to charge the PEBs. In the 3rd scenario, the PV-generated power, or the grid power is used to charge the ESS which will use to charge the PEBs when they arrive. In scenario 4, PEBs are charged through Solar PV if there is PV generation or

ESS power else power is purchased from the grid to charge the PEBs. The proposed energy management and mathematical model are described in Chapter 4.

2.2 Review of Electric Vehicle Technology

The main issue with ICE vehicles is fossil fuel consumption along with rising fuel prices and this causes two main problems: energy security and CO_2 emission to the environment. According to the observatory of economic complexity at the MIT media lab, oil is the spark of life for humans and is imported from politically unstable countries [46]. Considering the deficiency of fossil fuel and increment in the CO_2 emission, EVs reduce the reliance on transportation on crude oil and reduce GHG emissions. The vehicle technology is mainly divided into four main categories [47, 48] shown in Figure 2.3; moving from left to right is an electrification increase. The source of energy for a conventional vehicle is petrol or diesel fuel which is the main source of carbon radiation in the environment. However, HEV uses both sources of energy. Therefore, the carbon emission rate of a hybrid is less than for conventional combustion engine vehicles. The third and fourth types are also known as a zero-emission vehicle which depends on the hydrogen fuel cell and battery, respectively. The details of the different technologies will be discussed in the next few subsections.

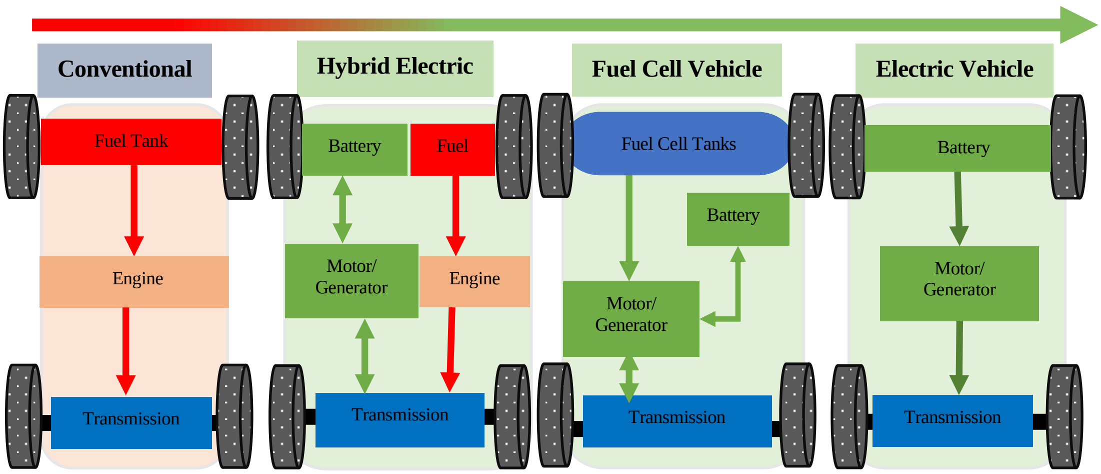

Figure 2.3 Electrification of Transportation.

2.2.1. Hybrid Electric Vehicle

Hybrid Electric Vehicle (HEV) have an IC engine and a battery both of which are used to propel the vehicle thus the source of energy can be a battery and/or internal combustion engine. Thus, the HEV is also known as a dual-power-source vehicle. HEVs are better for urban driving because the battery can be recharged by recapturing the kinetic energy of the vehicle into the battery through regenerative braking. In urban driving, the vehicle often does start and stop. Therefore, HEVs are better for urban driving than rural, or highway driving. Since the fully electric vehicle is in the early development stage, HEVs seem to be the most cost-effective solution so far probably for the next decade [49]. To minimise pollution, the HEV uses the ICE engine and electric motor in the most efficient way to save energy. The advantages of HEVs are as follows:

(i) Fuel efficiency and performance

(ii) Lower fueling cost

(iii) Reduce the CO_2 emission

(iv) Recover some of the energy from regenerative braking

(v) Use the existing fuel station.

The drivetrain is a collection of components that provides the power from the vehicle's battery or vehicle's engine to the vehicle's wheel. There are three types of HEV drivetrains: (i) series hybrid, (ii) parallel hybrid, and (iii) series-parallel hybrid [50]. The simplest configuration is the series drivetrain which provides power to the electric motor. The motor gets power either from a generator run by a gasoline engine or from the battery pack while, in the parallel drivetrain, the engine and motor work in parallel to generate power that propels the vehicle. However, the series-parallel hybrid merges the complication and advantages of both series and parallel drivetrains. Toyota Prius is an example of a series-parallel hybrid. In this study, the series-parallel hybrid vehicle consisting of the control, combustion engine, electrical system, and power split device is used as shown in Figure 2.4.

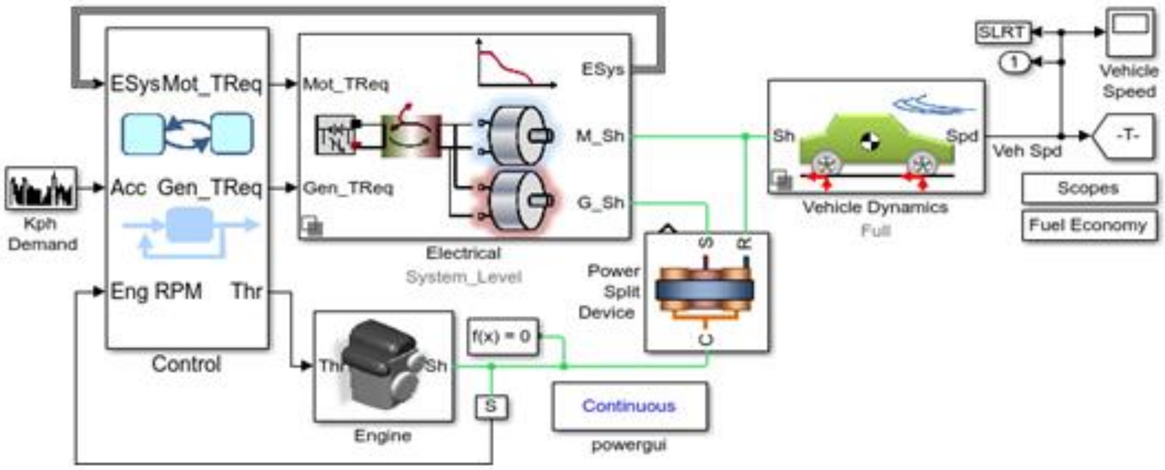

Figure 2.4 The Hybrid Electric Vehicle, Series-Parallel [51].

The controller gets motor speed, generator speed, brake, and acceleration information from the vehicle dynamics. The electrical section gets generator torque and motor torque from the controller which will decide when to charge and discharge the battery. Whenever a driver hits the brakes, the motor acts as a generator and starts to charge the battery; this is called regenerative braking [52], otherwise, it will consume power from a battery. The electrical section consists of a synchronous motor and drive, a synchronous generator and drive, a DC-DC converter, and a battery bank.

The ICE gets a throttle position from the controller which is used to regulate the amount of fuel or air entering the engine. The power split device as shown in Figure 2.4 is the brain of a hybrid vehicle that controls how the gasoline engine, generator, and electric motor work together. It allows the car to operate in series or parallel (independently both motor and gas engine and both can power up the car). The vehicle dynamic provides vehicle speed which depends upon the vehicle body, road inclination, and wind resistance.

Typical HEVs have four modes of operation [53] as shown in Figure 2.5. The modes of operations are as follows:

(i) **Start and Low to Mid-range Speeds**: During low to mid-range speeds or at the starting of the vehicle, the engine stops, and the vehicle is propelled by the battery alone.

(ii) **Driving Under Normal Conditions**: The power split device sends some of the power to run the generator and the rest of the power to drive the wheels directly. If there is excessive power, then it's used to charge the battery.

(iii) **Sudden Acceleration:** Both the battery and engine provide power during sudden acceleration.

(iv) **Deceleration:** The regenerative braking system converts the kinetic energy into electrical energy that is stored in the high-performance battery.

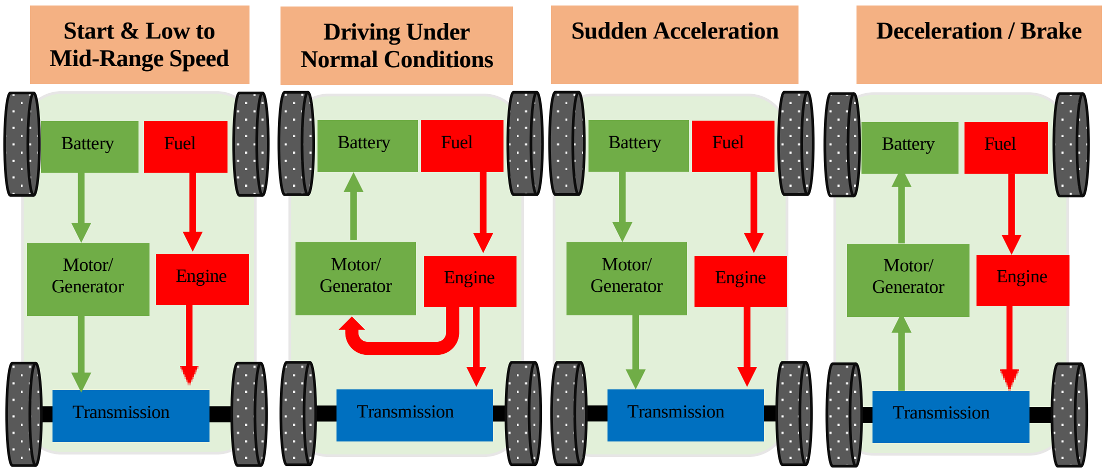

Figure 2.5 Hybrid Electric Vehicle Mode of Operations.

2.2.2. Electric Vehicle

Due to the potential benefits of EVs, the authors [54] transformed the series-parallel hybrid into the fully electric vehicle as shown in Figure 2.6 which can take the real electric vehicle movement data and predict the SOC of vehicles according to road inclination, vehicle weight, and wind resistance.

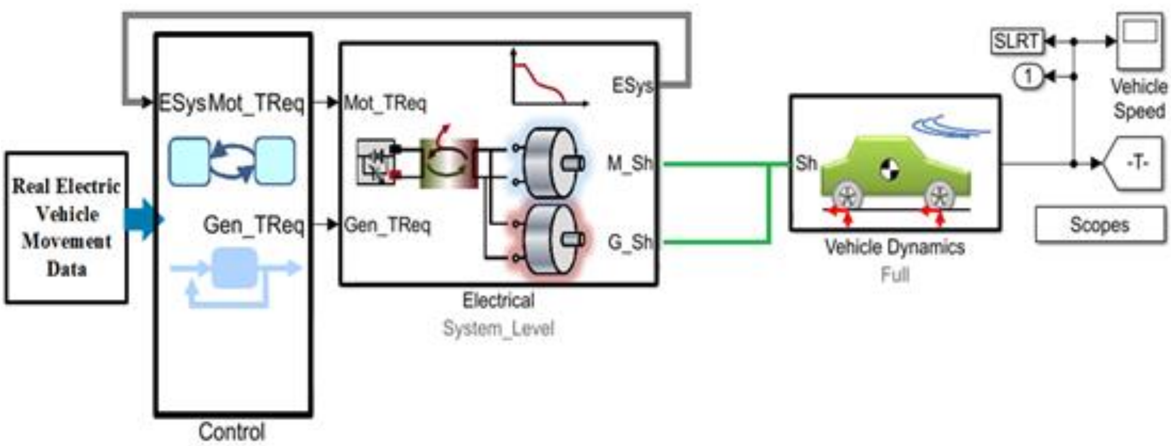

Figure 2.6 Electric Vehicle Model [54].

The fully electric vehicle uses only a battery power pack to propel the vehicle. Therefore, EVs are better for combatting global warming as compared to HEVs. The EVs use only the battery to propel the vehicle and have a regenerative braking system to recapture vehicles' kinetic energy into electrical energy to be stored in the battery. Therefore, EVs are better for urban driving, because in urban driving the vehicle often starts and stops; during which time the vehicle recaptures the kinetic energy into the battery. As compared to typical HEVs, the EVs have only two modes of operation which are as follows (see Figure 2.7):

(i) **All times:** Whenever the vehicle needs to move, the battery propels the vehicle

(ii) **Deceleration or Braking**: When the vehicle decelerates or brakes, the vehicle recaptures the kinetic energy into the battery using regenerative technology.

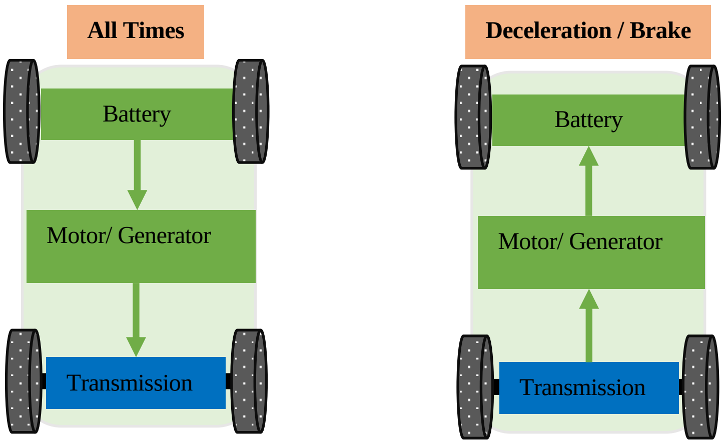

Figure 2.7 Electric Vehicle Mode of operations.

2.2.3. Fuel Cell Electric Vehicle

Fuel Cell Electric Vehicle uses electric powertrain like EVs; however, hydrogen is used as an energy source in the fuel cell tank. There is no tailpipe pollution, thus it is considered a zero-emission vehicle. Based on the powertrain configuration, the fuel cell electric vehicle is categorised into two types namely:

(i) Fuel Cell Electric Vehicle (FCEV)

(ii) Fuel Cell Hybrid Electric Vehicle (FCHEV)

The typical powertrain configurations of FCEV and FCHEV are shown in Figure 2.8

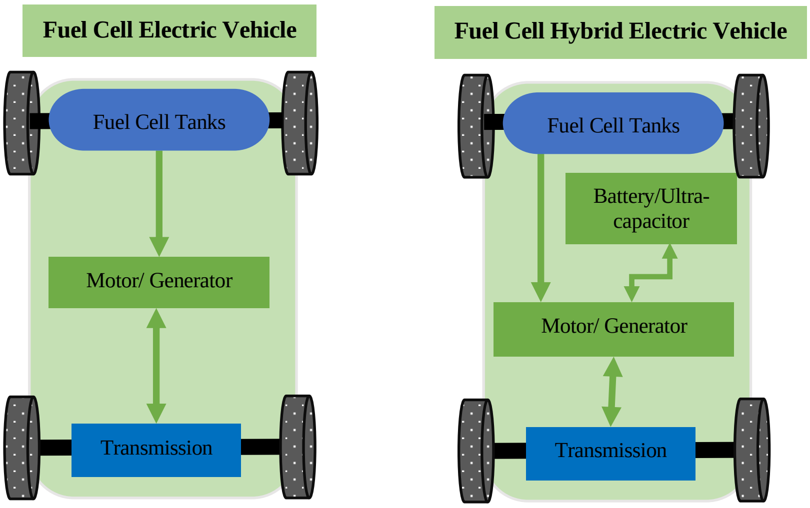

Figure 2.8 FCEV and FCHEV Powertrain configurations [55].

The FCEV is ideal for slow speed with smooth power demand applications such as buses, forklifts, and trams, etc. Nowadays FCEV manufacturers such as Hyundai, Toyota, and Honda, etc. are manufacturing high-performance FCEV vehicles in terms of fuel economy, and vehicle efficiency, by adopting various energy management techniques [56].

However, for high-speed operation, FCHEV adds another auxiliary ESS or ultracapacitor in the powertrain which can be charged, and discharged based on the vehicle power demand and supply. The fuel cell tank is used as the main source of energy and ESS or ultracapacitor is used for smooth and efficient operation [57]. The only drawback of the FCEV is the increase in weight due to the extra ESS or ultracapacitor in the powertrain.

The understanding of the EV charging methods is as important as understanding the EV technology described in the above section. Therefore, the next section will briefly describe the existing EV charging methods.

2.3 Review of EV Charging Methods

Battery exchange, wireless charging, and conductive charging are the main three charging techniques. The conductive charging is further divided into pantograph (Bottom-up and Top-down) and overnight charging as shown in Figure 2.9.

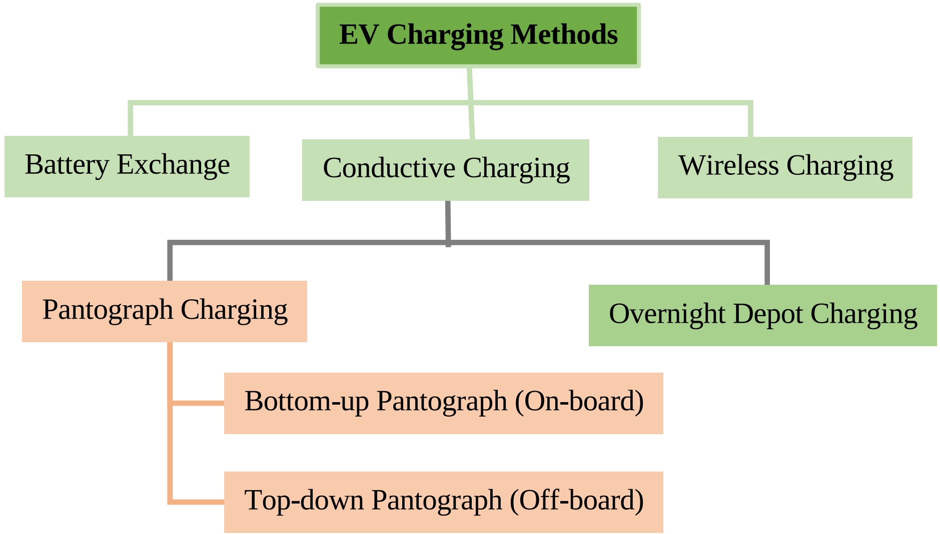

Figure 2.9 EV Charging Methods [58].

2.3.1. Battery Swap Station (BSS)

The battery swapping method is also known as "Battery Exchange" which is based on paying monthly rent for the battery to the BSS owner. The slow charging method of the BSS helps to extend the battery life. It is much easier to integrate the locally generated RESs such as Solar and Wind with the BSS system. One of the main advantages of this technique is the drivers do not need to get out of the vehicle and can replace the discharged battery very quickly. Moreover, the battery kept at the station can participate in the V2G (vehicle-to-grid) initiative [59, 60].

However, due to high monthly rental fees charged by the BSS owner, this type of EV charging technique is more costly than the fueling of the ICE engine because the BSS owner owns the EV batteries. This technique needs many expensive batteries as well as a sizeable area in which to store them. Also, the station may have a particular model of the battery, but the vehicles may have different battery standards [61, 62].

2.3.2. Wireless Power Transfer (WPT)

This technology is based on electromagnetic induction and uses two coils. The primary coil is placed on the surface of the road, and the secondary coil is placed inside the vehicle. Recently WPT technology has gained attention in EVs application because of its capability to allow the EV to recharge safely and conveniently. Also, it does not require a standard connector and can charge even while the vehicle is in motion [63].

However, the inductive power transfer is generally weak, and the air gap between the transmitter and receiver coils should be in the range of 20 to 100 cm for efficient power transmission. Moreover, eddy current loss is another issue in the WPT if the transmitter coil is not turned off. The information transfer between the transmitter and the EV should be real-time, and communication latency is another problem [64].

2.3.3. Conductive Charging (CC)

Conductive charging needs a direct connection between the vehicle and charging inlet and provides different charging facilities, e.g. level 1, level 2, and level 3 charging, and has high efficiency in charging due to the direct connection. The two power charging levels (Level 2, 3) are employed for a public charging station. The first two levels (Levels 1 and 2) have less impact on the distribution system. Conductive charging provides a V2G facility and reduces the grid loss, maintains voltage level, prevents grid power overloading, active power support, and can provide reactive power compensation by using the vehicle's battery [65, 66].

However, level 3 has different impacts on the distribution system such as voltage deviation [67], reliability of the system, and transfer/power loss. It increases not only peak demand but also affects the transformer life [67, 68]. It also needs a complex infrastructure, limited access to the electricity grid, and a standard connector/charging level [69]. The V2G technology requires intensive communication between grid and vehicle. Also, the V2G operation reduces the battery lifespan of the battery due to frequent charging and discharging. The charging station types including BSS, WPT, and CC stations are summarised in Table 2.1.

Table 2. 1 Summary of Reviews on Charging Methods

Types	Advantages	Disadvantages	Reference	Year
BSS	• Quick battery replaces (Fully charged) • BSS extend the battery life by slow charging • BSS help utilities in balancing the demand and load by using the V2G facilities • Easy to integrate with the locally generated RESs.	• More costly than ICE vehicle because of the monthly rent to BSS • The huge investment required for both equipment and batteries • Need a large stock of expensive batteries • Many areas needed to accommodate the batteries • Different EVs have different battery standards.	[59] [60] [61] [62]	2014 2017 2017 2018
WPT	• EV recharge it safely and conveniently • No need for any standard connector • No need for any standard Socket • Recharge when the vehicle is in motion.	• Power transfer is generally weak • The range of 20 to 100 cm for efficient power transmission • The transmitter and the EV should be real-time and communication latency.	[63] [64]	2018 2018
CC	• Provide multiple charging levels • Provide high efficiency • Coordinated V2G facility • Reduce the grid loss • maintain voltage level • prevent grid power overloading • Active power support.	• Complex infrastructure • Restriction to the electricity grid • Fast charging cause voltage instability in the distribution system • Need a standard connector/charging level • Grid power overloading will cause due to uncoordinated charging • V2G operation reduces the lifetime of the battery.	[65] [66] [67] [68] [69] [70]	2016 2017 2014 2018 2015 2013

For higher battery capacity and quick charging requirement applications such as buses and trucks, the following two charging techniques are utilised as discussed below:

Overnight Depot Charging: The overnight depot charging system can be designed for slow and fast charging. It is usually installed at the end of the lines and used for night-time charging. Thus, slow charging is the most favorable option because of the low charging impact on the distribution grid [25]. However, for higher battery capacity with quick charging requirement applications, the Pantograph charging technique is suitable.

Pantograph Charging: This type of charging is also known as opportunity charging. This kind of charging infrastructure is used for higher battery capacity and power requirement applications such as buses and trucks. This charging technique offers less investment in the bus battery thus reducing the bus investment cost, however the charging infrastructure cost increases [71]. Pantograph charging is further divided into the following two categories:

(i) **Top-down Pantograph:** The charging setup is mounted on the roof of the bus stop therefore it is commonly known as an off-board top-down pantograph. This method provides high power direct current which is already demonstrated in Singapore, Germany, New Zealand, and USA [72].

(ii) Bottom-up Pantograph: This type of charging method is suitable for those applications where the charging equipment is already installed in the bus. This is also known as an on-board bottom-up pantograph [72].

2.4 Review of EV Charging Configurations, Standards, Ports, and Connectors

In this section, the EV charging configurations such as on-board and off-board, charging standards including IEC and SAE, and the country-wise EV charging infrastructure and connectors are explained.

2.4.1. EV Charging Configurations

Most of the people in US have a daily driving range of less than 100 miles [73] considering this, charge anxiety is a more serious issue than range anxiety. To overcome the charge anxiety, the off-board charger is the better choice because it generally offers higher kW transfer and removes weight from the vehicle. The off-board charger means the charger is outside of the vehicle and provides DC power to the EV battery pack. The off-board EV charging configuration [74] as shown in Figure 2.10 uses the IEC mode 4 and SAE level 1 and Level 2 (see Table 2. 2).

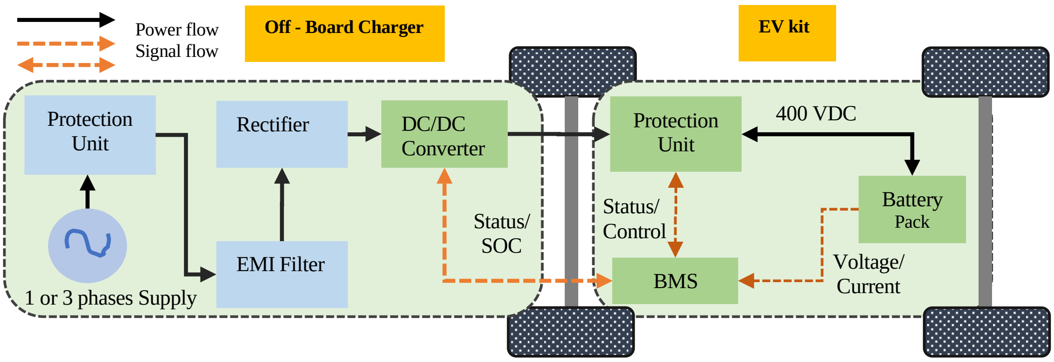

Figure 2.10 EV Charging Configuration for Off-board (DC Levels 1 and 2 or Mode 4).

However, the on-board charging offers lower kW transfer and adds weight to the vehicle. Because of the weight, space, and cost constraints the single-phase on-board chargers limit the transfer of high power [75, 76]. Therefore, it takes more charging time than the off-board charging configuration. The EV charging configuration for AC (Modes 1 and 2 and Level 1 and 2 for IEC and SAE standard respectively) requirements with on-board charger is demonstrated in Figure 2.11 [77, 78] and DC charging levels as described in Table 2.2.

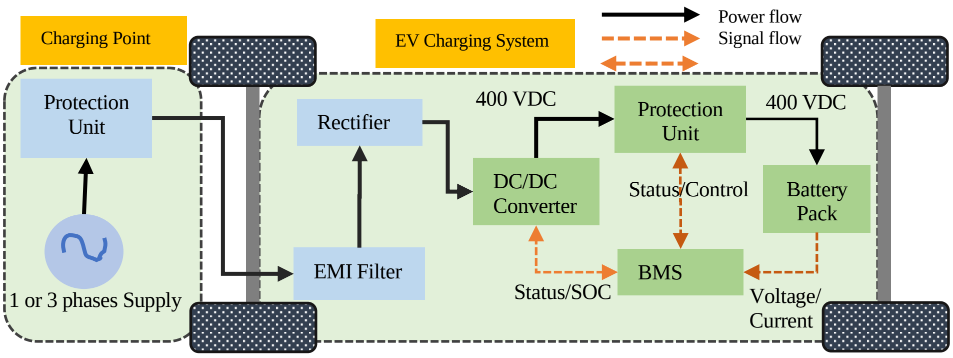

Figure 2.11 EV Charging Configuration for On-board (AC Levels 1 and 2).

Due to the increasing number of EVs the IEC and SAE in [79] proposed AC and DC charging standards for US and EU considering the voltage levels and current etc. (see Table 2.2). The details are further explained in the next subsection.

2.4.2. EV Charging Standards

Several EV charging standards are utilised around the globe to deal with EV charging infrastructure. For example, USA uses the IEEE and SAE standards, whereas Japan and Europe have their charging standard called CHAdeMO. Standards Administration of China (SAC) issues its standard named GB/T which is like the IEC standard. In SAE, the power level is called "Level" whereas, in IEC, the level of power is called "Mode". The ICE and SAE charging standards are summarized and presented in Table 2.2.

Table 2. 2 IEC and SAE Standards: Current and Voltage Level for AC and DC Charging

Standards	Phase	Level/Mode	Voltage (V)	Current (A)	Source
IEC62196	Single	Mode 1	120	16	AC
	Single	Mode 2	240	32	
	Single	Mode 3	250	32-250	
	DC	Mode 4	600	400	DC
IEC61851	Single	Mode 1	120	16	AC
	Single	Mode 2	240	80	
	DC	Mode 4	200-450	80	DC
SAEJ1772	Single	Level 1	120	16	AC
	Single	Level 2	240	32-80	
	DC	Level 1	200-450	80	DC
	DC	Level 2	200-450	200	

The charging Level 1/Mode 1 where most EVs charge at homes or offices overnight is used for slow charging. The level 2/ Mode2 and Level 3/ mode 3 charging modes are for both the public and private charging facilities and mode 4 in IEC and SAE is used for fast charging.

2.4.3. EV Charging Ports and Connecters

Different charging standards have been followed by different countries. The major differences between these standards are the charging ports and charging connectors as shown in Figure 2.12 and Figure 2.13, respectively. The SAE J1772, which is used in the USA, has the capability of charging both with AC and DC. Tesla introduced its charging connector which supports both AC and DC fast charging. In Europe, the combo is the popular connector. All these connectors are different in shape and pin-wise. However, the manufacturers are attempting to come up with a universal standard [80].

	USA		Japan	China		EU
AC Charging (Single/ Three Phase)						
						
Standards	SAE J1772		SAE J1772	IEC 62196	IEC 62196	IEC 62196-2
Levels/Modes	Level1, Level2		Level 1, Level 2	Mode 1, Mode 2	Mode 1	Mode 1, Mode 2
Phases	Single		Single	Single/Three	Single	Single/Three
DC Fast Charging and/or AC/DC Combo						
						
Levels	Level 1+ DC	Level 2+ DC	DC Fast Charging	DC Fast Charging		Fast Charging
Standards	SAE J1772Combo		CHAdeMO	GB/T 20234.3-2011		IEC 62196-3

Figure 2.12 EV Charging Ports

	USA		Japan	China	EU
AC Charging (Single/ Three Phase)					
					
Standards	SAE J1772		SAE J1772	IEC 62196	IEC 62196-2
Levels/Modes	Level 1, Level2		Level 1, Level2	Mode 1, Mode 2	Mode 1, Mode 2
Phases	Single		Single	Single/Three	Single/Three
DC Fast Charging & AC/DC Combo					
					
Levels	Level 2+ DC Combo	Supercharger	Fast Charging	DC Fast Charging	Fast Charging
Standard	SAE J1772	Tesla	CHAdeMO	GB/T 20234.3 - 2011	IEC 62196-3

Figure 2.13 EV Charging Connectors.

New Zealand imports EVs from Japan, Europe, and USA and does not have its own charging standards. Therefore, New Zealand follows the SAE, IEC, and Tesla standards shown in Figure 2.14.

AC Connectors and Pins			
	Type 1	**Type 2**	**Tesla**
		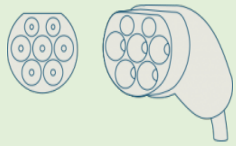	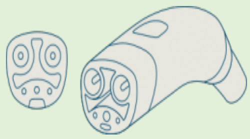
Standards	SAE J1772	IEC 62196	Tesla
Type	AC	AC	AC and DC Combo*
DC Connectors and Pins			
	Type 1	**Type 2**	**CHAdeMO**
	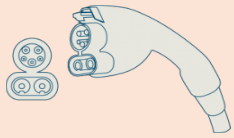	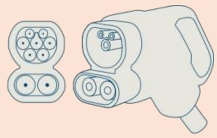	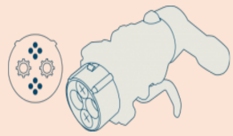
Standards	SAE J1772 (CCS Combo 1)	CCS Combo2	IEC 62196
Type	DC	DC	DC

Figure 2. 14 EV Charging Connectors and Pins Standards (New Zealand).

2.4.4. PEB Charging Connector

Auckland Transport has used Yutong electric buses for trial and, due to the successful results, some other bus companies in New Zealand have introduced electric buses in their fleets e.g., Go Bus and NZ bus, etc. EU charging standard is used in the Yutong electric bus charger. The charging gun has 3 phases and 5 wires as shown in Figure 2.15.

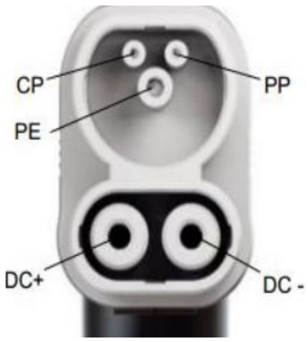

Pin Number	Pin Name	Pin Definition
1	DC+	Positive DC Wire
2	DC-	Negative DC Wire
3	PE	Protective Earthing
4	CP	Control guidance
5	PP	Connection Confirmation

Figure 2.15 Yutong Electric Bus Connector Comply with IEC62196-3-2011.

2.5 PEBDC Ecosystem Opportunities and Challenges

A detailed review of the opportunities and the challenges in designing a PEBDC is discussed below:

2.5.1. Opportunities

V2G Technology: V2G technology can turn the EVs power consumption challenges into opportunity. For example, the utilisation of EV batteries (more specifically PEB such as the Yutong electric bus battery which has 15 times bigger battery capacity than a Nissan Leaf EV), can be treated as a distributed energy system (DES) which can serve to overcome the grid challenges. Most of the public transport remains parked idly at the bus depot for about 40% every 24 hours [81]. During this idle parking time, the bus batteries can be connected to the grid for the implementation of the V2G technology presented by [82] to resolve various issues in a smart grid environment.

The recent V2G technology studies emphasised the operation of the deregulated electricity market. The authors in [83] suggest that electric vehicles cannot provide a bulk amount of power due to their smaller battery capacity and the higher unit energy cost compared to centralised generation. However, PEBs having 15 times bigger battery capacity than EV can provide more power; thus the utilisation of the fleet of PEBs can play an important and vital role in the ancillary service market such as spinning reserve and regulation [84].

V2V Technology: V2V technology can readily be accomplished in the current grid for power reserve. The PEBs in the bus depot can be utilised for V2V energy transfer to reduce the power trading loss between PEBs in the depot and power grid. In public transportation, bus scheduling is very critical. Thus, the PEB batteries should be charged enough to perform the scheduled trip. In case of unavailability of power from the grid, the V2V technology can be used to recharge the PEBs before departure from the depot. In this case, some of the PEBs in the depot will act as an ESS. There should be a charge management controller to exchange information such as battery charging and discharging state and level. This information is further used to ensure the SOC level of discharging and charging PEBs remains at 10% to 90% respectively, to overcome the PEB batteries' life degradation [85].

RES and PEBs in Bus Depot Ecosystem: A fleet of PEBs along with DGs in a bus depot charging ecosystem may be considered as microgrid as shown in Figure 2.2. The intermittency in a solar PV system and wind energy can be overcome by charging the PEBs when at the bus depot or by using the ESS to store the power generated by the RES. In this case, PEBs act as an ESS system. In this way charging PEBs from renewable sources can mitigate GHG emissions.

2.5.2. Challenges

Total Investment Cost: one of the biggest challenges in establishing a PEBDC ecosystem infrastructure is the total investment costs. These costs include i) equipment used in the depot ii) installation cost e.g., permit cost for the integration of depot charging ecosystem with the grid (grid connection / existing connection to grid up-gradation cost) and civil work, iii) operation and maintenance costs. The charger's cost is expected to decrease as the adoption of the EV increases also, there is a huge variation in the charger infrastructure cost among different EV suppliers. However, the installation cost may greatly reduce i) if there are any pre-existing connections ii) there is a simultaneous installation of several chargers reducing the overall grounding and components costs. The cost varies depending on the charger's power levels for example the installation cost of the public charging station is much higher than the private places. In addition to the installation cost, there is a continuous operation and maintenance cost which is taken to be 10 % of the total cost [45].

2.6 PEB Charging Impact on Electric Grid

EV charge scheduling and its impact on the distribution grid have already been studied by various researchers [86-89]. On the other hand, very few studies investigated PEBs fleets' scheduling. Even fewer researchers focused on the large-scale PEB charge scheduling corresponding to the depot charging infrastructure. The authors in [90] have analysed the electric bus fleet charging concepts: opportunity, flash, and depot charging and investigated the charging impact on the electrical grid. The power quality problems for a fast-charging station have been studied by the authors in [91] using the practical data (electric bus fleet) from Gothenburg, Sweden. Authors in [92] have analysed the charging impact on the grid considering the substation reserves in Hamburg, Germany. These studies focused on the potential issues related to the charging impact on the electrical grid but have not suggested any solution in terms of charging schedule.

Considering the battery swapping-based charging technology, the authors proposed optimisation methods for charge scheduling of electric bus fleets in [52, 93], and optimisation method for the rapid charging station method is proposed for electric buses considering both the cost of charging and battery losses [94]. In terms of wireless charging technology, the authors optimise the charging sequence for electric buses in one of the fast-charging stations in Beijing, China [53]. However, these studies do not apply to the PEB depot charging ecosystem. For depot charging, a mathematical model for scheduling a small fleet of buses up to 7 has been proposed [95]. This model takes the variable electricity price into account to minimise the charging cost of each electric bus in the depot. However, the authors did not consider the charging impact on the electrical grid neither did they consider the ESS or renewable energy resources such as wind or solar.

However, this thesis firstly optimises the PV size and location in a distribution system for a depot charging ecosystem considering the system loss minimisation. Secondly, a double-sided auction mechanism algorithm for the energy trading among the agents is proposed. Finally, two charge scheduling algorithms for i) overnight depot charging (consisting of Solar PV integrated with ESS) and, ii) pantograph charging (grid only) have been proposed. Also, the charging impact of charging both the scheme on the LV feeder has been analysed.

2.7 **Summary**

This chapter highlights the literature review on i) the State-of-the-Art Microgrid, ii) EV technologies, iii) EV charging Methods iv) EV charging configuration, standards, ports, and connectors, v) PEBDC ecosystem opportunities and challenges, and vi) PEB charging impact on the electrical grid. The details are presented as follows:

i) **The State-of-the-Art Microgrid:** Firstly, a detailed overview and architecture of the State-of-the-Art Microgrid have been presented. Secondly, the configurations of the proposed PEBDC ecosystem integrated with Microgrid and possible energy trading scenarios have been presented.

ii) **Review of the EV Technologies:** Firstly, the EV technologies including the HEV, EV, and FCEV have been presented. Secondly, EV Charging Methods such as BSS, WPT, and CC. Finally, EV charging configuration, standards, ports, and connectors defined by SAE J1772 and IEC 62196 adopted by different countries such as USA, Japan, China, Europe, and New Zealand have been presented.

iii) **Opportunities and Challenges**: The PEBDC ecosystem opportunities i.e. V2G, V2V, energy reserve market, and challenges such as total investment cost for the development of the charging infrastructure have been presented. This is further considered in the next chapter.

iv) **PEB Charging Impact on Electrical Grid:** PEB charging impact on the electrical grid in terms of fleet scheduling has been presented.

Chapter 3 DG Sizing and Allocation for PEBDC

This chapter is based on the work from the following journal publication in which the author of this thesis is the main author ("Analytical Hybrid Particle Swarm Optimization Algorithm for Optimal Siting and Sizing of Distributed Generation in Smart Grid" Journal of Modern Power Systems and Clean Energy, 1221-1230, 2020).

As noted in the Literature Review, the penetration of Distributed Generators (DG), specifically Photovoltaic (PV) or Wind Generators (WG) is rapidly increasing in the distribution network over recent years to reduce the voltage drop and the power losses [84]. The optimal sizing and allocation of DG in a Plug-In Electric Bus (PEB)charging ecosystem is necessary to obtain maximum benefits.

Therefore, this chapter firstly introduces the PSO algorithm and its application in DG sizing and allocation. Then, the objective function considering the boundary and power balancing constraints is discussed. Following that the impact of increasing the PEBs on LV feeders (IEEE Test Systems and KEPCO distribution system) has been presented. Finally, the two depot charging solutions are compared i.e., traditional, and futuristic in terms of technical, planning, economic, and environmental aspects.

3.1 Introduction

The conventional electrical grid is radial in structure and interconnected for electricity delivery from generation to load. One of the biggest issues with the conventional electrical grid is that the generation units are typically placed far away from the consumers and hence power losses occur during the power transmission and distribution. To alleviate this loss, a variety of solutions can be considered. Firstly, the transmission and distribution lines being a superconductor. However, currently, the cost of superconductor technology is high. Secondly, install the main generation unit near the end-user. Due to social issues and ecological pollution, this is also not applicable. Thus, more recently, the notion of the distributed generation has emerged which not only reduces the line losses but also offers a green, environment-friendly, and economical source of energy.

Important parameters of the electrical grid such as energy/power loss, power quality, voltage profile, stability, and reliability can be improved using advanced communication technologies and optimal DG placement and sizing. A different heuristic approach such as a genetic algorithm [96, 97], and simulated annealing [98] has been used for the optimal DG allocation and sizing. High computation cost is the main drawback of these approaches; however, Particle Swarm Optimisation (PSO) provides a significantly better computation efficiency [99]. The PSO algorithm is used for the optimal allocation and sizing of the DG units in a distribution network [99-102] considering the electrical grid technical challenges such as line loading, voltage profile, megavolt amperes (MVA) taken by the grid, and active losses. The reactive power loss is another challenge in the distribution system so the PSO algorithm is used for the optimal allocation and sizing of DG to minimise the reactive power losses [103].

To place an optimal DG size at an optimal location in a distribution system load flow analysis needs to be done then PSO algorithm is utilised and the detail is explained in Section 3.2.1.

3.2 PSO based DG Sizing and Allocation Algorithm

3.2.1. Load Flow Analysis

The main goal of optimal allocation and sizing of DG in a distribution system in this study is to minimise the active power loss and to improve the voltage profile. The active power loss shown in equation (3.1) is the objective function, which can be mathematically expressed as [104]:

$$P_{ij}^{loss} = \sum_{i=1}^{N}\sum_{j=1}^{N}[A_{ij}(P_iP_j + Q_iQ_j) + B_{ij}(Q_iP_j - P_iQ_j)] \tag{3.1}$$

Where P_{ij}^{loss} is the Active power loss between the bus *i* and *j*, *N* is the total number of buses in the distribution feeder P_i,P_j are the active power injected at bus *i* and *j*, respectively; and Q_i,Q_j are the reactive power injected at bus *i* and *j*, respectively and A_{ij}, B_{ij} are the sensitivity factors.

$$A_{ij} = \frac{x_{ij}}{V_i.Vj}Cos(\theta_i - \theta_j); B_{ij} = \frac{x_{ij}}{V_i.Vj}Sin(\theta_i - \theta_j); v_{ij} = 1,2,3.\dots.n \tag{3.2}$$

$$P_j = P_{DG_j} - P_{load_j}; Q_j = Q_{DG_j} - Q_{load_j} \tag{3.3}$$

P_{load_j} and Q_{load_j} are the active and reactive load, P_{DG_j} and Q_{DG_j} are the active and reactive power injected by DG_j at j bus, respectively. A single line diagram with a distributed generator in the distribution network having two adjacent nodes is shown in Figure 3.1.

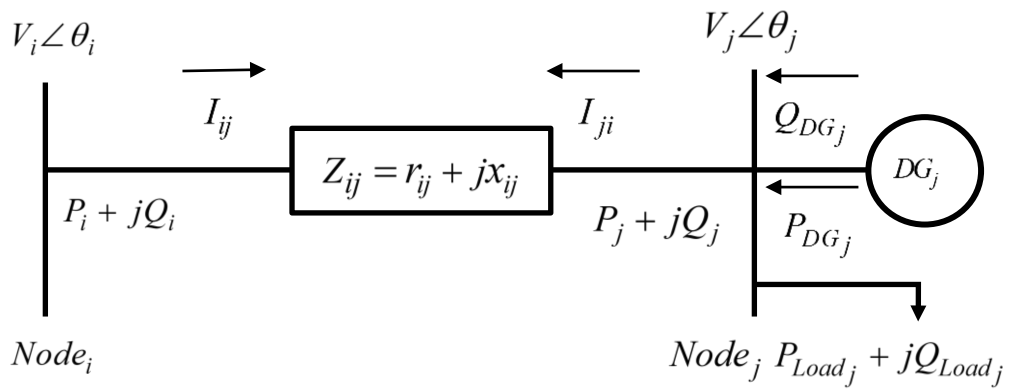

Figure 3. 1 Single line diagram of two adjacent nodes with DG in the distribution network.

3.2.2. Standard PSO Algorithm

PSO, a non-linear algorithm, was discovered by James Kennedy and Russell Eberhart in 1995 by observing the behavior of flying birds and fish flocking [105, 106]. The particles flying in the group have a certain velocity and position, thus, the authors proposed equations for both velocity and position. The current velocity of any particle in a group can be computed by adding the previous velocity and the distance between the personal flying experience called Personal best (P_{best}) and the flying experience of other particles in the group called global best (G^k_{best}). Every particle in the group changes their position according to P_{best} and G^k_{best}. The current velocity V_i^{k+1} can be calculated using equation (3.4)

$$V_i^{k+1} = V_i^k + C_1 r_1 (P^k_{best} - x_i^k) + C_2 r_2 (G^k_{best} - x_i^k) \quad (3.4)$$

Where x_i^k , V_i^k are the *i* particle's current position and current velocity at *k* iteration respectively, r_1,r_2 are the random number between [0,1], C_1,C_2 are the cognitive and social factor between [0,1]; and P^k_{best}, G^k_{best} are the personal and global best among all the particles in the group at *k* iteration, respectively. To compute the current position x_i^{k+1}, the current velocity is added to the previous position in equation (3.5)

$$x_i^{k+1} = x_i^k + V_i^{k+1} \tag{3.5}$$

The velocity of a particle in given search space is shown in Figure 3.2.

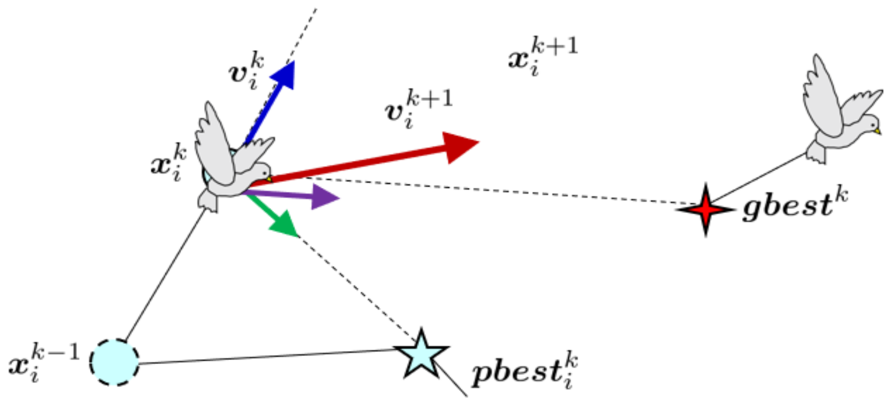

Figure 3. 2 Particles velocity update in a given search space [107].

The issues with the PSO algorithm are i) the local trapping and ii) it is strongly attracted towards the global best. The particles will tend towards its personal best which causes excessive wandering if C_1 is much higher thanC_2. On the other hand, if the C_2 is much higher than C_1, this causes the particle to be strongly attracted towards the global best which is not suitable because the particle moves away from the optimal value. Thus, to overcome this issue authors in [105, 106] set the acceleration coefficient value $C_1 = C_2 = 2$. The particles traveling in a group cooperate by exchanging information in the places they have visited. This cooperation between traveling particles should obey the following three rules as shown in Figure 3.3.

i) Avoid collision with neighboring birds.

ii) Match the velocity of neighboring birds.

iii) Stay near neighboring birds.

The triangles indicate the particles in the search space, the red and gray triangle shows the specific and neighboring particles, respectively.

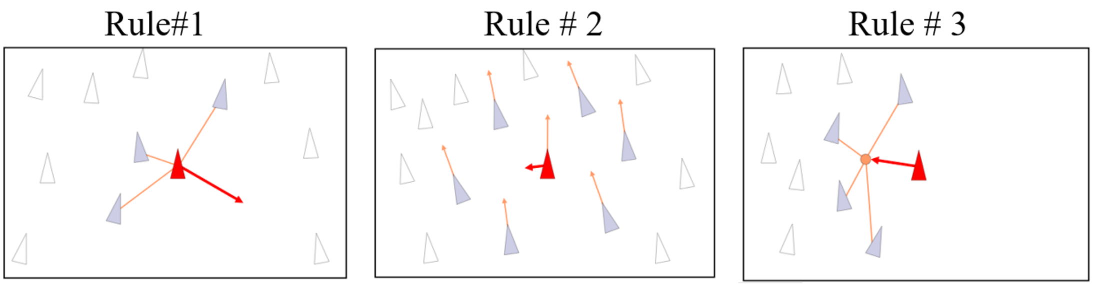

Figure 3. 3 Flying bird's cooperation rules.

3.2.3. PSO Algorithm Application in DG Sizing and Allocation

The PSO flow chart for the optimal DG allocation and sizing is shown in Figure 3.4.and the steps involved are as follows:

Step 1) System Input Data: In this step, i) bus data (e.g., bus number, bus types, bus angle, voltage magnitude, active and reactive load, active and reactive generation, ii) line data (e.g., nodes connection, resistance, reactance, ground admittance) and, iii) a total number of iterations are given to the algorithm.

Step 2) Load Flow Analysis: The exact loss formula is used to calculate the base case power loss and the load flow analysis is performed to calculate the current and voltage.

Step 3) Position and Sizing of DG: PSO is used to calculate the position and sizing of DG in a distribution network.

Step 4) Compute the total Active Power Loss: After placing the DG, the total power loss is computed using equation (3.1). The voltage limit should be in the allowable range throughout the nodes in the distribution network.

Step 5) Find the P_{best} and G_{best}: Power loss is calculated for each DG and is compared with the individual best. If this value is lower than the P_{best} then set this value a current P_{best} and record the DG position. The smallest active power loss among all the particles (DGs) in the simulation is the G_{best}

Steps 6) Position and Velocity: The velocity and position are updated using equation (3.4) and (3.5)

Step 7) Termination Criteria: The below conditions need to be satisfied for the loop termination, if not satisfied then add the iteration index $k=k+1$ and calculate the power loss using step 4. Loop termination conditions are as below:

i) No improvement

ii) If an acceptable solution is found

iii) Reached the maximum iterations (set for the loop termination)

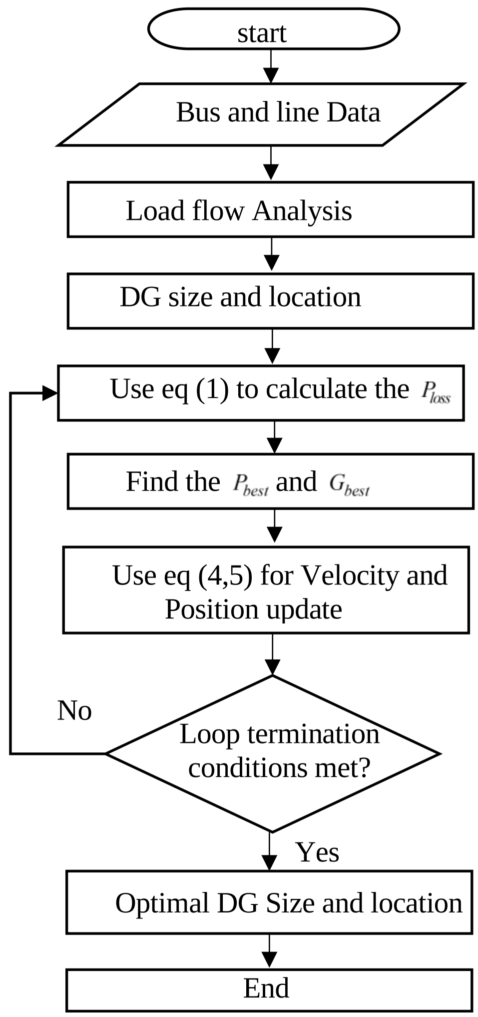

Figure 3. 4 PSO Flowchart for DG Placement and Sizing.

3.3 **Problem formulation**

3.3.1. Objective Function

The purpose of the objective function is to optimise the size and location of the DG unit to minimise i) DG deployment cost, ii) Violation cost and iii) Active power loss cost as shown in equation (3.6). The first term of the objective function shows the d-type DG deployment cost ($C_d^{DG}.T_d^{DG}$). There are different energy sources including non-renewable energy sources (diesel generator, gas turbines, and steam engine) and renewable energy sources (wind turbine, photovoltaic arrays, and fuel cells) which can be used as DG sources. Their deployment and maintenance costs are different. Thus T_d^{DG} is used to define the type of DG unit. The second term C_i^{viol} indicates the penalty cost for voltage limit violation at each node *i*. $V_i = 1$ if there is any voltage limit violation at any node *i* thus a penalty cost will be added. Otherwise $V_i = 0$ and no penalty will be added in the objective function. The third terms contain the active power loss in the distribution network.

$$Min\ F1\,(C^{DG},\ C^{Viol},\ C^{Loss}) = \sum_{d=1}^{D} C_d^{DG}\,.\,T_d^{DG} + \sum_{i=1}^{N} C_i^{viol}\,.\,v_i + \sum_{i=1}^{N}\sum_{j=1}^{N} C_{ij}^{loss}\,.\ p_{ij}^{loss} \tag{3.6}$$

The voltage at each bus should remain within certain limits, equation (3.7) defines the voltage violation limit.

$$v_i = \begin{cases} 1 & \boldsymbol{V^{min} \le V_i \le V^{max}} \\ 0 & \text{otherwise } \forall \boldsymbol{i = 1, 2, 3, \ldots. N} \end{cases} \tag{3.7}$$

The type of DG deployed at any bus *i* in the distribution network is shown in equation (3.8)

$$T_d^{DG} = \begin{cases} 1 & \text{if } d^{th} \text{ type DG is placed} \\ 0 & \text{otherwise } \forall d = 1,2,3, \ldots. D \end{cases} \tag{3.8}$$

3.3.2. Boundary Conditions

The maximum limit of power generated by DG d-type units is described in equation (3.9). The parameters P_d^{DG}, P_{DG}^{min} and P_{DG}^{max} represent the power generated by the d-type DG unit and its maximum and minimum power limit, respectively.

$$P_{DG}^{\min} \le P_d^{DG} \le P_{DG}^{\max} \qquad \forall d=1.2.3....D \tag{3.9}$$

The angle deviation limit DG d-type units are described in equation (3.10). The δ_i, $\delta_i{}^{max}$ and$\delta_i{}^{min}$ represent the angle at node *i* and it's the maximum and minimum allowable angle at any node *i*, respectively.

$$\delta^{\min} \le \delta_i \le \delta^{\max} \qquad \forall i=1.2.3....N \tag{3.10}$$

Each line has a current flow limit, the equation (3.11) represents the rated current. I_i and $I_i{}^{rated}$ represent the current at node *i* and its rated current, respectively.

$$I_i \le I_i^{rated} \qquad \forall i=1.2.3....N \tag{3.11}$$

3.3.3. Power Balancing

The sum of power generated by the DG unit and the amount of power injected by the substation should be equal to the total network load demand and the network losses which is represented in equation (3.12)

$$P^{S/S} + \sum_{d=1}^{D} P_d^{DG} = \sum_{i=1}^{N} P_i^{Load} + \sum_{i=1}^{N} \sum_{j=1}^{N} P_{ij}^{loss} \tag{3.12}$$

where, $P^{s/s}$, P_d^{DG} represent the power generated by the substation and d-type DG unit, respectively. The power demanded by the load and the power loss between node *i* and *j* is $P_i^{load}$and $P_{i,j}^{loss}$respectively.

3.4 Simulation and Results

The PSO algorithm is used to find the optimal location and size of the DG unit to overcome the loading impact due to the charging of PEBs in the distribution network. As the penetration of PEBs increases, so the loading on the grid will increase and therefore the PSO algorithm is utilised to find the optimal size and location for different PEBs penetration levels. Two IEEE test systems (i.e., IEEE-33 bus and IEEE-69 bus system) and one real distribution system i.e., KEPCO (Korea Electric Power Cooperation) have been tested. The grid voltage limit violation may occur as the PEBs penetration increases at different nodes for the IEEE-33 bus, IEEE-69 bus system, and KEPCO system. In all six scenarios, the bus voltages should remain within an acceptable bound i.e., 1 ± 0.05 p. u which can be seen in Figure 3.7, Figure 3.10, and Figure 3.13.

3.4.1. IEEE-33 Bus System

The IEEE-33 bus system is a radial distribution system with 33 buses, 32 branches with a total load of 2.3 MVAr and 3.715 MW, and the substation voltage is 12.66kV with a loading of 10 MVA [108] as shown in Figure 3.5.

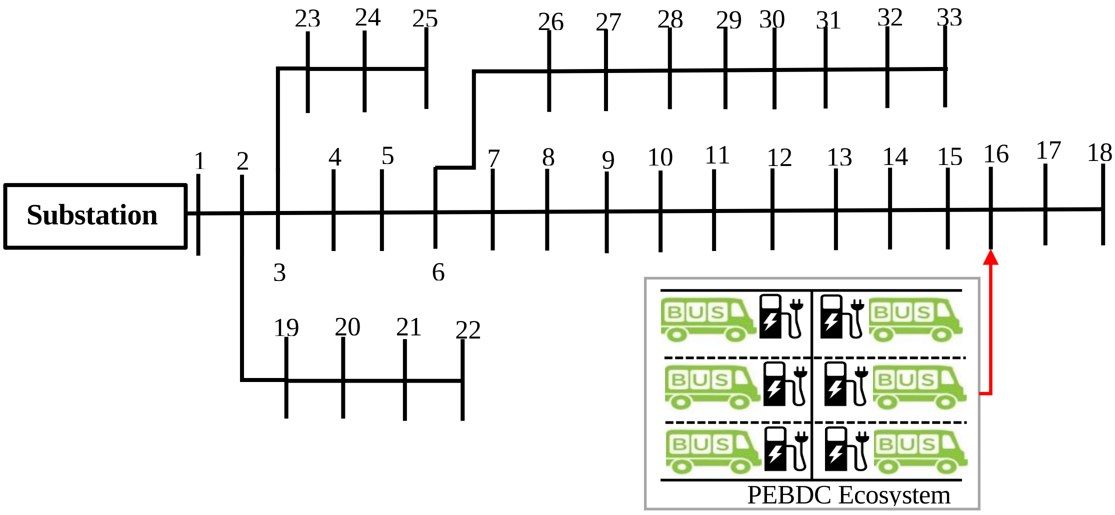

Figure 3. 5 IEEE 33 Bus System with PEBDC Ecosystem.

Impact of increasing PEB Penetration on LV Feeder Voltage- Without DG: As the number of PEBs increases, the extra load due to charging these PEBs in the PEBDC ecosystem connected with the LV feeder causes overloading of the distribution transformer. To observe these impacts, PEBs penetration was increased from 0% to 100%. If the LV feeder loading increases more than a specific loading level, then grid voltage violation occurs. This can be seen in the case of no DG (see Figure 3.6). Increasing the PEB penetration higher than bus node number 16 causes more voltage violations. For example, In Scenario 6 with 100% PEB penetration, the bus voltage fell below 0.7 p. u. as it can be seen in Fgiure 3.6.

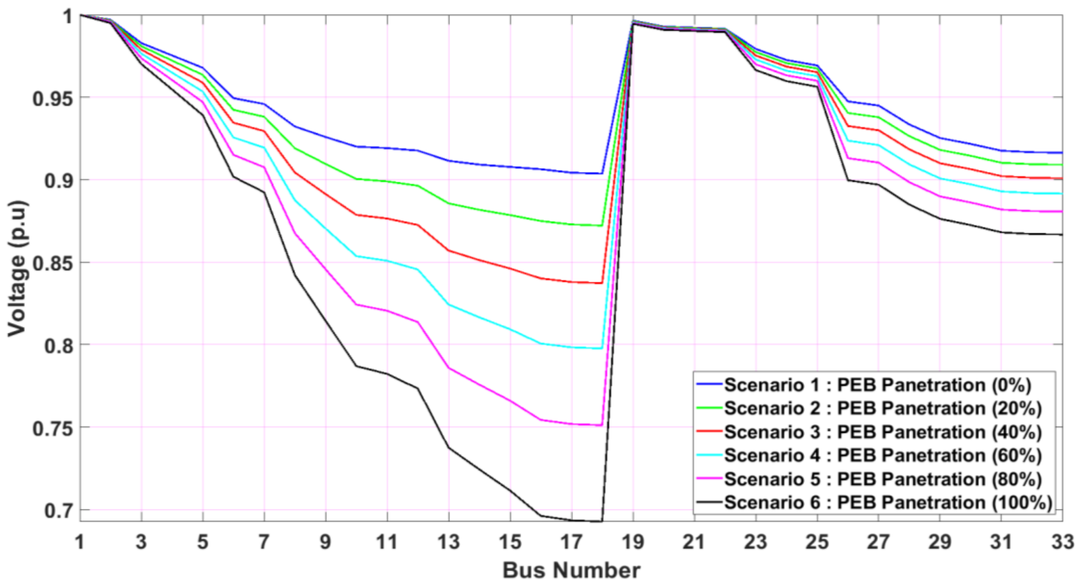

Figure 3. 6 IEEE 33 Bus System: Bus number Vs Voltage Profile- Without DG.

Impact of increasing PEB Penetration on LV Feeder Voltage- With DG: PSO algorithm is used for the optimal DG sizing and allocation to overcome the voltage violation and losses in the LV feeder. The voltage at each bus node should remain in a specific range as described in equation (3.7). The voltage profile at every bus after placing the optimal DG size at an optimal location has been shown in Figure 3.7. It is interesting to note that even with 100% PEB penetration, the bus voltage is within the specified limits.

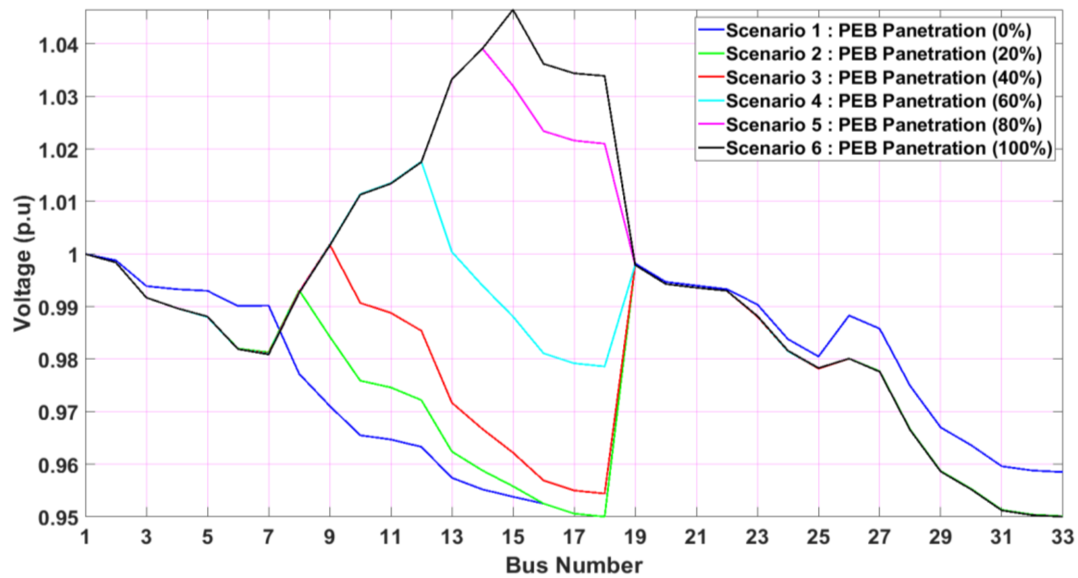

Figure 3. 7 IEEE 33 Bus System: Bus number Vs Voltage Profile- With DG.

The optimal DG size and location for 0% to 100% PEB penetration level with losses for the IEEE-33 bus system is shown in Table 3.1. It is interesting to notice that as the PEB penetration level increases the DG size is increased and its location is moving towards bus node number 16. This is due to the consideration of the PEB depot at node number 16.

Table 3. 1 IEEE-33 Bus System: DG size, Location, and losses for different PEB penetration level

Scenarios	PEB Penetration Level (%)	DG Size	Location	Losses
1	0	2.8875	7	0.1149
2	20	2.7390	8	0.1489
3	40	3.1939	9	0.1886
4	60	3.6503	12	0.2243
5	80	4.0910	14	0.2482
6	100	4.5130	15	0.2605

3.4.2. IEEE-69 Bus System

The IEEE-69 bus system is a radial system with 69 buses, 68 branches with a total load of 2694.60 MVAr, and 3802.19 MW and it has 12.66 kV substation voltage and a load of 100 MVA [109] as shown in Figure 3.8.

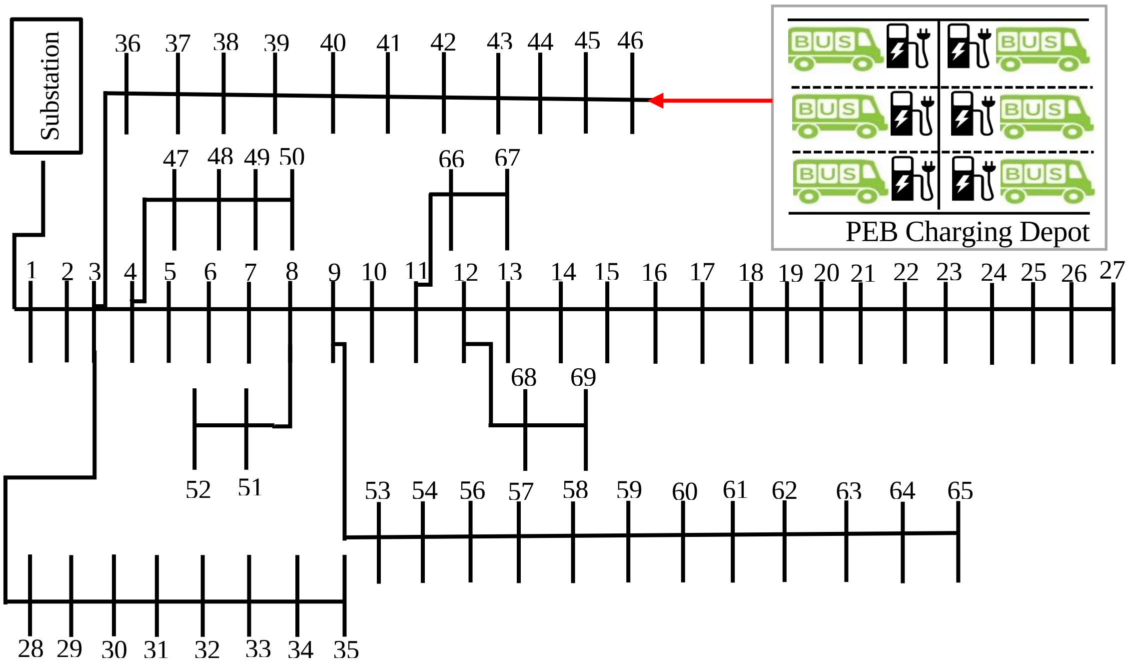

Figure 3. 8 IEEE 69 Bus System with PEBDC Ecosystem.

Impact of increasing PEB Penetration on LV Feeder Voltage- Without DG: To observe the charging impact of PEBs on LV feeder, the PEBs penetration level at bus node number 46 increased from 0% to 100% for the IEEE 69 bus system. Before placing the DG unit, grid voltage violation occurs as the PEBs penetration increases and the voltage violation occurs at different nodes. In all six scenarios, most of the bus voltages are not within an acceptable bound i.e., 1 ± 0.05 p. u which can be seen in Figure 3.9.

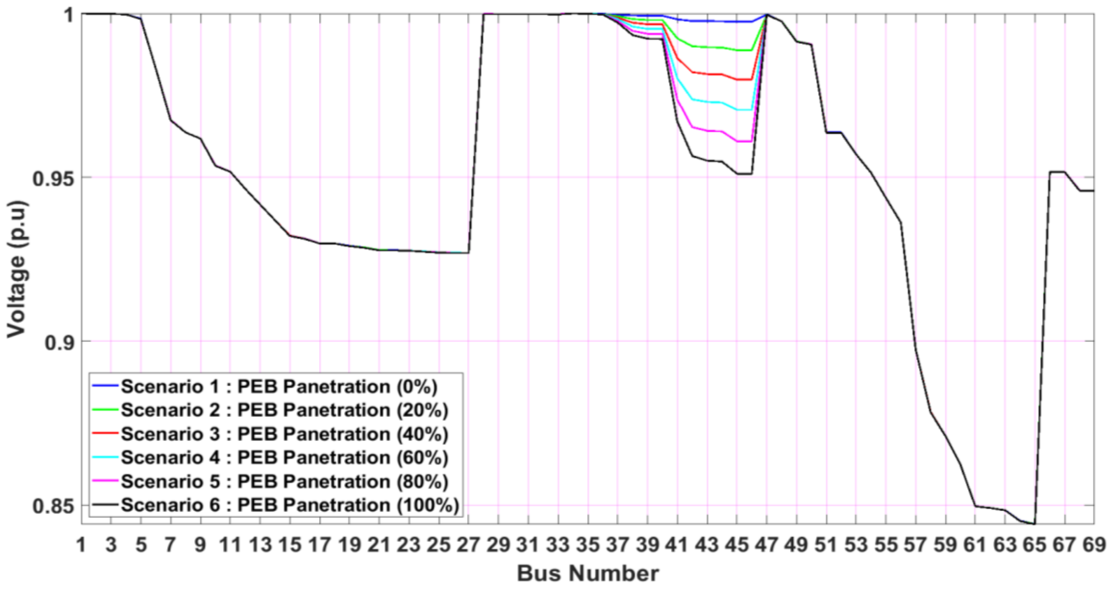

Figure 3. 9 IEEE 69 Bus System: Bus number Vs Voltage Profile- Without DG

Impact of increasing PEB Penetration on LV Feeder Voltage- With DG: The Optimal DG size and location for the IEEE-69 bus is achieved using the PSO algorithm for all six scenarios. It can be observed that even with the 100% PEB penetration all the buses are in the acceptable range which can be seen in Figure 3.10.

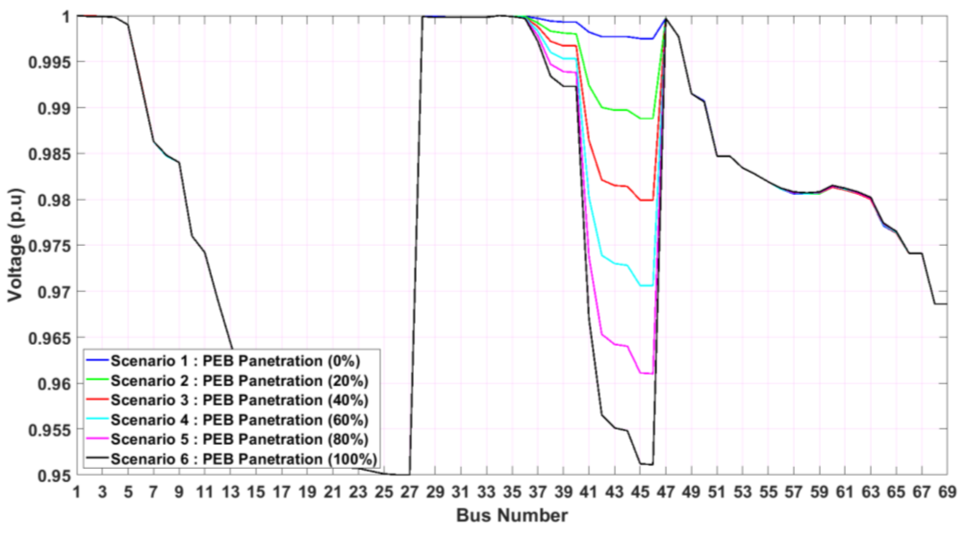

Figure 3. 10 IEEE 69 Bus System: Bus number Vs Voltage Profile- With DG.

The optimal size and location of the DG unit in the IEEE-69 bus distribution system for all six cases are shown in Table 3.2. It is interesting to notice that as the PEB penetration level increases at node 46 the DG size is increasing; however, its location is not changing. This is due to the higher load at bus number 61 as compared to other buses.

Table 3. 2 IEEE-69 Bus System: DG size, Location, and Losses for different PEB penetration level

Scenarios	**PEB Penetration Level (%)**	**DG Size**	**Location**	**Losses**
1	0	2.0827	61	0.1392
2	20	2.0834	61	0.1461
3	40	2.0841	61	0.1641
4	60	2.0849	61	0.1936
5	80	2.0867	61	0.2356
6	100	2.0878	61	0.2908

3.4.3. KEPCO Distribution System

KEPCO distribution system is also a radial system that has 4 feeders. The feeder number 1 has taken in this study which has 14 buses, 13 branches, and a total load of 6.0106 MW, 3.011 MVAr with 22.9 kV substation voltage, and 100 MVA loading [110] as shown in Figure 3.11.

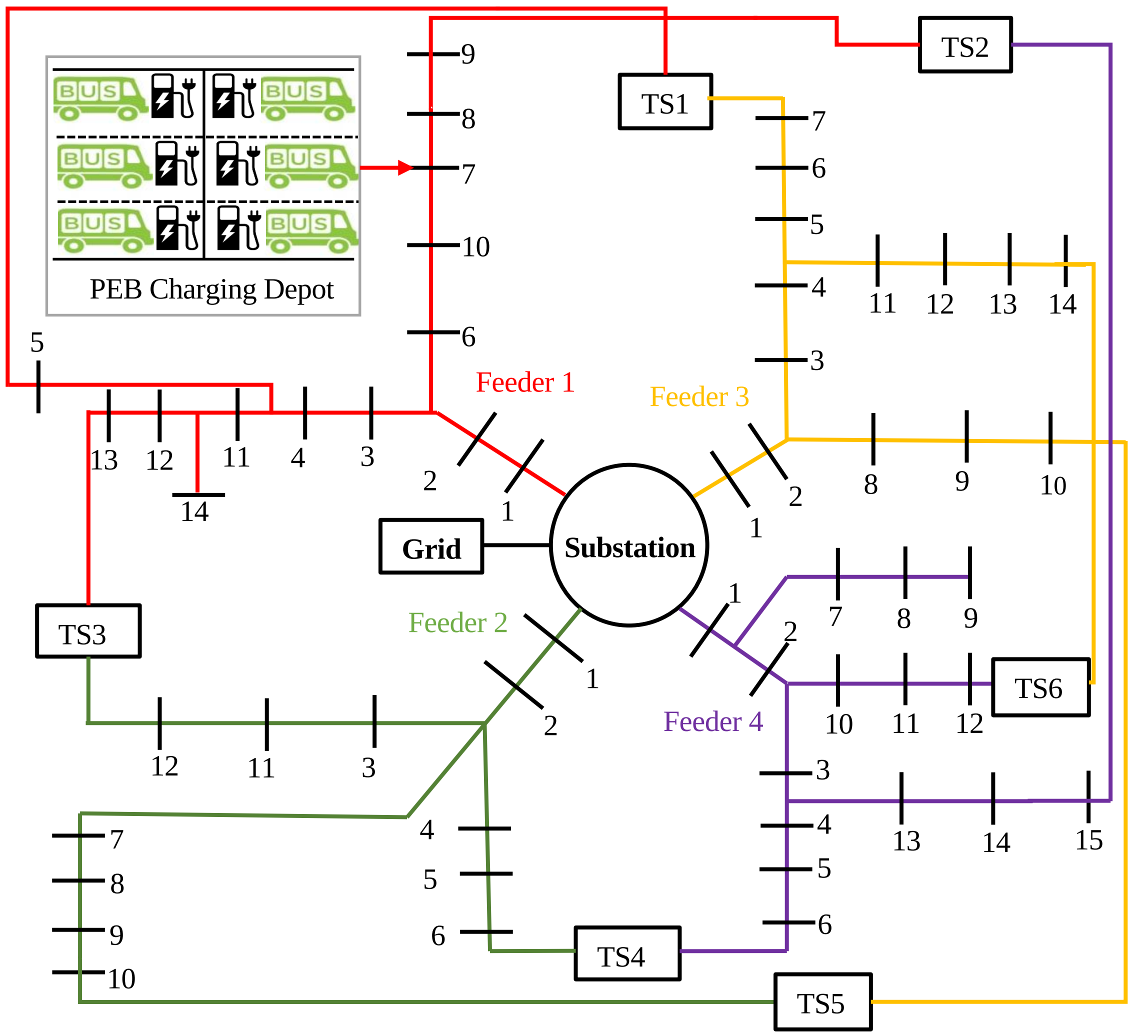

Figure 3. 11 KEPCO distribution System with PEBDC Ecosystem

Impact of increasing PEB Penetration on LV Feeder Voltage- Without DG: To make the study more interesting, an optimal DG sizing and allocation have been done for a practical distribution system i.e., KEPCO and voltage at each bus, and the system losses have been observed by increasing the PEBs penetration level from 0% to 100%. Before placing the DG unit, all the buses violate the voltage limits which can be seen in Figure 3.12.

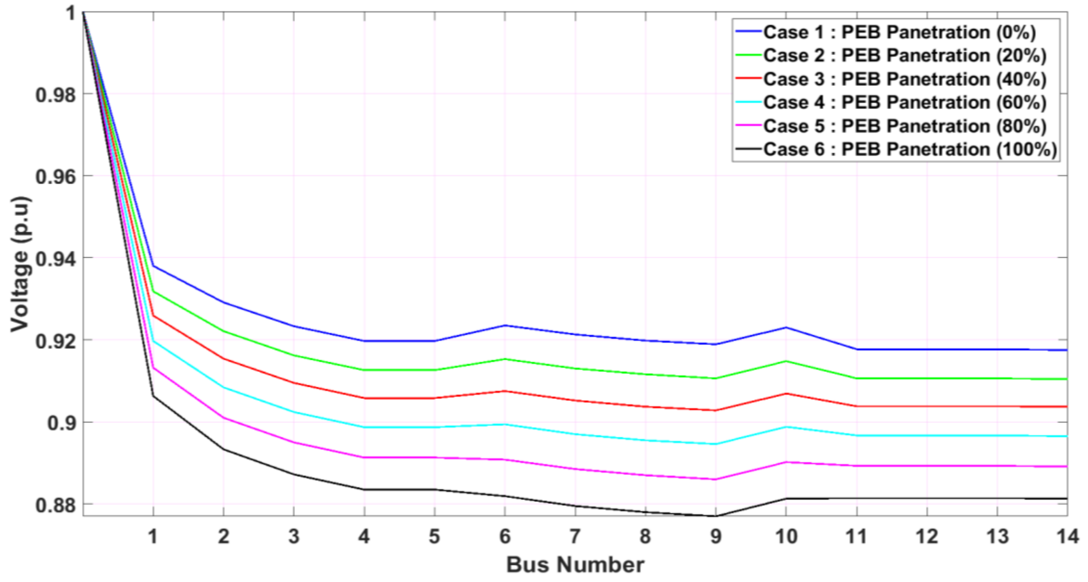

Figure 3. 12 KEPCO Distribution System: Bus number Vs Voltage Profile- Without DG.

Impact of increasing PEB Penetration on LV Feeder Voltage - With DG: To bring these violated bus voltages to an acceptable bound for the KEPCO distribution system, an optimal DG sizing and location has been done using the PSO algorithm for all six scenarios. It can be observed that in all six scenarios even with the 100% PEB penetration all the buses remain in the acceptable range. This can be seen in Figure 3.13.

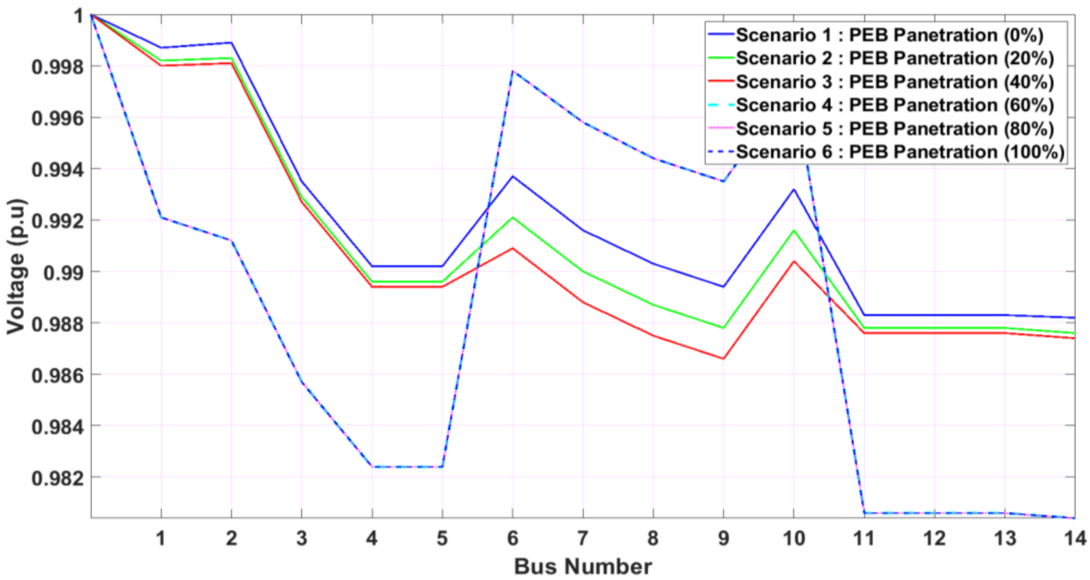

Figure 3. 13 KEPCO Distribution System: Bus number Vs Voltage Profile- With DG.

The optimal size and location of the DG unit for the KEPCO distribution system for all six scenarios are shown in Table 3.3. It is interesting to notice that, as the PEB penetration level increases at node 7 for scenarios 1-3, the DG size is increasing but the location is not changing;

rather it is fixed at bus number 3. However, in the case of scenarios 4-6, the location has changed from 3 to 7 and the DG size is also changed. This is because node number 3 has a much higher load compared to other buses, therefore the algorithm defines location 3 for scenarios 1-3. However, for scenarios 4-6, with more than 60% PEB penetration at node 7 causes the DG location to move to node number 7.

Table 3. 3 KEPCO Distribution System: DG size, Location, and Losses for different PEB penetration level

Scenarios	PEB Penetration Level (%)	DG Size	Location	Losses
1	0	5.8581	3	0.3190
2	20	6.2711	3	0.0364
3	40	6.5857	3	0.0418
4	60	6.6857	7	0.0462
5	80	6.7876	7	0.0462
6	100	7.1915	7	0.0462

3.5 **Depot Charging Solution for PEBs**

3.5.1. Vector's Distribution Network

The central North Island and the South Island supply electricity to Auckland with six 220 kV and two 110 kV circuits. All eight circuits are terminated at the Otahuhu grid exit point (GXP) with 110 kV and 220 kV busbars. Vector, the distribution company, is comprised of three components: Sub-transmission (22 kV, 33 kV, and 110 kV), distribution network (11 kV and 22 kV), low voltage network (400 V and 230 V) and it receives electricity from the national grid owned by Transpower. The general structure of the Vector distribution network is shown in Figure 3.14.

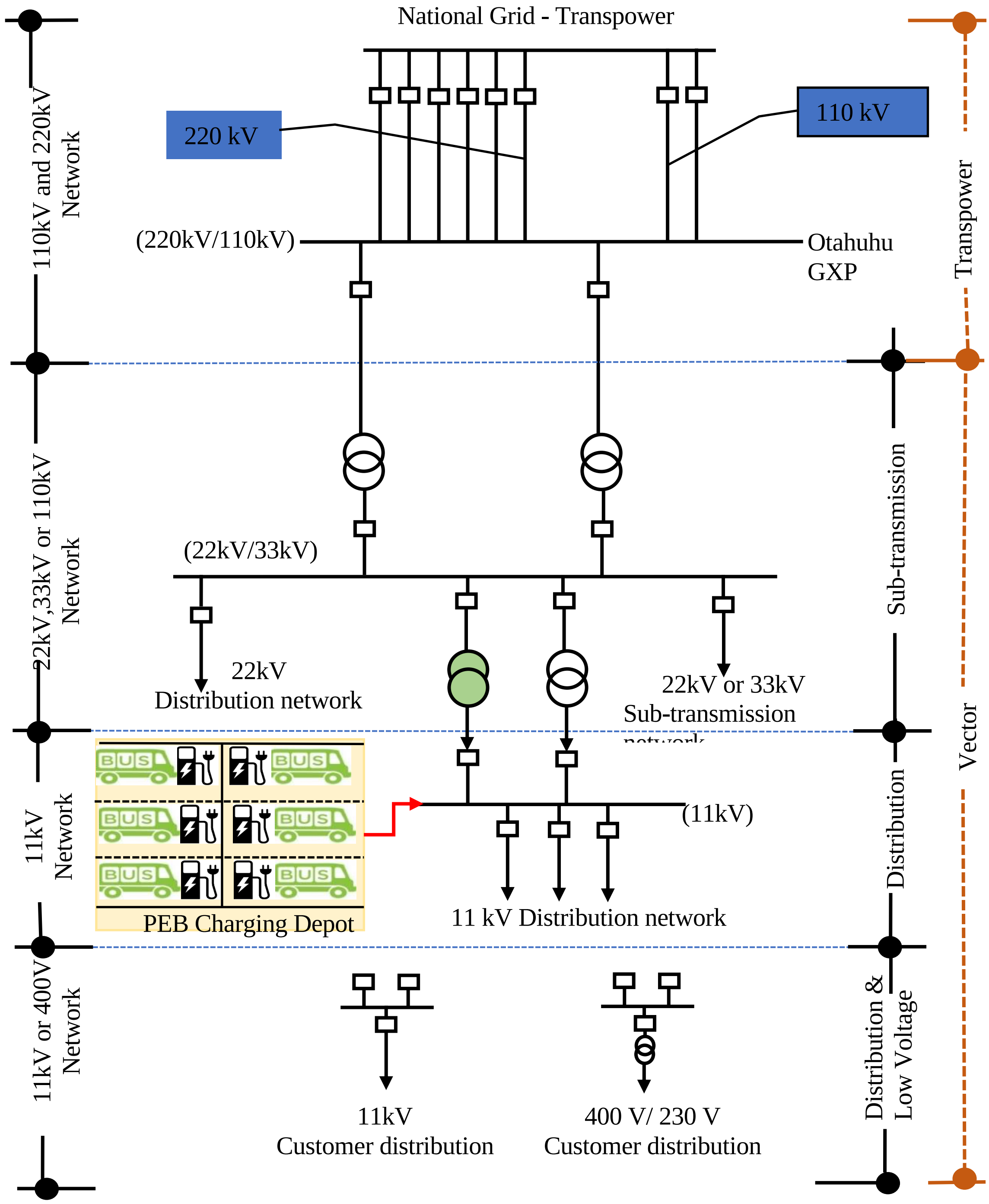

Figure 3. 14 Vector's Distribution Network Auckland.

The grid close to sub-transmission has a high power flow capability (fault level) but has less capacity further away. The PEB depot charging station can be connected to either the distribution network (11 kV) or the low voltage network (400V). Due to the thermal capacity of grid components and the voltage quality, there is a limit to the amount of power input or output at a point in a grid [111]. These factors need to be considered while designing a PEB charging depot. Based on the subscribed power, each customer that is connected to the grid pays the cost for a connection as well as transmission fees [112]. A PEB depot charging station connection cost to the grid is expensive due to the short and high-power peak that occurs only during charging the PEBs. Because of these load characteristics, the implementation of a charging station specifically PEBs (having large batteries) impacts the stability of the power distribution grid [25]. If the power taken by the PEB depot charging exceeds the grid capacity, then the grid owner must find another solution. This is described in the next subsection.

3.5.2. Depot Charging: Traditional vs Futuristic Solution

The solutions for an overpower obtianed from the grid due to charging PEBs in a bus depot are i) traditional reinforcement solution, ii) Futuristic solution (renewable energy resources integrated with ESS) [113]. A detailed comparison of these two solutions is given in Table 3.4.

Table 3. 4 Comparison of Traditional vs Futuristic Depot Charging Solution

Aspects	Issues	Traditional Solution	Futuristic Solution
Technical	Voltage dip/rise	Network reinforcement Generation tripping Capacitor banks Limits/bands for demand and generation	Coordination between the Solar PV generation and ESS storage
	Hosting Capacity	Network reinforcement	PV integrated with ESS and V2G
	Intermittent	NA	Resolved using the ESS
Planning	Modeling of Data	Operation condition (Worst cases)	Time-series models
	Network calculations	Deterministic	Probabilistic
	Network constraint violations	Completely avoided	Risk acceptance
	Objective Function	Single Objective Cost (Transformer)	Multi-objectives Carbon emission reduction Cost (PV and ESS)
Economic	Cost (NZ$)	Transformer (100 kVA) $ 15,525 [114]	PV (100 kW): $ 41,100 ESS (500 kWh): $ 130,000
	Life cycle (year)	45	PV 25 ESS 10
	Maintenance	Negligible	10%
Environmental		Emission	Emission Free
		Unsustainable	Sustainable

3.6 **Summary**

In this chapter, the PSO algorithm and its application for the DG sizing and allocation have been presented, the summary of the study is as follows:

i) **Load flow analysis** is the most essential and reasonable approach to analysing the voltage at each node, the branched power flow, and the losses in the system. Therefore, load flow analysis has been done before and after determining the optimal DG size and location using PSO and then is compared the system losses.

ii) **Optimal DG sizing and location** for two IEEE Test Systems (i.e., IEEE 33 and IEEE 69) and one practical distribution system (Korea Electric Power Cooperation) have been performed to minimise the i) DG deployment cost, ii) the violation cost and iii) the active power loss cost while considering all necessary constraints.

iii) **PEBs penetration** has been increased from 0% to 100% in the PEBDC ecosystem and then find the optimal DG size and location for the LV feeder to i) keep the voltage at each node in a specific limit, ii) find the optimal location and size, and iii) to minimise the system losses. This has been tested on the IEEE-33, IEEE-69 bus test system, and Korea Electric Power Cooperation distribution system.

iv) **Finally, the comparison between traditional and futuristic** depot charging solutions has been done considering i) technical, ii) planning iii) economic, and iv) environmental aspects. Having discussed the aspects of sizing and location of the PEBDC ecosystem, the management of the energy flow in the system is considered in the next chapter.

The PEB Depot Charging Ecosystem is connected with the distribution system thus we calculated the optimal DG size and location using PSO in Chapter 3. To perform the energy trading among the depot entities, an efficient Energy Management System (EMS) for the PEBDC ecosystem needs to be developed which is proposed in Chapter 4.

Chapter 4 Energy Management of PEBDC Ecosystem

This chapter is based on the work from the following journal publication in which the author of this thesis is the main author ("A Novel and Cost-efficient Energy Management for Plug-In Electric Bus Depot Charging Ecosystem" Electric Power System Research, 2021).

The integration of renewable Distributed Generations (DGs) has been a serious concern over the reliable and satisfactory operation of the distribution system due to the intermittent nature of DGs. One of the solutions being proposed is the utilisation of an Energy Storage System (ESS). However, without an appropriate energy management system, the integration of PV and ESS in a PEBDC ecosystem can have an adverse effect on the LV feeder.

Therefore, this chapter firstly presents an efficient Energy Management System (EMS) for the PEBDC ecosystem. Secondly, the EMS mathematical modeling consisting of PV, ESS, and chargers is developed. The different costs such as investment, operation, and maintenance and the constraints related to PV, ESS, charger, grid, and load are considered in the model are presented. Finally, in the results and discussion section, the energy trading among the parties involved in the PEBDC ecosystem for all four seasons i.e., Summer, Autumn, Winter, and Spring are presented.

4.1 Introduction

The fast-growing participation of electric vehicles more specifically PEBs and higher building energy consumption arising from increased urbanisation will place a heavy burden on the power system [115]. The integration of renewable energy such as PV system along with the ESS into the PEBDC ecosystem not only provides the solution to this problem but also provides advantages such as i) surplus energy exported back to the grid to generate revenue for the depot owner ii) PV panel has very low maintenance cost – it's just needed to clean the panel couple of the times a year [116], ii) provide 20-25 years warranty and have no wear and tear because there are no moving parts in the PV system [117].

However, the downsides are i) initial investment cost in the PV system is high, but the solar technology cost will go down due to the research and development in the PV technology [118, 119].

ii) Bigger area required, therefore, only suitable for a place such as an airport, cricket stadium, or soccer field with a lot of solar panel spaces available on the rooftops and, iii) intermittency is the major problem of the PV system.

However, an effective integration and energy management of ESS and PV in the depot charging ecosystem can lead to i) smoothing of the intermittency impact [120], ii) peak load reduction on the distribution grid [121], and iii) reduce the energy cost for the depot owner [122]. Considering the intermittent nature of solar PV, varying loads (PEB and building), and grid energy prices, an energy management system (EMS) is compulsory to monitor, control, and improves the economics of all the parties involved in the energy trading.

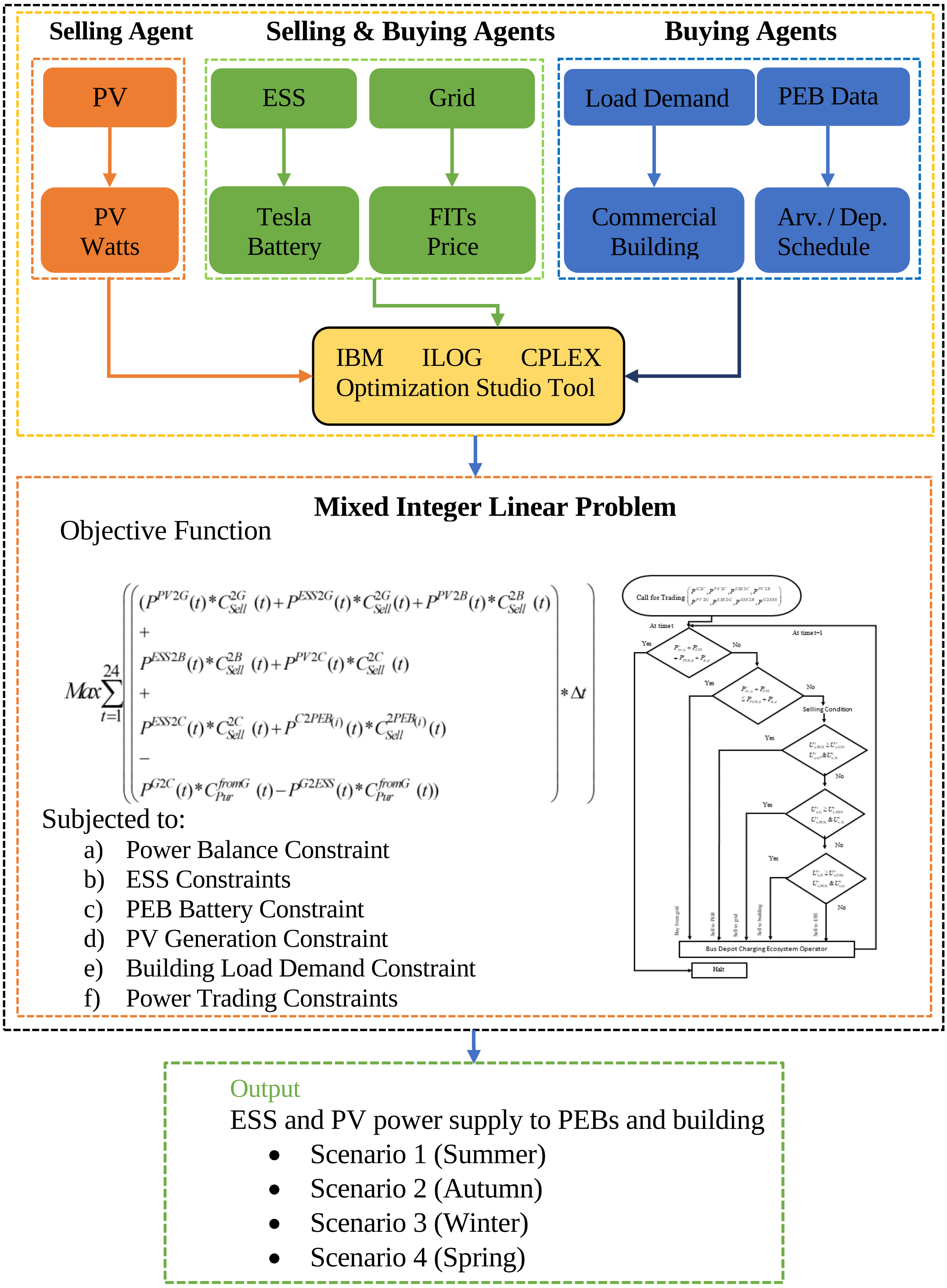

Figure 4. 1 A Framework of the Proposed Study.

Figure 4.1 shows the framework of the proposed study. Firstly, agent data such as selling (PV), selling and buying (ESS and grid), and buying (load and PEBs) are provided as inputs into the IBM ILOG CPLEX optimisation studio. Secondly, to perform the energy trading among the agents in the PEBDC ecosystem, an optimal EMS system is proposed which is subject to the optimal participation of the agents in the energy trading and guarantees the power flow between the selling and purchasing agents. The constraints such as total power generation and consumption, ESS charging and discharging, PEB battery safety, PV generation, building load demand, and power trading constraints are considered in the mathematical model. Lastly, the output in the form of ESS and PV power supply to PEBs and building are shown for all four seasons.

4.2 Proposed Energy Management System

The proposed EMS is based on the double side auction [123]. By definition, the double-sided auction is a process of selling and buying goods to multiple buying and selling agents. The potential buying and selling agents communicate their respective bids to the market institution and then the market institution chooses one price and clears the market [124]. In the PEBDC ecosystem scenario, ESS, PV, and grid act as a selling agent, while PEB, ESS, and grid act as a buying agent, and the aggregator act as a market institution. The buying and selling agents could participate in the energy market trading individually. However, the participation of individual agents at a system level is not feasible due to the following two reasons:

i) The power demand volume of individual buying agent may be lower than the required minimum volume to take part in the energy trading market, and

ii) The number of energy trading consumers/participants can be larger therefore the individual trade would be challenging to achieve.

Therefore, an aggregator is introduced to simplify the energy trading interaction between the selling and buying agents. A proposed EMS for the integration of PV, ESS, PEB, building, and grid in a PEBDC ecosystem is shown in Figure 4.2.

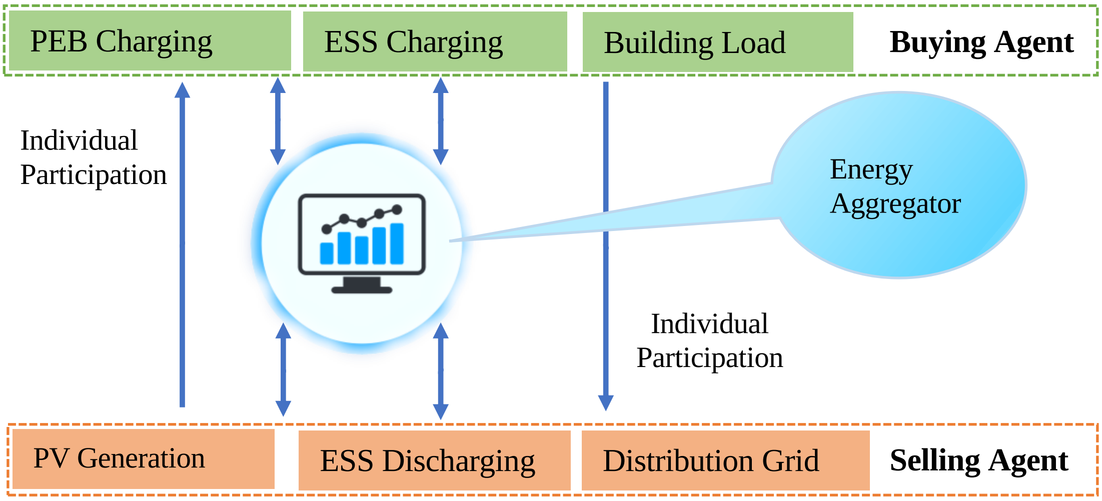

Figure 4. 2 Components of the Proposed Energy Management System.

The proposed EMS implemented in the following three management steps:

i) In the primary management step, the energy aggregator in the EMS gathers information and sends instructions to each selling and purchasing agent.

ii) The secondary management step deals with the balancing of total available power from PV, ESS (discharging), and grid (as a source), and total load demand from PEBs, building, grid (as a load), and ESS (charging).

iii) The tertiary management step will minimise the economic structure of the PEBDC ecosystem by performing the optimal energy trading among the buying and selling agents.

4.2.1. Model Description

The PEBDC ecosystem consists of Bus Depot Owner (BDO) (that owns the PV, ESS, and chargers), PEBs, and access to the building(s) and the grid as shown in Figure 4.3. The role of energy aggregator (third party agent) in the EMS is to gather information and send instructions to each selling agent such as PV, ESS (discharge), grid and buying agents PEB, building, ESS (charging), and to the grid which is connected with a local micro source controller using a bidirectional communication system. The micro source controller coupled with the solar PV system will allow the flow of energy (surplus or deficit) to the AC bus or the grid through the distribution panel. The distribution panel will step up the voltage when the energy flows from PV and ESS to the grid and step down the voltage when the energy flows from the grid to the AC bus. The BDO will perform the energy trading among the agents in the PEBDC ecosystem while considering the

Feed-in Tariffs (FITs) pricing scheme, PEB arrival/ departure schedule, building load, available energy in the ESS, and PV generation.

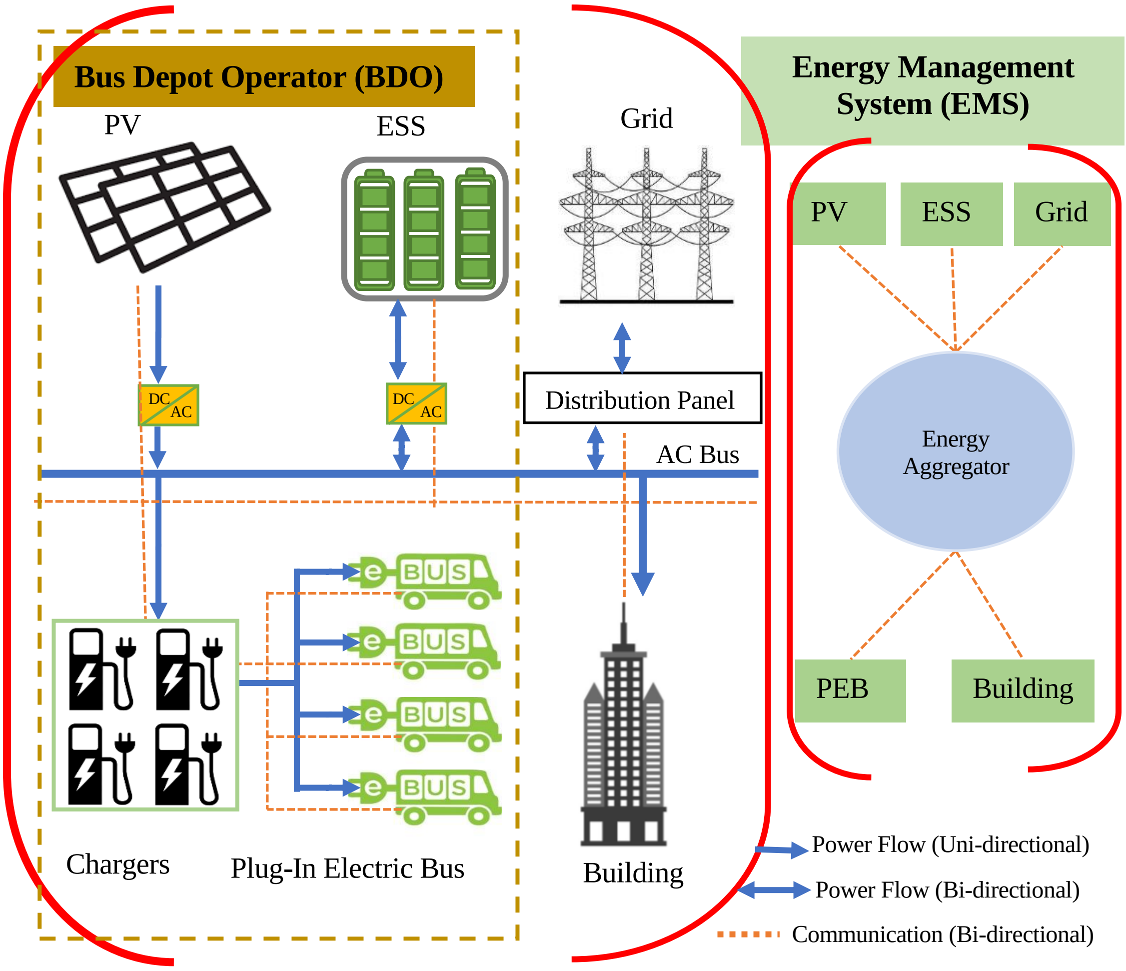

Figure 4. 3 A Comprehensive Energy Management System for PEBDC Ecosystem.

Figure 4.4 shows the flow chart of the proposed model which works on the double-sided auction-based algorithm. This algorithm provides a trading platform for the selling and buying agents which aim to search for the highest bidding agent from all the purchasing agents (PEB, building, ESS, and grid) in the bus depot and then performs the energy trading while buying the power from the grid during the low tariff or using the PV generation. The surplus power in ESS or PV production is feedback to the grid or building to fulfill the power demanded by the loads (building and grid).

In the flow chart firstly, the call for energy trading at any time interval t will check the balance of total available power between the selling agents (PV, and ESS (discharging)) and purchasing agents (PEB, building, and ESS (charging)). Then, in the case of surplus or deficit power, the EMS will take part in energy trading. If the sum of PV power production and available power in the ESS is less than the demanded load (PEB and building) then the aggregator will purchase the power from the grid to fulfill the demanded power else the power is sold to the purchasing agent depending on the best bids offered by the agents. After the balanced condition is achieved, the EMS checks at t+1 and repeats for every 10-minute intervals.

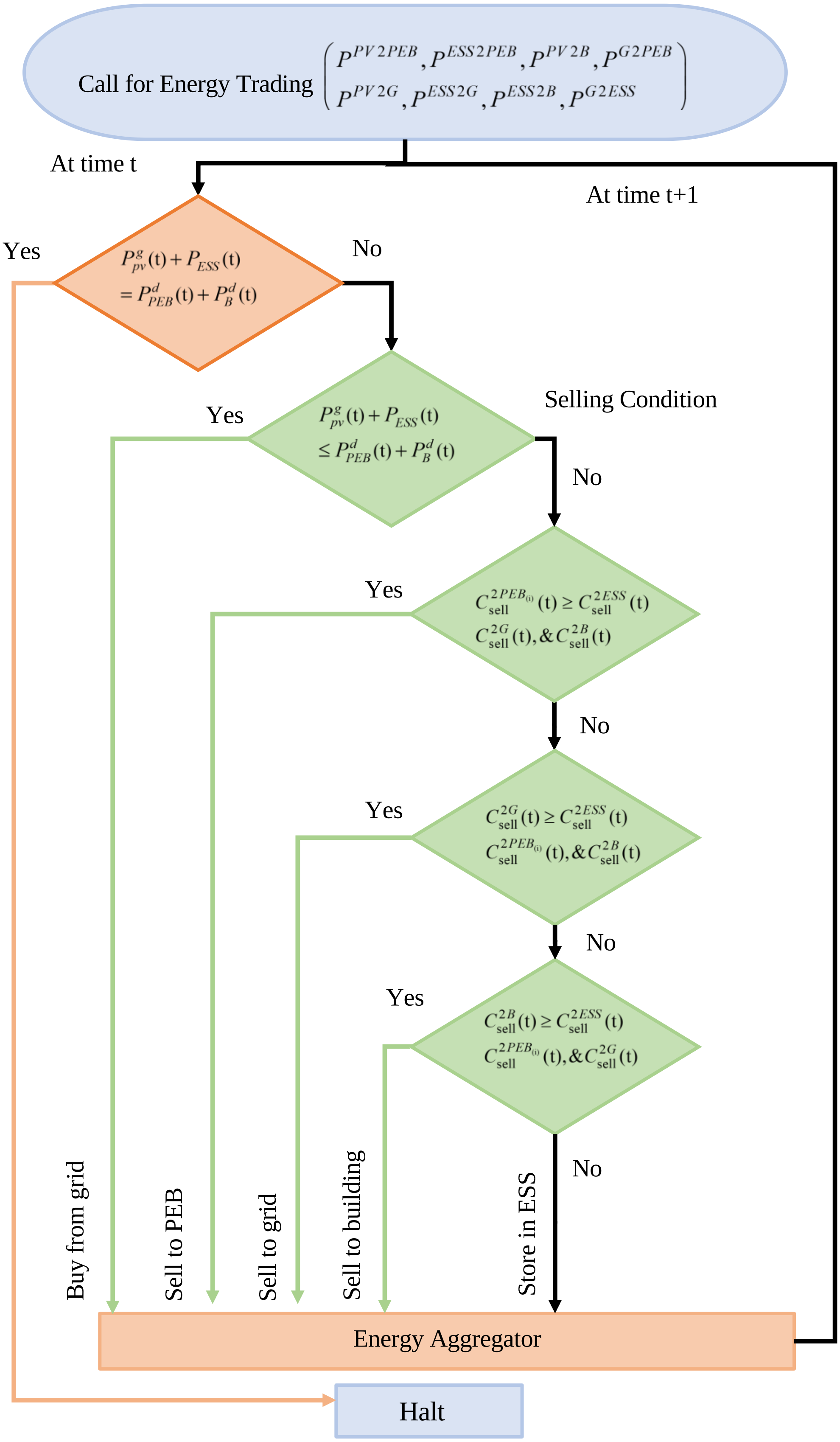

Figure 4. 4 Flow Chart of the Proposed Energy Management Model.

4.2.2. Assumptions

i) The PEBDC ecosystem is located at the Auckland airport where a 100 kW PV system is integrated with 500kWh ESS and 12 chargers are available.

ii) Every charger has two charging guns and thus 12 chargers (for peak, off-peak, and normal time) are required to charge 44 PEBs (at different times) and this is the maximum charging capacity of the BDO.

iii) To maximise the daily BDO profit, ESS buys and stores power from the grid when its price is low. At other times, the power stored in ESS and that generated by the PV system may be exported back to the grid or sold to a building at 2/3 or 1/3 of the purchase cost from the grid,[125] respectively, shown in Figure.4.5.

iv) The solar profile irradiation of the city of Auckland[126], charger price from Idaho National Laboratory [127], and FITs prices from a distribution company Electra [128] are used as real-world data in the simulations.

v) PEB owner is agreed to purchase the power from the BDO at a higher price than the actual price on the grid for the time intervals (1:00-7:00) am.

4.3 Mathematical Model

The purpose of the aggregator in the PEBDC Ecosystem is to purchase electric power from the main grid and/or use the generated power from the PV system and/or available power in the ESS to fulfill the power demanded by the purchasing agent such as a fleet of PEBs and/or a building. The aggregator generates profit by purchasing the electric power from the grid and storing it in the ESS while the grid price is low and sells it back to the grid when the grid offers a higher price.

In this study, a MILP optimisation model has been formulated to maximize the PEBDC Ecosystem profit by performing energy trading among the selling and purchasing agents. The total system costs (capital investment, operation, and maintenance) of PV, ESS, and PEB chargers per day [23] shown in Table 4.2 are also considered during the simulation.

Table 4.1 PEBDC Ecosystem Components Costs (NZ$).

System Components	PV	ESS	Charger
System Size	100 kW	500kWh	50 kW
Price per W/Wh	0.411	0.260	N/A
Estimated life span (year)	25	10	25
Total System Cost	41,100	130,000	45,000
Recovery cost/day	3.67	4.986	2.99

4.3.1. Cost Model

The total cost of the PEBDC Ecosystem consists of two parts: capital investment cost C_I and operation & maintenance cost $C_{O\&M}$ for PV, ESS, and chargers as described in equation (4.1).

$$C_{Total} = C_I + C_{O\&M} \tag{4.1}$$

As a general rule, $C_{O\&M}$ is assumed to be 10% of the total investment cost [23]. The present worth factor (PWF) [129] is used to transform the total cost into an annualised total present cost shown in equation (4.2). Where annual real interest rate (r = 6%) = nominal interest rate – inflation rate [130] and N is the lifetime of PV, ESS, and charger.

$$PWF_{r,N} = \frac{(1+r)^N - 1}{r(1+r)^N} \tag{4.2}$$

4.3.2. Objective Function

The objective function is formulated as a MILP problem for the daily BDO profit maximisation shown in equation (4.3). The salvage value is the estimated resale value of an asset at the end of its useful life which is calculated using the depreciation rate of 40% for ESS and charger and 16% for the PV (New Zealand power generation and electrical reticulation systems assets) [130]. The total investment cost, salvage value, and PWF of PV, ESS, and charger are different, therefore the total daily present cost (recovery) for each one is calculated separately.

$$\frac{profit^{Max}}{day} = \frac{Re\,v^{Max}}{day} - (\frac{(C^{PV}_{total} - S_{PV}) * PWF_{PV}}{365} + \frac{(C^{ESS}_{total} - S_{ESS}) * PWF_{ESS}}{365} + \frac{(C^{C}_{total} - S_{C}) * PWF_{C}}{365}) \tag{4.3}$$

Where the parameters C^{PV}_{total}, C^{ESS}_{total}, C^{C}_{total}, S_{PV}, S_{ESS}, S_C, PWF_{PV}, PWF_{ESS} and PWF_C are the total investment cost, salvage value and present worth factors of the PV, ESS, and charger, respectively. The first term of equation (4.3) shows the maximised revenue (Rev) generated by BDO per day, the second, third, and fourth terms show the total daily present cost of PV, ESS, and charger, respectively.

The energy trading is performed between the grid, PEB, and the building for 24 hours. The revenue per day generated by BDO in time slot *t* is calculated as described in equation (4.4) and it depends on the selling and purchasing energy cost between PV2G, PV2B, ESS2G, ESS2B, C2PEB, G2C, and G2ESS. Δt is the resolution time (10 minutes).

$$\frac{Re\,v^{Max}}{day} = Max \sum_{t=1}^{24} \begin{cases} ((P^{PV2G}(t) * C^{2G}_{Sell}(t) + P^{ESS2G}(t) * C^{2G}_{Sell}(t) + P^{PV2B}(t) * C^{2B}_{Sell}(t) \\ + \\ P^{ESS2B}(t) * C^{2B}_{Sell}(t) + P^{PV2C}(t) * C^{2C}_{Sell}(t) \\ + \\ P^{ESS2C}(t) * C^{2C}_{Sell}(t) + P^{C2PEB(i)}(t) * C^{2PEB(i)}_{Sell}(t) \\ - \\ P^{G2C}(t) * C^{from\,G}_{Pur}(t) - P^{G2ESS}(t) * C^{from\,G}_{Pur}(t)) * \Delta t \end{cases} \tag{4.4}$$

4.3.3. Design Constraints

Power Balance Constraints: The stable PEBDC Ecosystem indicates that the total power generation and the power consumption should be equivalent at any time interval *t*. The power supplied by the source (ESS, PV, and grid) and demanded by the load (PEB, building, and grid) are represented in equation (4.5)

$$P^{ESS}_s(t) + P^{PV}_s(t) + P^{G}_s(t) = P^{PEB}_d(t) + P^{B}_d(t) + P^{G}_d(t) \tag{4.5}$$

ESS Constraints: The maximum and minimum SOC limit is used to preserve the batteries' lifespan [129] which is defined in equation (4.6). Equations (4.7-4.9) represent the maximum amount of power that the ESS can provide to the building, charger, and grid, respectively [131, 132].

equation (4.10) represents the maximum power that the ESS can take from the grid. As the ESS cannot charge and discharge at the same time, equation (4.11) represents the charging and discharging binary variables. Equations (12) and (13) define the ESS's charging and discharging limit, respectively.

$$SOC_{\min}^{ESS}(t) \le SOC^{ESS}(t) \le SOC_{\max}^{ESS}(t) \tag{4.6}$$

$$P^{ESS2B}(t) \le P_{\max}^{ESS}(t) \tag{4.7}$$

$$P^{ESS2C}(t) \le P_{\max}^{ESS}(t) \tag{4.8}$$

$$P^{ESS2G}(t) \le P_{\max}^{ESS}(t) \tag{4.9}$$

$$P^{G2ESS}(t) \le P_{\max}^{ESS}(t) \tag{4.10}$$

$$X(t) + Y(t) \le 1 \qquad X(t), Y(t) \in [0,1] \tag{4.11}$$

$$\left(P^{PV2ESS}(t) + P^{G2ESS}(t)\right) * \eta_{char} X(t) \le \left(P_{\max}^{ESS}(t) - P_{\min}^{ESS}(t)\right) * Y(t) \tag{4.12}$$

$$\left(P^{ESS2B}(t) + P^{ESS2G}(t) + P^{ESS2C}(t)\right) / \eta_{dis} \le \left(P_{\max}^{ESS}(t) - P_{\min}^{ESS}(t)\right) * X(t) \tag{4.13}$$

PEB Constraints: The energy safety level, charging limit, SOC update of $PEB_{(i)}$ at any time interval t is defined in equations (14-16) respectively.

$$SOC_{\min}^{PEB(i)}(t) \le SOC^{PEB(i)}(t) \le SOC_{\max}^{PEB(i)}(t) \tag{4.14}$$

$$\left(P^{C2PEB_{(i)}}(t)\right) * \eta_{char} \le \left(P_{\max}^{PEB_{(i)}}(t) - P_{\min}^{PEB_{(i)}}(t)\right) * Y(t) \tag{4.15}$$

$$SOC^{PEB_{(i)}}(t+1) = SOC^{PEB_{(i)}}(t) + \left(P^{C2PEB_{(i)}}(t)\right) * \Delta t * \eta_{char} \tag{4.16}$$

Charger Constraints: The maximum amount of power that chargers can take from the grid, PV, ESS at any time interval t is defined in equations (4.17- 4.19) respectively. Equation (4.20) determines the maximum amount of power that a charger can obtain from the ESS, PV, and grid, respectively to charge the PEBs.

$$P^{G2C}(t) \le P_{\max}^{C}(t) \tag{4.17}$$

$$P^{PV2C}(t) \le P_{\max}^{C}(t) \tag{4.18}$$

$$P^{ESS2C}(t) \le P_{\max}^{C}(t) \tag{4.19}$$

$$\left(P^{ESS2C}(t) + P^{PV2C}(t) + P^{G2C}(t)\right) * \eta_{char} \le \left(P_{\max}^{C}(t) - P_{\text{mix}}^{C}(t)\right) \tag{4.20}$$

Reverse power flow Constraints: As the ESS, building, grid, and charger, are integrated into the PEBDC Ecosystem, the constraint equations (4.21-4.27) are required to prevent reverse power flow.

$$P^{PV2ESS}(t) \geq 0 \tag{4.21}$$

$$P^{PV2B}(t) \geq 0 \tag{4.22}$$

$$P^{PV2G}(t) \geq 0 \tag{4.23}$$

$$P^{PV2C}(t) \geq 0 \tag{4.24}$$

$$P^{G2B}(t) \geq 0 \tag{4.25}$$

$$P^{G2C}(t) \geq 0 \tag{4.26}$$

$$P^{ESS2B}(t) \geq 0 \tag{4.27}$$

Solar PV Generation Constraints: The PV generation limit is defined in equation (4.28) and the balance between the total PV power production and consumption due to (Grid, ESS, PEBs, and Building) is defined in equation (4.29).

$$0 \leq P_g^{pv}(t) \leq P_g^{pv}(max)\,(t) \tag{4.28}$$

$$P^{PV}(t) = P^{PV2G}(t) + P^{PV2ESS}(t) + P^{PV2C}(t) + P^{PV2B}(t) \tag{4.29}$$

Load demand Constraints: Total load demand depends upon the number of PEBs in the PEBDC Ecosystem and total building load. Equation (4.30) defines the total load boundary limit (building and PEBs) for the proposed model. Where $X_L^{PEB_{(i)}}(t)$, $X_L^B(t)$and $X_L^{total}(t)$ are the load due to $PEB_{(i)}$, building, and the total load at any time interval t. The balance between the building load demand and the total power supply (due to ESS, PV, and Grid) is shown in equation (4.31).

$$0 \leq X_L^{PEB_{(i)}}(t) + X_L^B(t) \leq X_L^{total}(t) \tag{4.30}$$

$$X_L^B(\mathrm{t}) = P^{ESS2B}(t) + P^{PV2B}(t) + P^{G2B}(t) \tag{4.31}$$

4.4 **Results and Discussions**

A simulation has been performed for the energy management of the PEB depot charging ecosystem considering the middle months of all four seasons Summer, Autumn, Winter, and Spring corresponding to January, April, July, and October, respectively. The real-world data from Yutong PEBs [133], Sky Bus's arrival and departure schedule[134], and FITs scheme for the grid [128] shown in Figure .4.5 are used in the simulation. Power is purchased from the grid and stored in ESS during low tariffs and is sold back to the grid or to a contracted building at times of high tariff. Overnight charging offers an intelligent and cost-effective solution for both the BDO and PEB owner to charge a large fleet of vehicles during the nighttime.

Charging the PEBs during off-peak hours (1:00–6:50 am) can minimise the negative impacts on the power distribution network. Therefore, the price of selling electricity to the PEB is set higher for this period (black line in Figure 4.5) so that the trading occurs during this period in the simulation.

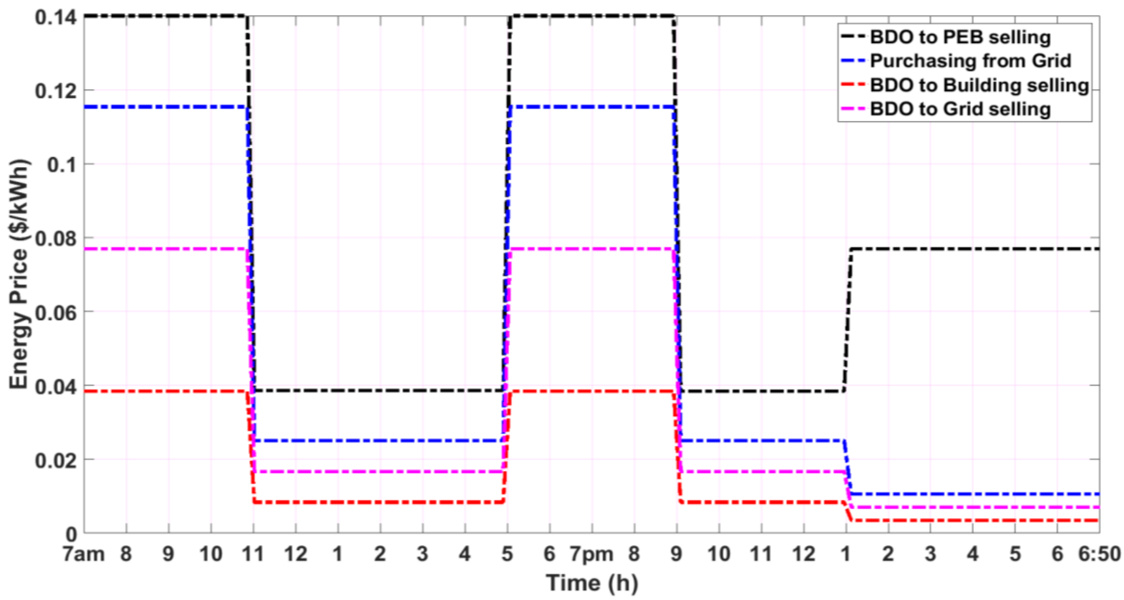

Figure 4. 5 Proposed FITs scheme for PEBDC Ecosystem.

4.4.1. Energy trading among PEBDC Ecosystem's agents

Energy trading (selling and buying) among the agents (PV, ESS, Building, PEBs, and grid) in the PEBDC Ecosystem for a whole day for four different seasons namely scenario 1 (summer), scenario 2 (Autumn), scenario 3 (winter) and scenario 4 (spring) are shown in Figure 4.7, Figure 4.9, Figure 4.11, and Figure 4.13, respectively.

According to the proposed FIT scheme, when the price on the grid is low, ESS will charge from the grid and use this energy to charge the PEBs are sell it back to the grid when the price on the grid becomes high. The detailed analysis of each season is as follows.

Scenario 1 (Summer): Figure 4.6a presents a whole day ESS charging and discharging status. The positive and negative power values on the y-axis represent the ESS charging from PV/grid and discharging from ESS to building/grid/PEBs, respectively. The ESS SOC is updated in each time interval using equation (4.32).

$$SOC^{ESS}(t+1) = SOC^{ESS}(t) + \left(P^{G2ESS}(t) + P^{PV2ESS}(t)\right) * \Delta t * \eta_{char} - \left(P^{ESS2G}(t) + P^{ESS2B}(t) + P^{ESS2C}(t)\right) * \Delta t / \eta_{dis} \quad (4.32)$$

The grid and building offer a high price from (7:00-11:00 am) therefore, ESS sells power to the grid and building. However, ESS is charging from (11:00-5:00 pm) from PV and grid for future use. During the time interval (6:00-9:00 pm) some of the available power in the ESS is sold to the grid and the rest is used to charge PEB1 and PEB6 from (7:10–9:00 pm) respectively. Two PEBs (PEB1 and PEB6) arrived at the depot at 7:00 pm, and 7:50 pm, respectively [134] charged using ESS.

However, PEB12 which arrived at 9:00 is not charged using the PV or ESS. This is because of the unavailabilty of PV energy and ESS is charging at the arrival of PEB12 (ESS charging and discharging can not occur at a same time to preserve the battery lifespan). Again from (9:00 pm - 6:50 am), the ESS is charging from the grid and PV (if available) to fully charge the ESS for the next day's use. The balance between the total PV power production and consumption (due to, Grid, ESS, PEBs, and Building) is performed using equation (4.29) and the result is shown in Figure 4.6b.

To reduce the load on the distribution feeder due to higher building energy consumption arising from increased urbanisation, the stored power in the ESS is used to supply power to the building when it is available. The balance between the building load demand and the total power supply (due to ESS, PV, and Grid) is performed using equation (4.31) and the result is shown in

Figure 4. 6 c.

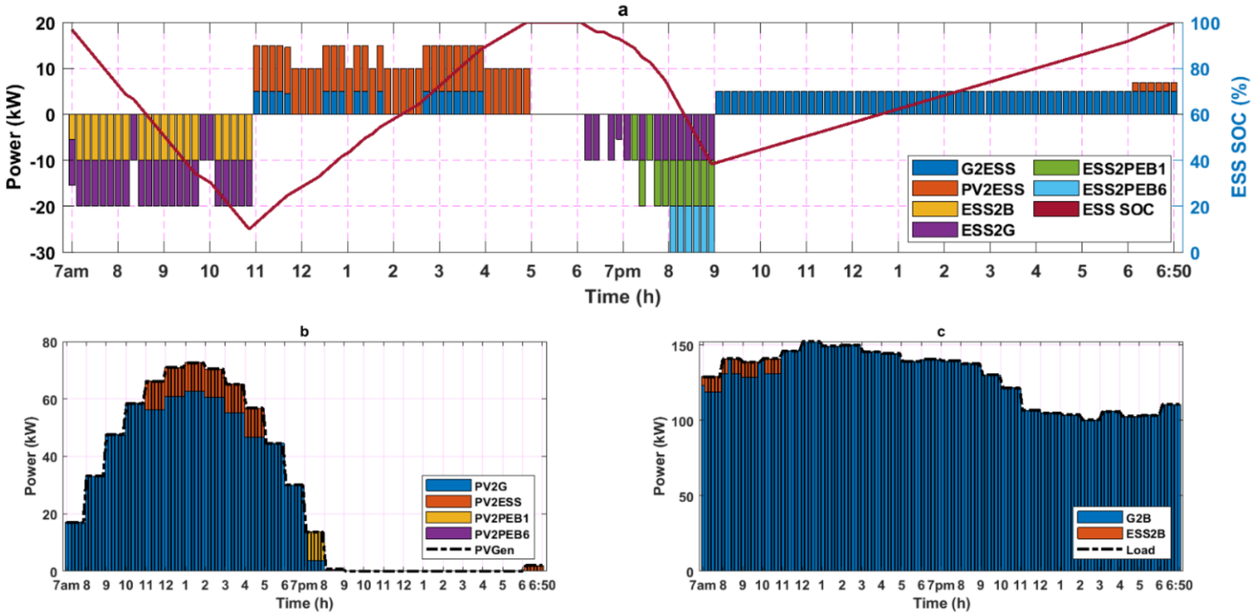

Figure 4. 7 a) SOC of ESS in a single day; b) PV Generation and Supply c) Building Load Demand and Supply (Summer).

Figure 4.7a and Figure 4.7b show the amount of power provided by ESS to (building (B), Grid (G) and PEBs) and PV to (G, ESS, and PEBs) respectively for the summer season. It is interesting to note that only 1% of PV-generated power is used to charge the PEBs as shown in Figure 4.7b. The reason is the 1st and 2nd PEBs are arriving at 7:00 and 7:10 pm respectively and the PV generation is available until 8:00 pm. Therefore, PV to PEBs charging occurs for the time interval 7:10 pm – 8:00 pm.

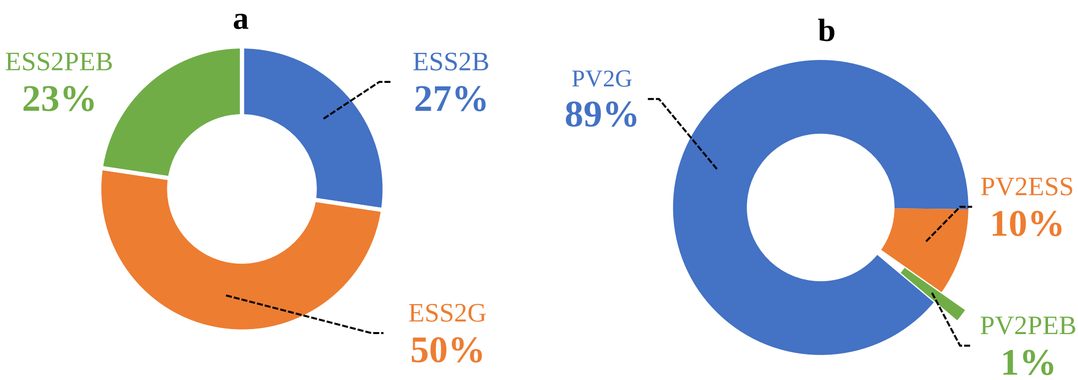

Figure 4. 8 Power provided by a) ESS to B, G, and PEBs; b) PV to B, G, and PEBs (Summer).

Scenario 2 (Autumn): According to the FITs scheme, the PV-generated power is exported back to the grid or sold to the building/PEBs. Figure 8. shows a single-day ESS charging and discharging status, PV generation, and building load demand and supply for the Autumn season. As compared to summer, the PV power generation is only for the time interval 8: 00 am - 6: 50 pm which is half for the autumn season as can be seen in Figure 8.b

In New Zealand, Autumn month's temperatures are cooler than summer, therefore the building load demand (due to hot water usage) for the Autumn season is slightly higher than summer and this is served by the grid the ESS (see Figure 8.c).

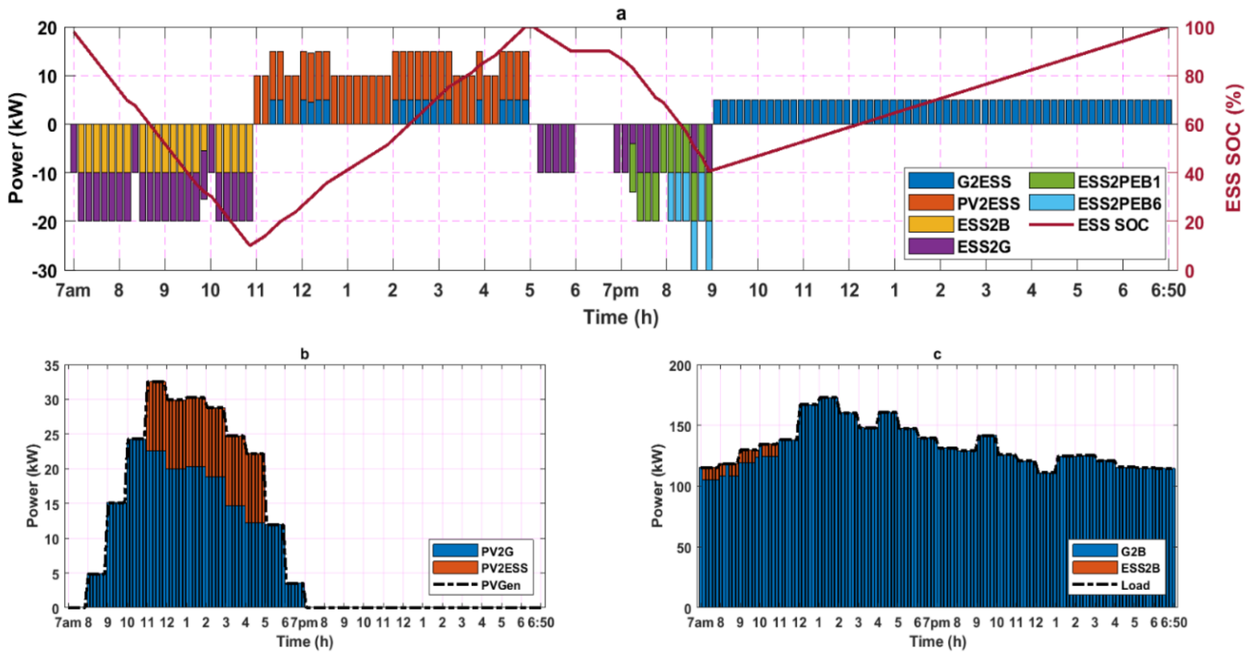

Figure 4. 9 a) SOC of ESS in a single day; b) PV Generation and Supply c) Building Load Demand and Supply (Autumn).

Figure 9a and Figure 9b show the amount of power provided by ESS to (B, G, PEBs) and PV to (G, ESS, and PEBs) for the autumn. It is interesting to note that the PV generation in autumn does not match with the PEB arrival therefore, the energy trading between PV to PEB is zero. However, ESS is selling the stored power to grid, building, and PEBs which is 49%, 28%, and 23% respectively as can be seen in Figure 9a. The power generated by PV is selling to Grid and ESS which are 74% and 26% respectively shown in Figure 9b.

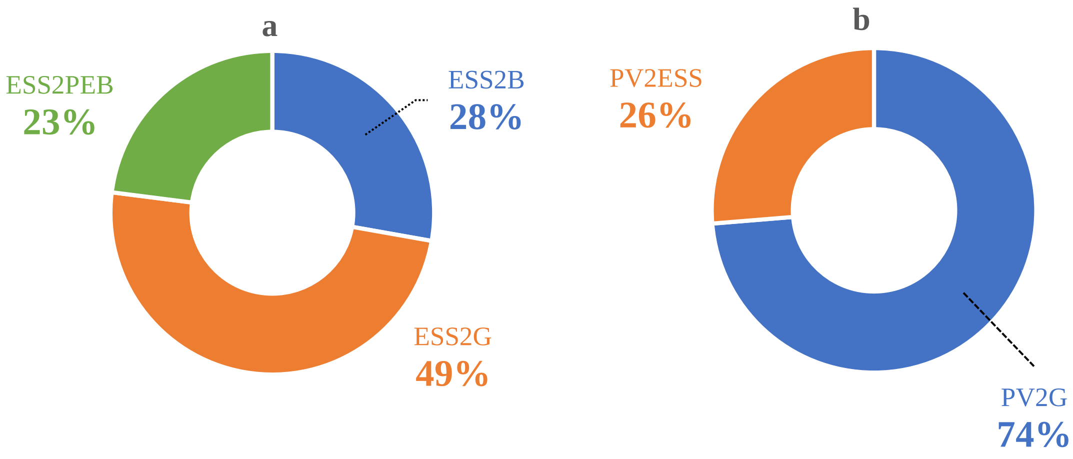

Figure 4. 10 Power provided by a) ESS to B, G, and PEBs; b) PV to B, G, and PEBs (Autumn).

Scenario 3 (Winter): A single-day ESS charging and discharging status, PV generation, and building load demand and supply for the winter season are shown in Figure 4.10. In winter, the sun is lower in the sky and hence there is limited PV power generation and only for the time interval 9: 00 am - 6: 00 pm. Thus, the generation is much less compared to the other three seasons as can be seen in Figure 4.10b. Moreover, in winter, due to the cold weather, there is more electricity usage (due to hot water) therefore, the building load demand in the winter season is higher than for any other season. This building load demand is served by the grid and ESS (see Figure 4.10c).

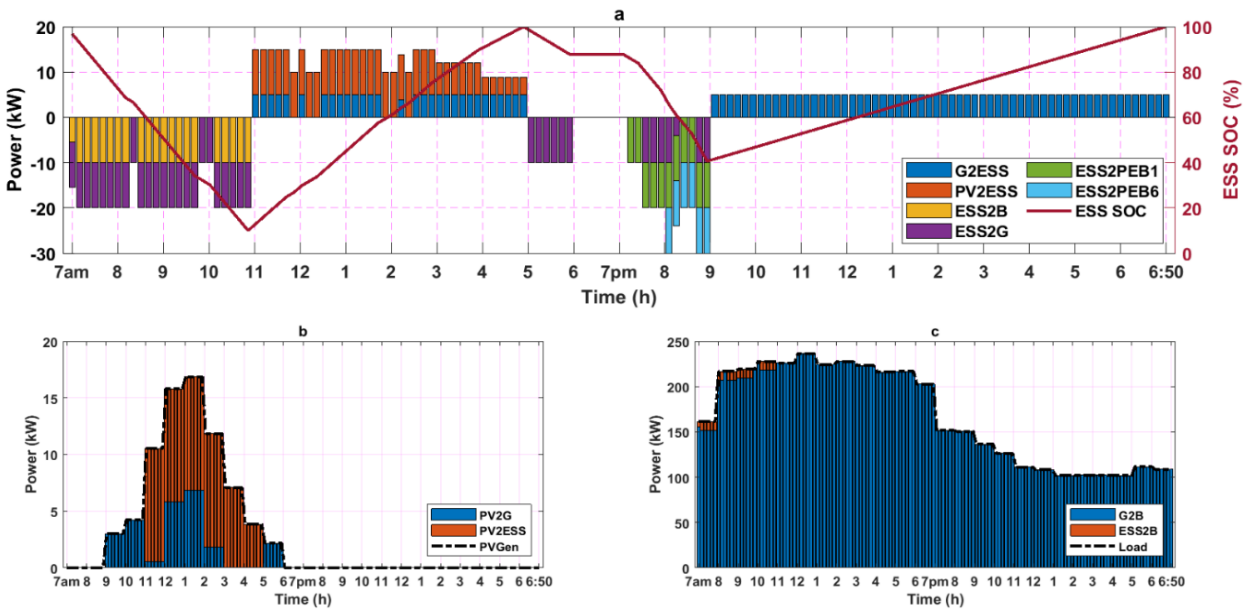

Figure 4. 11 a) SOC of ESS in a single day; b) PV Generation and Supply c) Building Load Demand and Supply (Winter).

Figure 4.11a and Figure 4.11b show the amount of power provided by ESS to (B, G, PEBs) and PV to (G, ESS, and PEBs) for the winter season. Similar to the autumn season, the PV generation does not match with the PEB arrival therefore, energy trading between PV to PEB is zero.

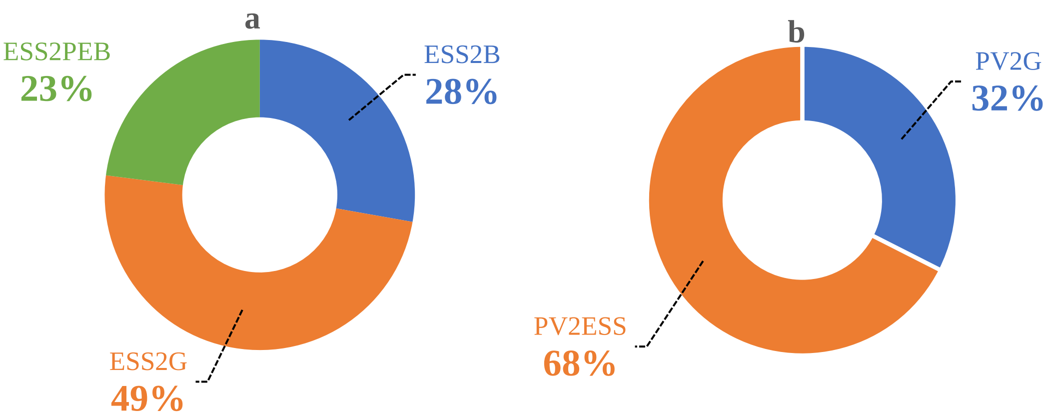

Figure 4. 12 Power provided by a) ESS to B, G, and PEBs; b) PV to B, G, and PEBs (Winter).

Scenario 4 (Spring): Figure 4.12a shows a single-day ESS charging and discharging status, PV generation, and building load demand and supply for the winter season. In the spring season, the PV power generation is much higher than in autumn and winter (7:00 am - 7:00 pm). The power generation can be seen in Figure 4.12b. Furthermore, the building load demand for the spring season is lower than in winter and autumn due to less electricity usage (more specifically less hot water usage). This demand is served by the grid and ESS (see Figure 4.12c).

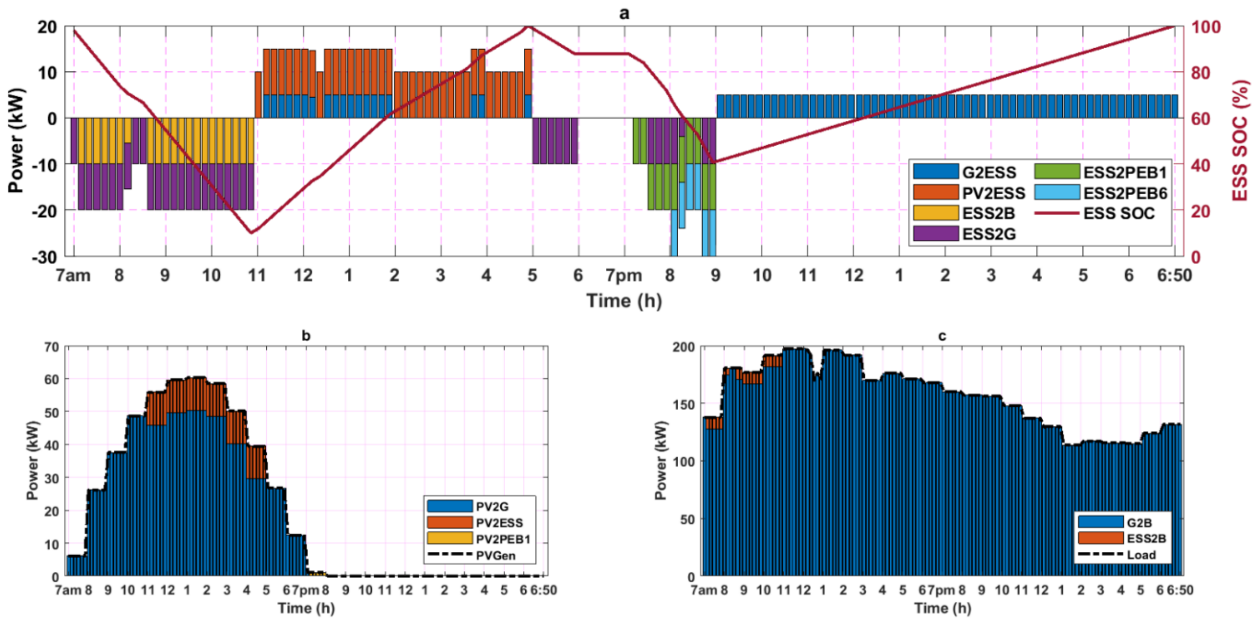

Figure 4. 13 a) SOC of ESS in a single day; b) PV Generation and Supply c) Building Load Demand and Supply (Spring).

Figure 4.13a and Figure 4.13b show the amount of power provided by ESS to (building, grid and, PEBs) and PV to (grid, ESS, and PEBs), respectively for the spring season. ESS sells the stored power to the grid, building, and PEBs which is 49%, 28%, and 23%, respectively as can be seen in Figure 4.13a. Similar to autumn and winter, in the spring season, the PV-generated power does not match with the PEB arrival thus, the energy trading between PV to PEB is zero. However, ESS used 13% of PV generation and the rest of 87% is sold to the grid.

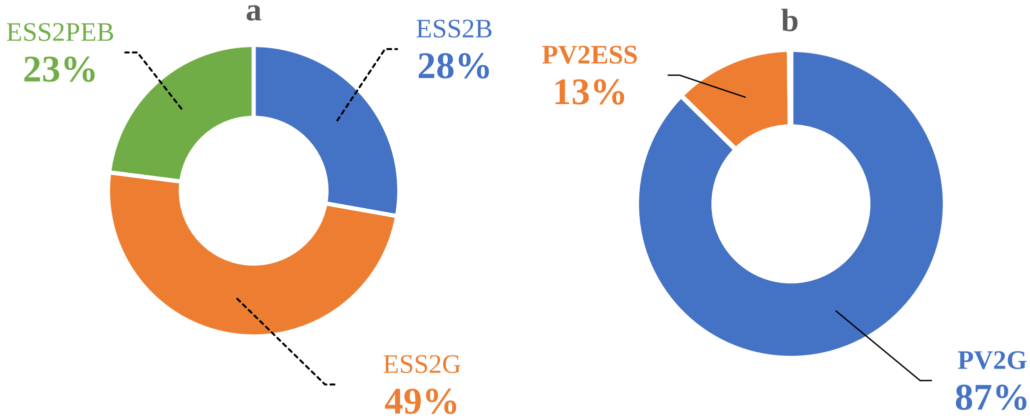

Figure 4. 14 Power provided by a) ESS to B, G, and PEBs; b) PV to B, G, and PEBs (Spring).

It is interesting to note that the winter season has less profit and the summer season has the highest profit. The daily profits gained by the BDO during each season are shown in Table 4.3.

Table 4. 2 Daily Seasonal Profit (NZ$)

Seasons	**Months**	**Profit**
Summer	January	231.684
Autumn	April	119.781
Winter	July	85.8222
Spring	October	181.196

4.5 **Summary**

This chapter presents an efficient energy management system for the PEBDC ecosystem integrated with an LV Feeder. The key findings of this chapter are as follows:

i) **The proposed cost-efficient energy management system** is based on a double-sided auction mechanism that provides a platform to perform energy trading among the selling and buying agents in the PEBDC ecosystem.

ii) **A MILP model in CPLEX** is developed considering the capital investment, operation & maintenance, and depreciation costs for installing PV, ESS, and charger. The objective of the developed mathematical model is to maximise the daily profit of the BDO owner by performing energy trading among the selling agents (PV, ESS (discharge), grid), and purchasing agents (grid, ESS (discharge), PEBs). The energy trading and the daily profit are analysed for all four seasons.

iii) **Real-world data** from Yutong PEBs, SkyBus arrival, and departure schedule, FITs scheme for the grid, and the load for one of our campus buildings is used. The constraints such as power balance, ESS, PEB, grid, charger, PV, generation, and demand are considered in the simulation.

In this Chapter, energy trading among the depot entities has been performed using the proposed efficient Energy Management System (EMS) in the Eco Charging station. PEBs are coming to refuel in the eco charging station thus the charge scheduling and discharging model for PEBs is proposed and discussed in Chapter 5.

Chapter 5 Charge Scheduling Algorithms and Discharging Model

This chapter is based on the work from the following journal publication in which the author of this thesis is the main author ("Plug-In Electric Bus Depot Charging with PV and ESS and Their Impact on LV Feeder" Energies, 21-39, 2020).

Plug-in Electric buses (PEBs) help the transition process towards zero emissions and provide more sustainable transportation when the flow of energy is optimally managed as discussed in the previous Chapter. However, because PEBs have bigger battery capacity and thus have higher charging time than the normal EVs and a PEB charge scheduling and discharging model is mandatory for charging infrastructure development.

This chapter firstly presents the system configuration considering i) Framework of the proposed study, ii) Assumptions iii) PEB Depot charging ecosystem iv) Skybus route, and v) Skybus fleet arrival and departure schedule. Secondly, the proposed PEB charge scheduling algorithms i.e., overnight and pantograph are presented. Thirdly, in the results and discussion section, the proposed charge scheduling algorithms are used to determine the impact of charging PEBs on LV feeder for different travel periods i.e., peak, normal and off-peak. Finally, a comparison of these two charging schemes has been done.

5.1 Introduction

PEBs are the promising alternative to conventional buses to provide a sustainable, economical, and efficient mode of transportation [135, 136]. Therefore, European cities such as Geneva, Stockholm, Madrid, Valladolid, London, Amiens, and Paris are shifting towards electric buses to decarbonise and to reduce air pollution; the details are as follows:

i) **Geneva (Switzerland):** In 2013, ABB demonstrated the flash charging technology for Geneva airport to the city's international exhibition center, Palexpo. The bus battery can be recharged at a selected stop with a 400kW charger for 15 seconds. At the end of the bus line, only 3 to 4 minutes are required to fully recharge the batteries. This project used an electric bus manufactured by the HESS company which is 18.7-metres long and can carry up to 135 passengers [108].

ii) **Stockholm (Sweden):** In 2015, Siemens and Scania electrified a 2 km motorway with two 150 kW chargers for hybrid trucks. The Stockholm project had numerous replications such as a 60 kW DC charger at Stuttgart airport, two twin chargers at Geneva airport, and two 300 kW chargers installed at Gothenburg.

iii) **Madrid (Spain)**: In 2017, a pilot project was introduced in Madrid for one bus line having 42 stops. This system uses 8 minutes of charging time during traveling and fully charges during night-time. It is planned to bring 88 electric buses in Madrid by the end of 2020 [137].

iv) **Valladolid (Spain):** In 2017, VECTIA (a sustainable urban transport company) commissioned five plug-in hybrid buses for the Valladolid city center. The bus uses a Lithium Titanite Oxide (LTO) battery which has a capacity of 45 kWh. These buses are recharged at the end of the bus line using five pantographs with a charging capacity of 150 kW and this can be scaled up to 300 kW [137].

v) **London (United Kingdom):** In 2017, ABB commissioned a pantograph recharging scheme installed at the Shudehill Interchange. A Volvo 7900e electric bus having a battery capacity of 76 kWh can be recharged using a pantograph at selected stopovers with 3 to 6 minutes of energy boosts. This allows running the bus 24/7 [72].

vi) **Amiens (France):** In 2017, Amiens let the biggest contract in Europe: 43 electric buses supplied by Irizar, a Spanish manufacturer [138]. These buses have a battery capacity between 90 and 150 kWh and recharge through a 500kW rated pantograph in approximately 5 minutes.

vii) **Paris (France):** In 2018, The RATP group (a state-owned public transport operator comprising 4,700 buses including 800 hybrid and 74 electric buses) and Ile-de-France Mobilities (the organisation which controls and coordinates the public transport network operating in the Paris-area) launched a tender to buy 1,000 electric buses and to electrify two bus lines [139]. At the end of 2020, the first series of the tender should be let; these will use the depot charging technique [138] to minimise the charging impact on the grid.

Most of the above research is based on pantograph recharging. However, the electrification of public transportation through pantograph leads to a phenomenon of peak load that impacts the stability of LV (Low Voltage) feeder [140] compared to depot charging [141]. Also, it is important to design the PEBs charging schedule during the infrastructure planning of depot charging, while considering the nexus between the transportation network and power grid. The scheduling of PEBs charging time in a depot charging station is challenging due to:

i) **Physical structure limitations:** 1) the number of chargers, 2) the charging capacity of each charger, and 3) space (number of PEBs in a charging station for a specific time).
ii) **Power grid limitation**: large scale PEBs electrification causes an intense burden on the power grid. Therefore, the total load on the grid must be balanced with its maximum capacity to avoid expensive peak load costs.
iii) **PEBs limitations:** 1) Limited battery capacity, 2) require considerable charging time, 3) strict operation tasks (arrival and departure) so the PEB needs to be fully charged before departure. 4) Another PEB limitation is heating. Especially in the summer, heat dissipation at charging stations can be a serious issue; depending on the number of chargers and the power demand.

5.2 System Configuration

5.2.1. A Framework of the Proposed Study

Figure 5 .1 shows the framework of the proposed study. 1) According to the PV outputs, available power in the ESS, grid limit, load (building and PEBs), and Skybus arrival and departure schedule, the PEBs in the PEBDC Ecosystem starts to charge. 2) The capital, depreciation, operation, and maintenance costs ESS, PV, and chargers are considered component costs.

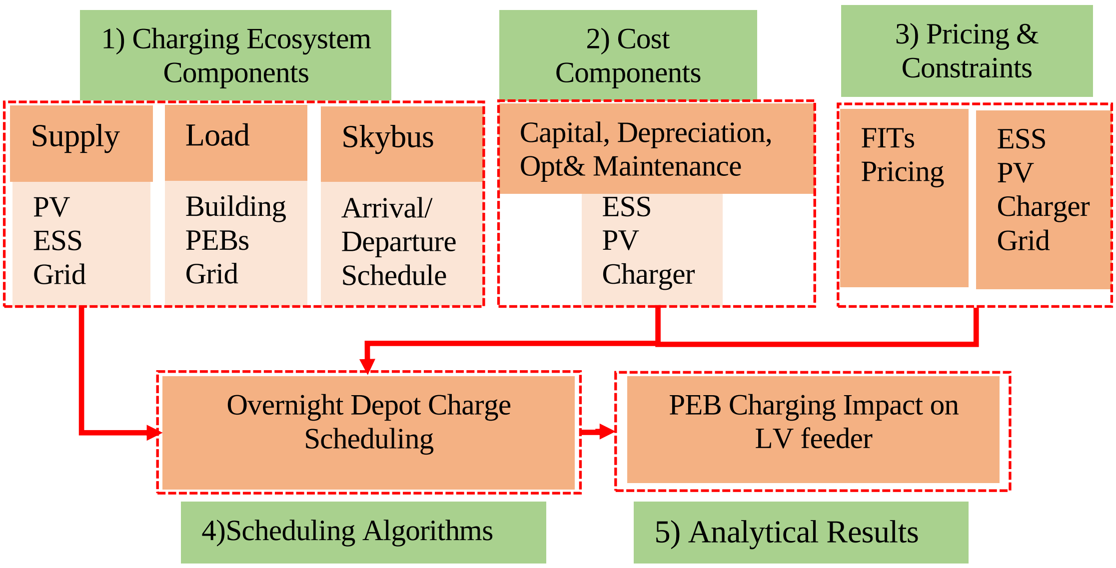

Figure 5. 1 A Framework of the Proposed Study.

3) The FITs pricing, constraints related to ESS, PV, charger, and grid are also considered during the simulation. 4) The study aims to develop two charge scheduling algorithms using the MILP model in IBM ILOG studio with CPLEX solver for the PEBs coming in to charge their batteries in the depot while considering the nexus between transportation and the power grid. The constraints (PV, ESS, and grid limit), capital investment, operation and maintenance, and depreciation costs of PV, ESS, charger, and FITs price of the grid are considered in the scheduling algorithm. 5) Finally, the analytical results of the PEBs charging impact on the LV feeder are presented.

5.2.2. Assumptions

The following assumptions have been considered:

i) The PEBDC Ecosystem is located at the Auckland airport where a 100 kW PV system is integrated with 500kWh ESS and 12 chargers are available.

ii) Every charger has two charging guns and thus 12 chargers (peak, off-peak, and normal time) are required to charge 44 PEBs (at different times) and this is the maximum charging capacity of the depot.

iii) To maximise the daily BDO profit, ESS buys and stores power from the grid when its price is low. At other times, the power stored in ESS and the power generated by the PV system may be exported back to the power grid at 2/3rd of cost from the grid [125], and at a contract rate to the PEB owner as shown in Figure 5.7.

iv) PEB owner has agreed to purchase the power from the BDO at a higher price than the actual price on the grid for the time intervals (1:00-7:00) am.

v) In the Depot Charge Scheduling Algorithm, the charger draws only 5kW, whilst the Pantograph Charge Scheduling Algorithm uses more than 250 kW at ten-minute intervals from the grid.

vi) The solar profile irradiation of the city of Auckland [126], charger price from Ecotricity New Zealand [142], and FITs prices from a distribution company Electra [128] are used as real-world data in the simulations.

5.2.3. PEB Depot Charging Ecosystem

The PEB depot charging ecosystem consists of BDO (as a charging service provider that owns the PV, ESS, and charger), PEBs, and the grid as shown in Figure 5. 2.

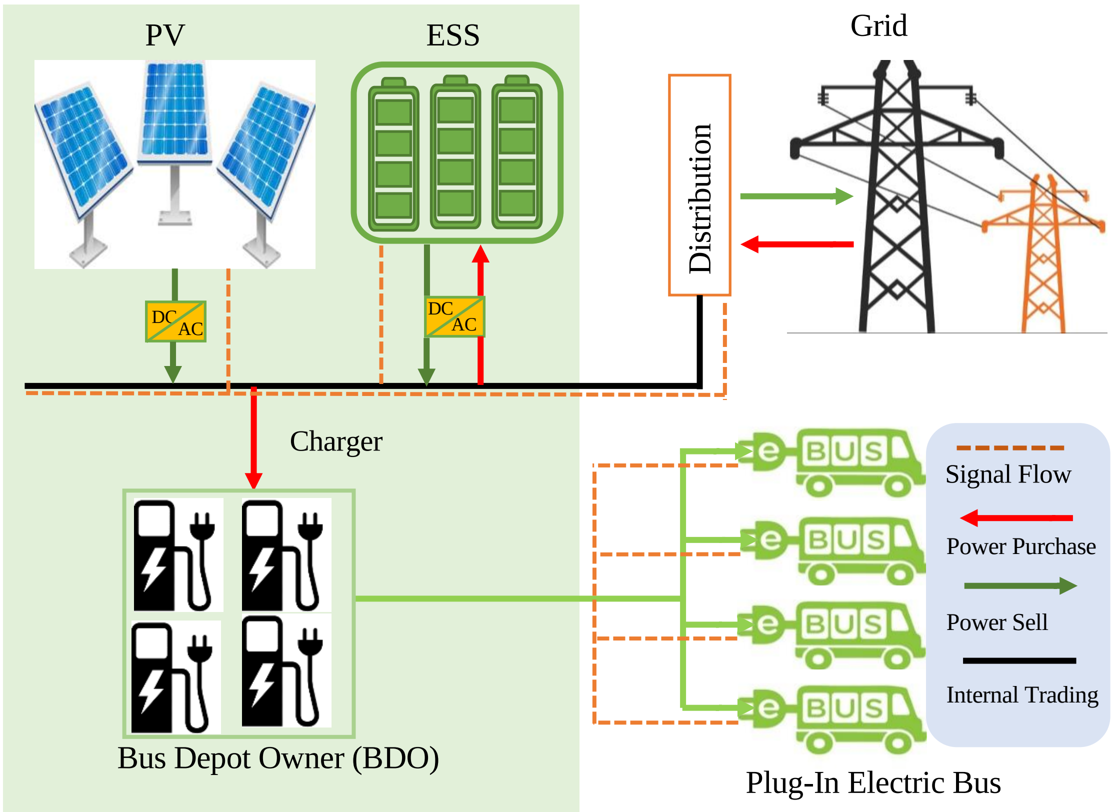

Figure 5. 2 PEB Depot Charging Ecosystem.

The PEBs arrive at the depot to charge up their batteries. In external trading, the BDO pays when it purchases power from the grid for its ESS and chargers (red arrow), and generates revenue when it sells power to the PEBs and/or grid (green arrow). However, in internal trading, such as PV to chargers/ESS or ESS to the chargers, the BDO does not need to pay anything because the BDO owns these entities (black line) during optimisation. Lithium-ion batteries are used as the ESS. When the PEBs arrived at the charging station, the BDO should charge all the PEBs before their next scheduled departure [134]. To maximise the daily BDO profit, the proposed algorithm will charge the PEBs using PV or ESS resources if available; otherwise, from the grid. The total system cost (capital investment and operation & maintenance) of PV, ESS, PEB, and charger per day [130] are shown in Table 5.1.

Table 5. 1 PV, ESS and Charger Total System & Recovery Costs (NZ$)

System Components	**PV**	**ESS**	**Charger**
System Size	100 kW	500kWh	50 kW
Price per W/Wh	0.411	0.260	N/A
Estimated life span (year)	25	10	25
Total System Cost	41,100	130,000	45,000
Recovery cost/day	3.67	4.986	2.99

5.2.4. Skybus Route

Skybus is an airport bus service for commuters travelling between the Auckland airport and Auckland Central Business District (CBD) as shown in Figure 5. 3. Its route has 12 stops and covers a total distance of 20.5 km in an average time of 52 minutes.

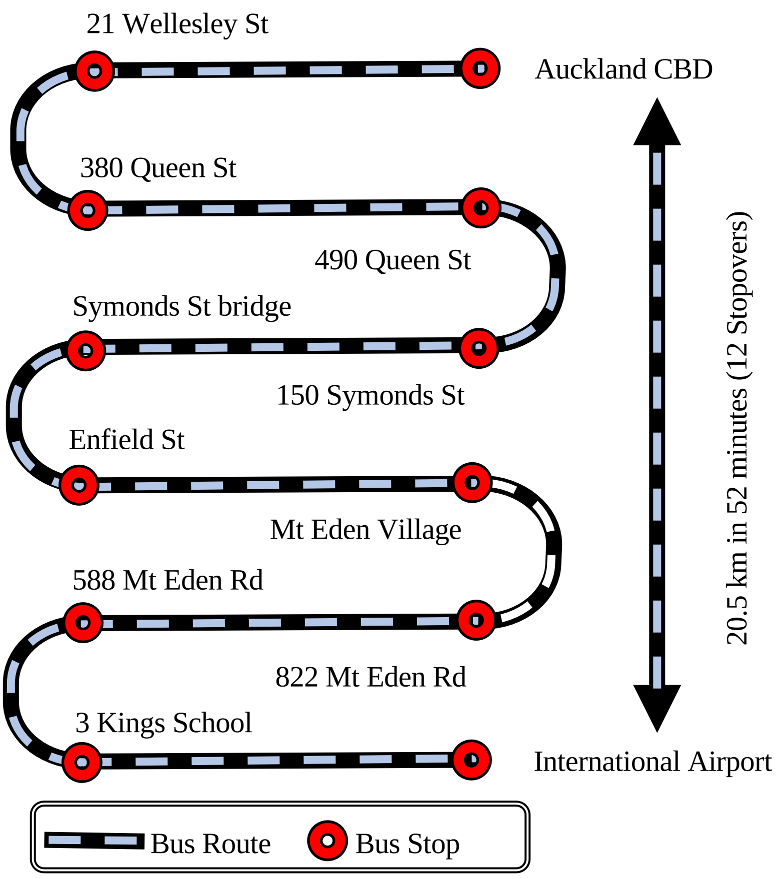

Figure 5. 3 Skybus Route between Auckland Airport and Auckland CBD.

5.2.5. Skybus Fleet Arrival and Departure Schedule

The SkyBus has three intervals i.e. peak, off-peak, and normal time which operates in 10, 30, and 20 minutes time intervals as shown in Figure 5.4 and required 24, 8, and 12 PEBs respectively with half of them in each direction between the Auckland airport and CBD.

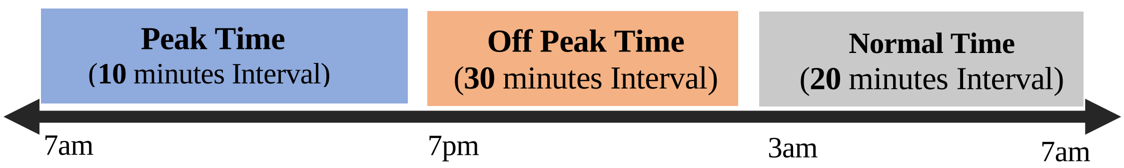

Figure 5. 4 Skybus Departure Time Intervals.

5.2.5.1 Peak, Off-peak, and Normal Time

The detailed timetable (arrival and departure) for peak, off-peak, and normal time intervals are described in Table 5.2, Table 5.3, and Table 5.4, respectively. To validate the proposed algorithms, simulations have been performed and results of the 1st, 6th, and 12th PEB for peak time 1st, 2nd, and 4th PEB for off-peak time and 1st, 3rd, and 6th PEB for normal time interval are discussed in Section 6.

Table 5. 2 Skybus Arrival and Departure Schedule (Peak Time)

Round Trip#	PEB#	To City		Stopovers	To Airport		Stopovers	Status
		Departure	Arrival		Departure	Arrival		
1	1	7:00 am	7:52	0:08	8:00	8:52	0:08	Road
	2	7:10	8:02	0:08	8:10	9:02	0:08	Road
	3	7:20	8:12	0:08	8:20	9:12	0:08	Road
	4	7:30	8:22	0:08	8:30	9:22	0:08	Road
	5	7:40	8:32	0:08	8:40	9:32	0:08	Road
	6	7:50	8:42	0:08	8:50	9:42	0:08	Road
	7	8:00	8:52	0:08	9:00	9:52	0:08	Road
	8	8:10	9:02	0:08	9:10	10:02	0:08	Road
	9	8:20	9:12	0:08	9:20	10:12	0:08	Road
	10	8:30	9:22	0:08	9:30	10:22	0:08	Road
	11	8:40	9:32	0:08	9:40	10:32	0:08	Road
	12	8:50	9:42	0:08	9:50	10:42	0:08	Road
2	-	-	-	-	-	-	-	Road
3	-	-	-	-	-	-	-	Road
4	-	-	-	-	-	-	-	Road
5	-	-	-	-	-	-	-	Road
6	1	5:00	5:52	0:08	6:00	6:52pm	0:08	Station
	2	5:10	6:02	0:08	6:10	7:02	0:08	Station
	3	5:20	6:12	0:08	6:20	7:12	0:08	Station
	4	5:30	6:22	0:08	6:30	7:22	0:08	Station
	5	5:40	6:32	0:08	6:40	7:32	0:08	Station
	6	5:50	6:42	0:08	6:50	7:42	0:08	Station
	7	6:00	6:52	0:08	7:00	7:52	0:08	Station
	8	6:10	7:02	0:08	7:10	8:02	0:08	Station
	9	6:20	7:12	0:08	7:20	8:12	0:08	Station
	10	6:30	7:22	0:08	7:30	8:22	0:08	Station
	11	6:40	7:32	0:08	7:40	8:32	0:08	Station
	12	6:50	7:42	0:08	7:50	8:42	0:08	Station

Table 5. 3 Skybus Arrival and Departure Schedule (Off-Peak Time)

Round Trip#	PEB#	To City		Stopovers	To Airport		Stopovers	Status
		Departure	Arrival		Departure	Arrival		
1	1	7:00 pm	7:52	0:08	8:00	8:52	0:08	Road
	2	7:30	8:22	0:08	8:30	9:22	0:08	Road
	3	8:00	8:52	0:08	9:00	9:52	0:08	Road
	4	8:30	9:22	0:08	9:30	10:22	0:08	Road
2	-	-	-	-	-	-	-	Road
3	-	-	-	-	-	-	-	Road
4	1	1:00 am	1:52	0:08	2:00	2:52 am	0:08	Station
	2	1:30	2:22	0:08	2:30	3:22	0:08	Station
	3	2:00	2:52	0:08	3:00	3:52	0:08	Station
	4	2:30	3:22	0:08	3:30	4:22	0:08	Station

Table 5. 4 Skybus Arrival and Departure Schedule (Normal Time)

Round Trip#	PEB#	To City		Stopovers	To Airport		Stop-overs	Status
		Departure	Arrival		Departure	Arrival		
1	1	3:00	3:52	0:08	4:00	4:52	0:08	Road
	2	3:20	4:12	0:08	4:20	5:12	0:08	Road
	3	3:40	5:32	0:08	4:40	5:32	0:08	Road
	4	4:00	4:52	0:08	5:00	5:52	0:08	Road
	5	4:20	5:12	0:08	5:20	6:12	0:08	Road
	6	4:40	5:32	0:08	5:40	6:32	0:08	Road
2	1	5:00	5:52	0:08	6:00	6:52am	0:08	Station
	2	5:20	6:12	0:08	6:20	7:12	0:08	Station
	3	5:40	6:32	0:08	6:40	7:32	0:08	Station
	4	6:00	6:52	0:08	7:00	7:52	0:08	Station
	5	6:20	7:12	0:08	7:20	8:12	0:08	Station
	6	6:40	7:32	0:08	7:40	8:32	0:08	Station

5.3 **PEB Charge Scheduling Algorithms**

This study aims to formulate and analyse the charge scheduling algorithms for PEBs recharging their batteries in the PEB depot. The battery capacity of PEBs is bigger and thus their charging power is larger than private EVs. Thus, charging of PEBs causes very high energy consumption and has a negative impact on the distribution grid. Therefore, emerging technologies such as ESS, PV, and charging control methods deployed in a distributed generation are used to reach this goal. A coordination strategy (charging/discharging) between the selling and purchasing agents in the PEBDC Ecosystem is implemented to increase the robustness of the system. PEBs have a strict operation task (the arrival and departure schedule), therefore they need to be fully charged before the next scheduled trip. Keeping this strict operation task in mind, the following two algorithms are proposed.

i) Depot charge scheduling:

ii) Pantograph charge scheduling:

These two proposed charge scheduling algorithms along with the battery discharge model are applied to a fleet of SkyBus PEB and both the algorithm are tested for three different periods as shown in Figure 5. 5.

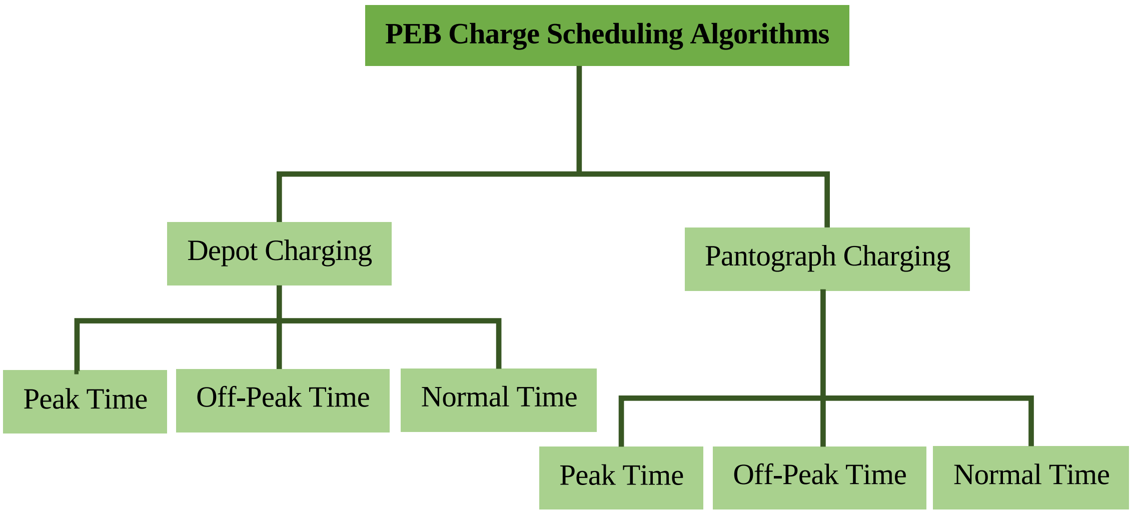

Figure 5. 5 PEB Charge Scheduling Algorithms.

In the PEB charge algorithm, the energy trading among the selling/purchasing agents i.e., PV, ESS, grid, and PEBs are considered for depot charging. However, in the case of a pantograph, the power source is only the grid as shown in Figure 5.6a.

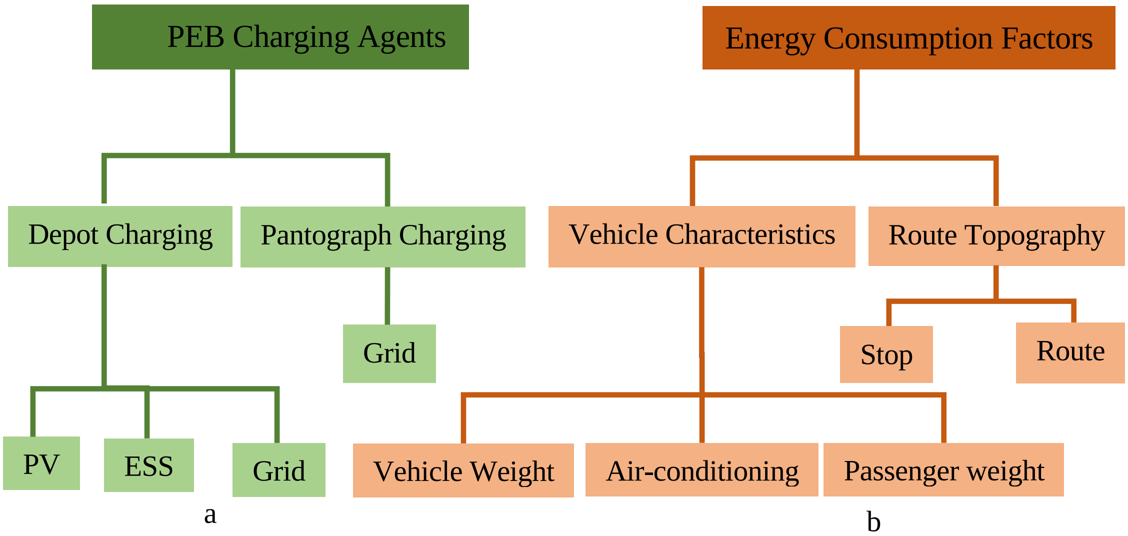

Figure 5. 6 a) PEB Charging Agents for Charging Algorithms b) Energy Consumption Factors for Battery Discharging Model.

The energy required to drive a vehicle depends on several vehicle energy consumption factors as shown in Figure 5.6b. These are considered in the battery discharging model.

In the case of New Zealand, the inclusion of the route topography in the simulation is important because the roads are hilly and become slippery during the rainy season, therefore, PEBs consume high power during up-hill driving. If the PEBs are going too fast downhill and the driver brakes, the motor is used as a generator and the vehicle recovers energy into its battery using its regenerative braking system.

The integration of PEBs into the distribution grid can be enhanced when their charging takes place mostly during off-peak times. This coordinated scheduling of charging is referred to as coordinated charging [143]. Moreover, when the charging power can be limited or controlled, the negative impact of PEBs on the distribution system can be further mitigated. However, not every grid operator is equipped to control the charging power. Such coordination of charge scheduling and the potential limit of charging power give rise to algorithms as follows:

5.3.1. Overnight Depot Charge Scheduling Algorithm

The Depot charging is also known as overnight charging. In this charging technique, the batteries are charged while in the depot, typically with a manual plug. The range of overnight-based depot charging buses is more than the pantograph-based charging technique. This is due to the power capacity of the charger. In overnight charging the buses are charged only at night time and use during daytime. However, in pantograph-based charging, the buses are charged at another terminal of the bus route. Thus, a smaller battery capacity is required. The algorithm I address the charging time scheduling of the PEB fleet during the night time using three available power resources in the PEBDC Ecosystem i) PV power production (if available), ii) available power in the ESS (charged during day time from PV) and/or iii) use the grid to charge the fleet of PEBs. Both the charging schedule of PEBs and charging power from the grid can be coordinated, and limited, respectively, based on the available capacity of the charger [142, 144].

Firstly, the algorithm will check the initial SOC of PEBs when they arrive at the charging station, then the algorithm will charge the PEBs using the PV power production (if available) or existing power in the ESS or otherwise from the grid up to a controlled limit based on the FITs scheme and without affecting their departure schedule. Due to the coordination between PEBs charging and grid limit, the proposed depot charge scheduling algorithm can mitigate the overloading problem in the LV feeder.

Algorithm I: Overnight Depot Charge Scheduling Algorithm and Battery Discharging Model.

1: Input: Obtain i) PEB arrival and departure schedule, maximum allowable charging power of each PEB and charger, initial and final SOC of PEBs and ESS, PV generation, price of selling electricity to PEB, and electricity buying price from the grid, and ii) PEBs energy consumption (due to the vehicle weight (v), air-conditioning unit (a), passenger weight (p), route topology(r), and stop (s)) for the depot charge scheduling algorithm and battery discharging model respectively, at any interval time *t*.

2: Procedure

PEB Charging

3: for all $t < T$ do

4: Lookup PEBs arrival and departure schedule (Table 5.2, Table 5.3, and Table 5.4)

5: **If** PEBs are in the charging station **then**

6: for all $i < I$ do

7: Optimise:

8: Max PEBs charging power using $P^{PEB_{(i)}}(t) = P^{PV2C_{(i)}}(t) + P^{ESS2C_{(i)}}(t) + P^{G2C_{(i)}}(t)$

9: $s.t \begin{cases} \sum_{t=A_i}^{L_i} SOC^{PEB(i)}(L_i) = SOC_{max}^{PEB(i)} \\ \sum_{x=1}^{chargerNo} P^{G2C(x)}(t) \leq P_{max-limit}^{G2C}(t) \end{cases}$

10: end for

11: else

PEB Discharging

12: When PEBs will be on the road, energy will consume and SOC update according to:

13: $\begin{cases} SOC^{PEB(i)}(t+1) = SOC^{PEB(i)}(t) - E_c^{PEB(i)}(t) \\ E_c^{PEB(i)}(t) = \sum_{t=1}^{T}(E_c^v + E_c^a + E_c^p + E_c^s + E_c^r) \\ P^{ESS2PEB(i)}(t) + P^{PV2PEB(i)}(t) + P^{G2PEB(i)}(t) = 0 \\ \forall t = 1,2,3,\ldots T \ \ \forall i = 1,2,3,\ldots N \end{cases}$

14: end for

15: Output: Optimised the charging schedule and charging power of each PEB's battery from integrated PV, ESS and grid for the time interval *t* = 1…,24h (with 10 minutes time intervals).

Where *i,* and *x* are the PEB and charger number, $SOC^{PEB(i)}(L_i)$,$SOC_{max}^{PEB(i)}$are the SOC (leaving from the depot) at time *t* and maximum SOC of PEB_i respectively,$A_i$and $L_i$are the starting and leaving charging time of PEB_i,$P_{nax}^{G2C(x)}$is the maximum power that the grid can provide to *x* charging pole, the efficiency is represented as η_i. This $E_c^{PEB_{(i)}}(t)$ denotes the total energy consumption due to vehicle weight, air-conditioning unit, passenger weight, route, and stop, respectively.

Steps (1-10) show the PEB charge scheduling algorithm. Step 8 maximises the charging power drawing by$PEB_i$from PV, ESS, and grid. Step 9 ensures i) PEBs are fully charged before departure, and ii) avoid power consumption exceeding the grid limit. Steps (11-14) show the PEB battery discharging model. Step 13 ensure i) PEBs SOC updates each time interval t, according to the energy consumptions$PEB_{w,a,p,r,s}^{Enr_cons}(t)$ ii) PEB battery is not charging from PV, ESS, and grid during the journey.

5.3.2. Pantograph Charge Scheduling Algorithm

One of the issues with the depot charging is that it requires more charging time. Thus, buses need to have a bigger battery to complete the scheduled trip which significantly increases the investment cost [145]. Keeping this issue in mind pantograph charge scheduling is presented in Algorithm II.

Algorithm II Pantograph Charge Scheduling Algorithm and Battery Discharging Model.

1: Input: Obtain i) arrival and departure schedule, maximum allowable charging power, initial and final SOC of each PEB, electricity selling/buying to PEB and/or from the grid, and ii) PEBs energy consumption for the pantograph charge scheduling algorithm and battery discharging model respectively, at any interval time *t*.

2: Procedure

PEB Charging

3: for all $t < T$ do

4: Lookup PEBs arrival and departure schedule (Table 5.2, Table 5.3, and Table 5.4)

5: If PEBs are in the charging station **then**

6: for all $i < I$ do

7: Optimize:

8: Max PEBs charging power using $P^{PEB_{(i)}}(t) = P^{G2C_{(i)}}(t)$

9: $s.t \left\{ \sum_{t=A_i}^{L_i} SOC^{PEB(i)}(L_i) = SOC_{max}^{PEB(i)} \right.$

10: end for

11: else

PEB Discharging Model

12: PEBs are on the road and the energy will consume according to:

13:
$$\begin{cases} SOC^{PEB(i)}(t+1) = SOC^{PEB(i)}(t) - E_c^{PEB(i)}(t) \\ E_c^{PEB(i)}(t) = \sum_{t=1}^{T}(E_c^v + E_c^a + E_c^p + E_c^s + E_c^r) \\ P^{ESS2PEB(i)}(t) + P^{PV2PEB(i)}(t) + P^{G2PEB(i)}(t) = 0 \\ \forall t = 1,2,3,\ldots T \ \ \forall i = 1,2,3,\ldots N \end{cases}$$

14: end for

15: Output: Optimise the charging schedule and charging power of each PEB's battery from the grid for the time interval $t = 1\ldots,24$ h (with 10 minutes time intervals).

Steps (1-10) show the PEB pantograph-based charge scheduling algorithm. Step 8 maximises the charging power drawing by PEB *i* from the grid. Step 9 ensures all PEBs are fully charged before their departure. Steps 11-14 show the PEB_i battery discharging model. Step 13 ensures PEBs SOC updates each time interval *t*. This $E_c^{PEB(i)}(t)$ denotes the total energy consumption due to vehicle weight, air-condition unit, passenger weight, route, and stop, respectively.

5.4 **Results and Discussion**

Simulation has been performed for the SkyBus fleet using real-world data from Yutong PEBs [133] and SkyBus's arrival and departure schedule [134]. The electricity purchasing price from the grid (Blue dotted line) [128] and Genesis Energy (one of the biggest distributions and generation companies in New Zealand) offer Selling back to grid price (Magenta dotted line) which is *2/3rd* of the purchasing price [125]. According to these two prices, and the selling to PEB price (Black dotted line) is set in the proposed FITs scheme for the bus depot ecosystem shown in Figure 5.7. The proposed Depot and Pantograph Charge Scheduling algorithm has been tested and analysed the charging impact of PEBs using K-9 feeder in Manurewa, Auckland, New Zealand.

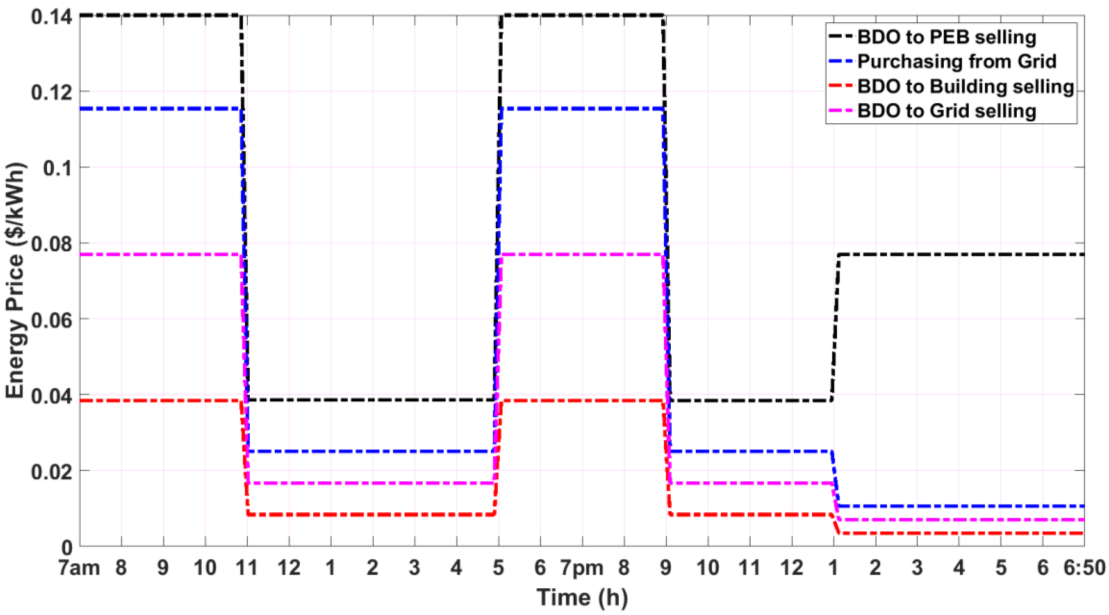

Figure 5. 7 Proposed feed-in tariffs scheme for Bus Depot Charging Ecosystem.

To validate the proposed battery discharging model, diverse vehicle characteristics such as vehicle weight, passenger weight, air-conditioning unit, and route topology such as route and stops affecting the driving range of the vehicle are all used in the proposed PEB discharging model. The simulation has been performed using Yutong PEBs (374 kWh) for three test cases: i) fully loaded the bus with air conditioning unit fully on; ii) 50% loaded bus with air conditioning unit partially on, and iii) fully unloaded bus with air conditioning unit off. Table 5.5 shows the energy consumption rate for each test case.

Table 5. 5 One Trip Energy Consumption for Skybus (Airport-City)

Test Cases	Energy Consumption (Yutong)	Energy Consumption					Total Energy Consumption (one trip)
		Vehicle Characteristic			Route Topography		
		Vehicle Weight	A/C Unit	Passenger Weight	Route	Stops	
1	1.36kWh/km	16 KWh	3.3 kWh	3.1 kWh	2.6KWh	5.4kWh	30.40 kWh
2	1.26kWh/km	16 kWh	1.65kWh	1.55 kWh	1.3 kWh	5.4kWh	25.90 kWh
3	1.07kWh/km	16 kWh	0 kWh	0 kWh	0.65kWh	5.4kWh	22.05 kWh

5.4.1. Depot Charge Scheduling Algorithm

The simulation results and discussions of the depot charge scheduling algorithm for three scenarios including the peak, off-peak, and normal time are given in the subsections.

Scenario 1 (Peak time): The SOC updates of PEB1, PEB6, PEB12 (corresponding to test cases I, II, and III, respectively, in Table 5.5) with 374kWh battery capacity in the PEBDC Ecosystem at each time interval under depot charging for the whole day are shown in Figure 5.8a. .Each of the three PEBs was on the road (with different energy consumption rates) until 7:00 pm, 7:50 pm, and 8:50 pm, respectively, after which they started to charge in the bus depot charging station. Between 7:00–9:00 pm, the price on the grid is high, and thus PEB1 and PEB6 are charged from ESS. After 1:00 am, all three PEBs are charged from the grid as the price and load on the grid are low. The SOC updates of all three PEBs shown in Figure 5.8a are calculated using equation (5.1).

$$SOC^{PEB(i)}(t+1) = SOC^{PEB(i)}(t) + \left(P^{ESS2C}(t) + P^{G2C}(t) + P^{PV2C}(t)\right) * \Delta t * \eta_{char} \tag{5.1}$$

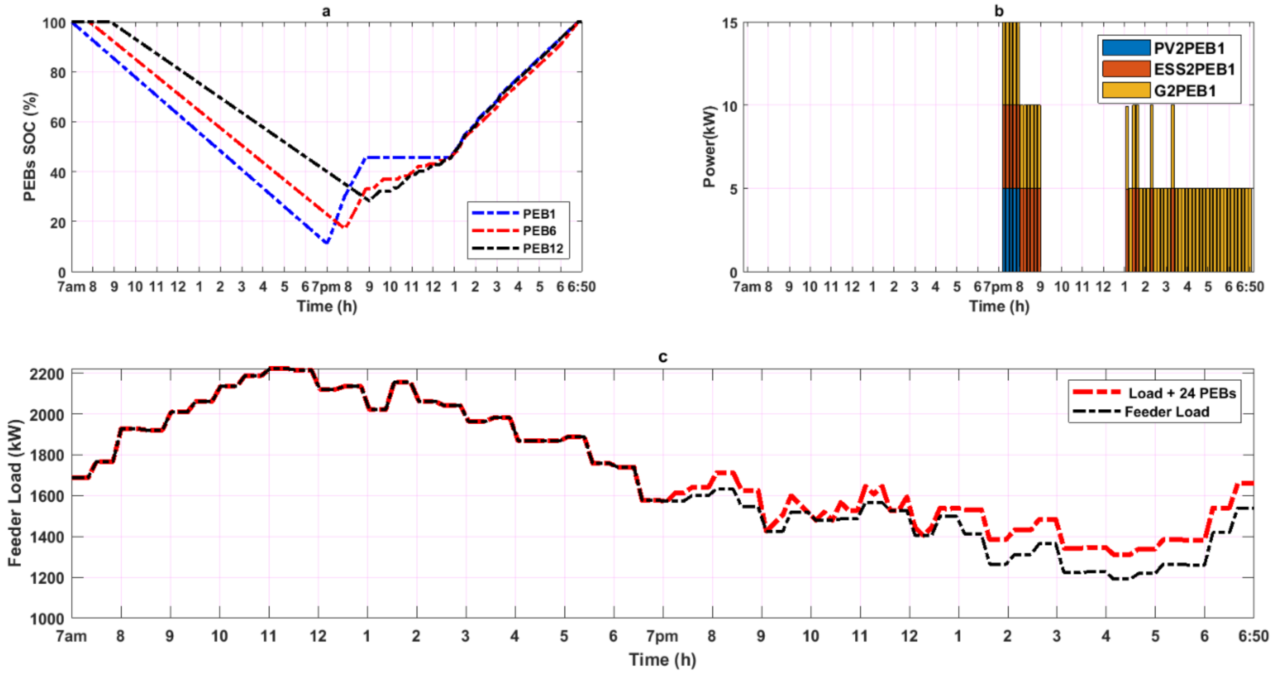

Figure 5. 8 Peak travel a) SOC of 3 PEBs; b) PEB1 charging from PV, ESS, and grid and c) Impact of charging 24 PEBs on the LV Feeder.

Considering the negative impact on the power distribution network, a limit of 5 kW is set on the allowable power injection from the grid which overcomes the transformer overloading issue. The power generated by PV, available power in the ESS, and a limited amount of power from the grid are used to charge the PEBs. As an example, the power taken by PEB1 from PV, ESS, and grid is shown in Figure 5.8b. Moreover, charging the whole fleet has also much less effect on the distribution feeder as can be observed in Figure 5.8c.

Scenario 2 (Off-peak time): During the off-peak travel, PEB1, PEB2, and PEB4 were on the road (different energy consumption rate shown in Table 5.5) until 3:00 am, 3:30 am, and 4:30 am, respectively, after which they started to charge between 3:00 - 8:00 am. The SOC updates of PEB1, PEB2, and PEB4 are shown in Figure 5.9a. The power generated by PV, available power in the ESS, and a limited amount of power from the grid are used to charge the PEBs. As an example, the power taken by PEB1 from PV, ESS, and the grid is shown in Figure 5.9b and the loading impact of all 8 PEBs is shown in Figure 5.9c.

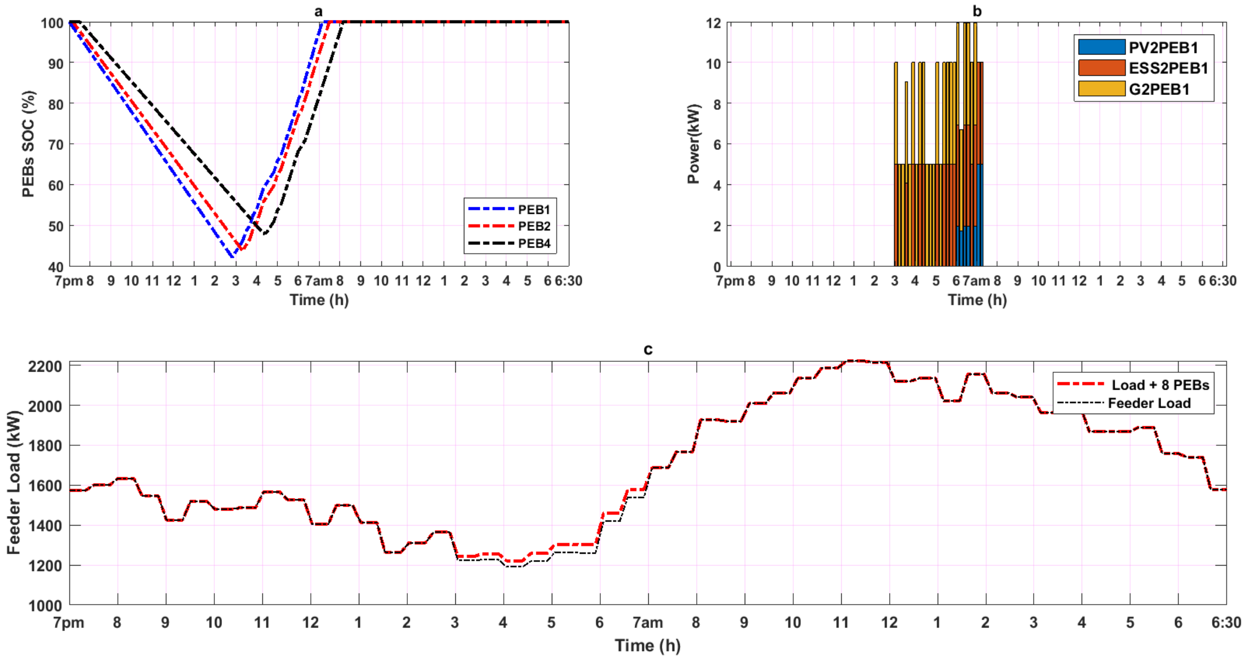

Figure 5. 9 Off-peak travel: a) SOC of 3 PEBs; b) PEB1 charging from PV, ESS, and grid, and c) Impact of charging 8 PEBs on the LV Feeder.

Scenario 3 (Normal): During the normal travel period, PEB1, PEB3, and PEB6 were on the road (different energy consumption rates are shown in Table 5,5) until 7:00 am, 7:40 am, and 8:40 am, respectively, after which they started to charge between 7:00 - 10:00 am. The SOC updates of PEB1, PEB3, and PEB6 are shown in Figure 5. 10a. The power generated by PV, available power in the ESS, and a limited amount of power from the grid are used to charge the PEBs. As an example, the power was taken by PEB1 from PV, ESS, and the grid is shown in Figure 5. 10b, and the loading impact of all 12 PEBs is shown in Figure 5. 10c.

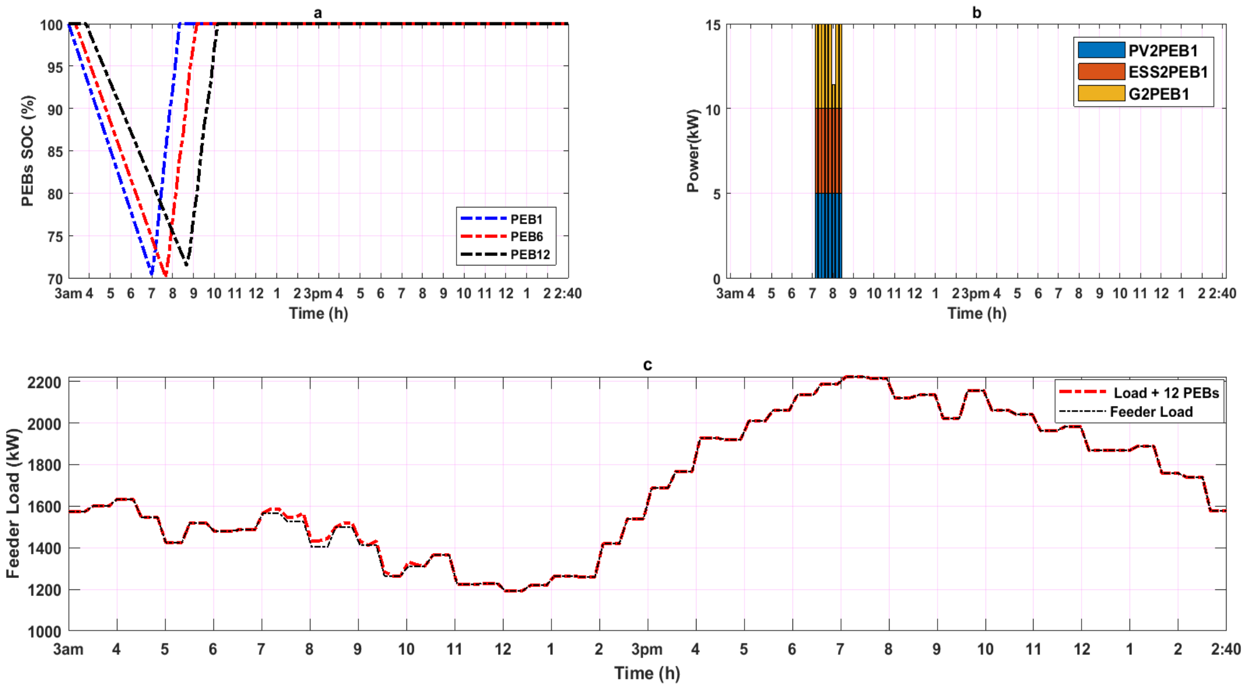

Figure 5. 10 Normal travel: a) SOC of 3 PEBs; b) PEB1 charging from PV, ESS, and grid, and c) Impact of charging 12 PEBs on the LV Feeder.

5.4.2. Pantograph Charge Scheduling Algorithm

The simulation results and discussions of the pantograph charge scheduling algorithm for three scenarios including the peak, off-peak, and normal time are given in the subsections.

Scenario 1 (Peak time): The SOC updates of PEB1, PEB6, PEB12 (corresponding to test cases I, II, and III, respectively, in Table 5.5) with 374kWh battery capacity in the bus depot charging station at each time interval under pantograph charging for the whole day is shown in Figure 5. 11. The slope of PEB1 and PEB6 are steeper than PEB12 due to higher SOC consumption per trip of PEB1 and PEB6 compared to PEB12.

PEB1, PEB6, and PEB 12 are charged upon their arrival at 7:00 pm,7:50 pm, and 8: 50 pm respectively as shown in Figure 5. 11a. The extra load due to charging PEBs in the distribution substation causes transformer overloading. The transformer loading refers to the apparent power (kVA) which should be less than the transformer's kVA rating. If the load demand goes more than the transformer kVA rating, then the transformer can be overloaded [146]. The loading impact of charging three PEBs and all 24 PEBs (charging at 7:50 pm) on the distribution feeder is shown in Figure 5. 11b and Figure 5. 11c, respectively.

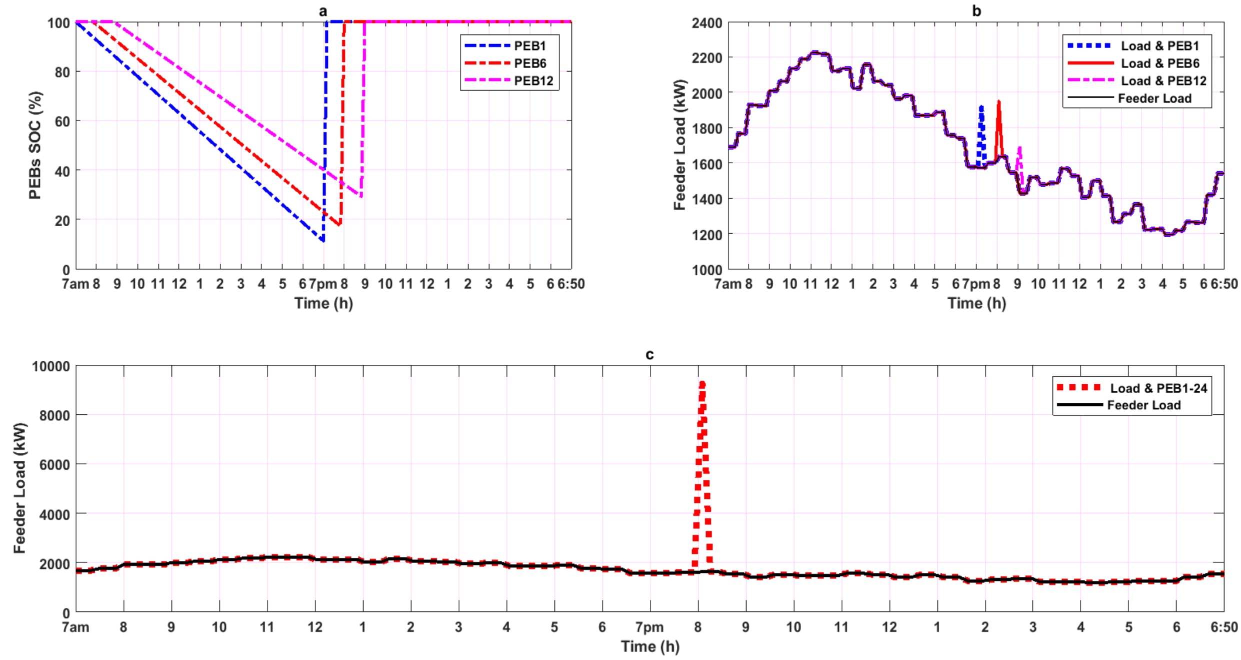

Figure 5. 11 Peak travel: a) SOC of 3 PEBs; b) Impact of charging 3 PEBs and c) Impact of charging 24 PEBs on the LV Feeder.

Scenario 2 (Off-peak time): In the case of off-peak travel, PEB1, PEB2, and PEB4 were on the road (different energy consumption rates shown in Table 5.5) until 3:00 am, 3:30 am, and 4:30 am, respectively. The PEB1, PEB2, and PEB 4 are charged upon their arrival and the SOC update is shown in Figure 5. 12a. The loading impact of charging three PEBs, and all 8 PEBs (charging at 3:30) on the distribution feeder are shown in Figure 5. 12b and Figure 5. 12c, respectively.

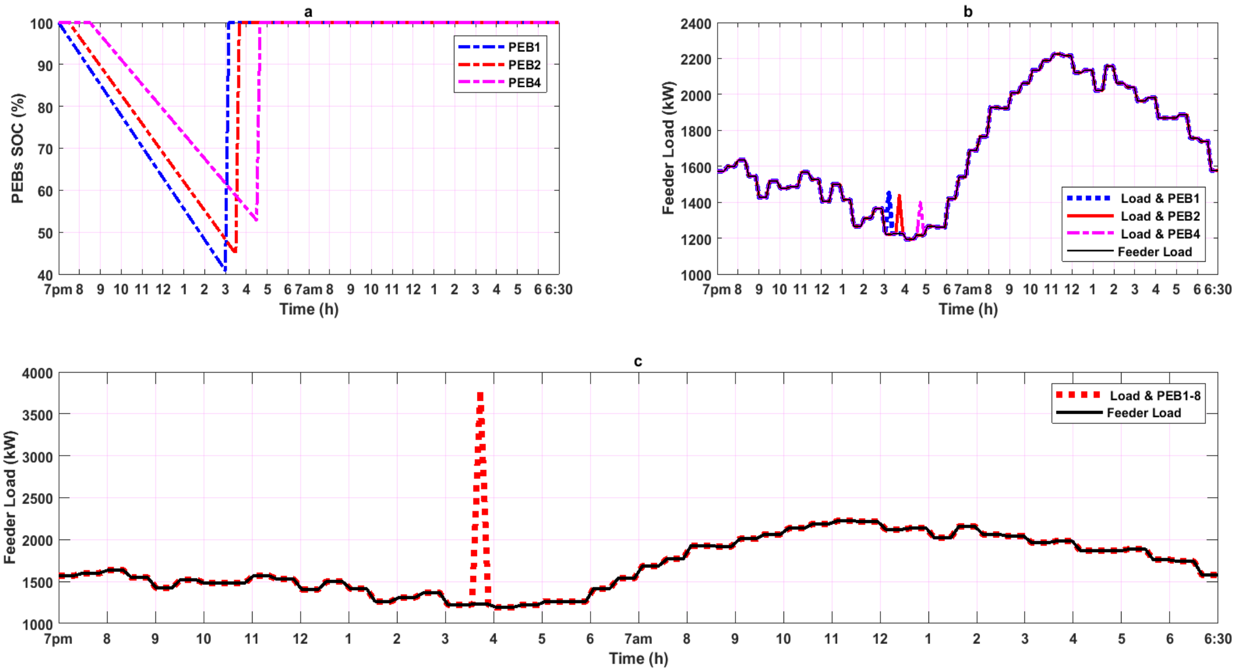

Figure 5.12 Off-Peak travel: a) SOC of 3 PEBs; b) Impact of charging 3 PEBs and c) Impact of charging 8 PEBs on the LV Feeder.

Scenario 3 (Normal): During the normal travel period, PEB1, PEB3, and PEB6 were on the road (different energy consumption rates shown in Table 5.5) until 7:00 am, 7:40 am, and 8:40 am, respectively, after which they started to charge. The SOC updates of PEB1, PEB3, and PEB6, and their loading impact on LV feeder are shown in Figure 5.13a and Figure 5.13b respectively, and the loading impact of all 12 PEBs is shown in Figure 5.13c.

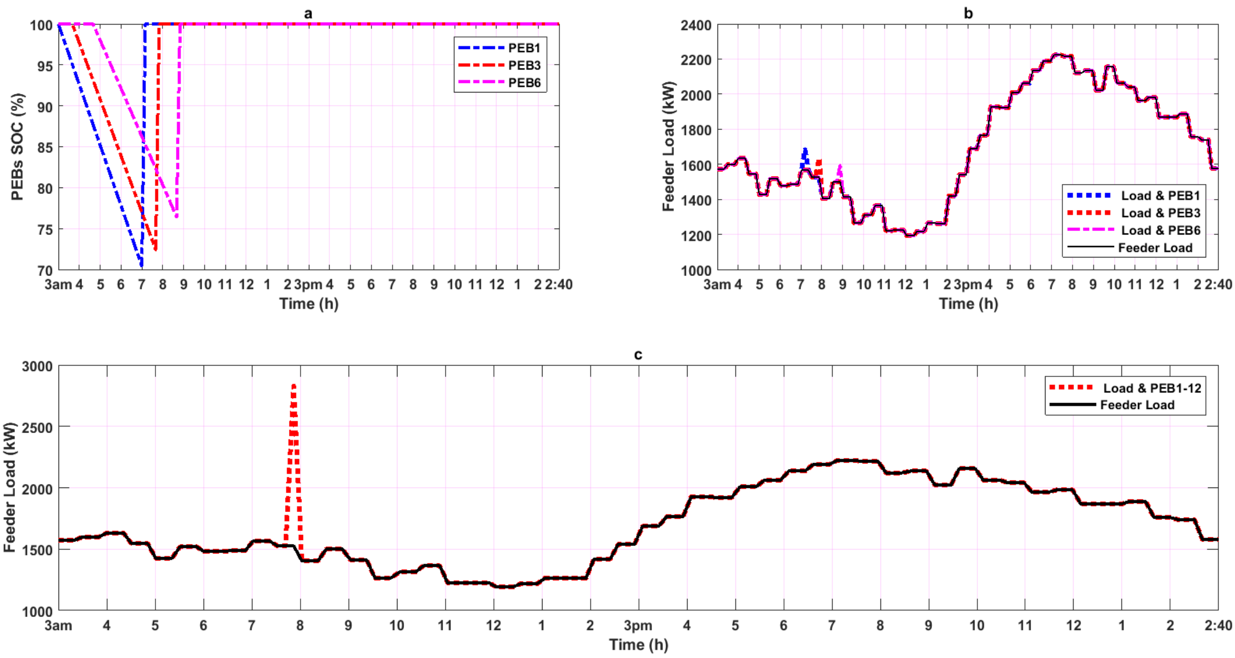

Figure 5. 13 Normal travel: a) SOC of 3 PEBs; b) Impact of charging 3 PEBs and c) Impact of charging 12 PEBs on the LV Feeder.

5.4.3. Depot vs Pantograph Charging Scheme Comparison

Each of the charging schemes has its advantages and disadvantages and, during the selection, the nine factors should be considered as described in Table 5.6.

Table 5. 6 Comparison of Depot and Pantograph Charging

S. No	Characteristics	Charging Scheme		Reference
		Depot	**Pantograph**	
		Plug-in Electric Bus		
1	Bus Battery Capacity	Typically>200 kWh	Typically >40-120kWh	[147]
2	Bus Range	200 to 300 km	Unlimited theoretically	[148]
3	Charging power	40–120 kW	Up to 600 kW	[149]
4	Bus Weight	More	Less	[150]
5	Bus Cost	High	Low	[149]
6	Charging time	4-6 hours	3-6 minutes	[151]
		Charging Infrastructure		
7	Transformer	No need to upgrade	Need to upgrade	[71]
8	Grid Stability	High	Low	[152]
10	Location	Depot charging	En-route charging	[153]
11	BDO Profit	High	Low	[25]

5.5 **Summary**

This chapter presents two charge scheduling algorithms i.e., i) Depot charging ii) Pantograph charging, and a discharging model for PEBs. The key findings of the work are presented as follows:

i) **In the PEB charge scheduling algorithm,** the selling/purchasing agents i.e., PV, ESS, and grid in the PEBDC ecosystem are used for charging the PEB. However, in pantograph PEBs are charged only from the grid.

ii) **In PEB discharging model,** several vehicle energy consumption factors including i) vehicle characteristics such as vehicle weight, air-conditioning unit, and passenger weight, and ii) route topography i.e., route, and stop are considered for the buses charging their batteries in both the depot and with pantograph charging.

iii) **Physical structure limitations**: number of the chargers, charging capacity of each charger, space, and power grid limitation (large-scale PEBs electrification causes an intense burden on the power grid). PEBs limitations: i) consume high charging power, ii) required considerable charging time, ii) Another PEB limitation is heating. Especially in the summer, heat dissipation at charging stations can be a serious issue; depending on the number of chargers and the power demand. iv) strict operation task (arrival and departure) so all PEBs need to be fully charged before the next day's departure.

iv) **The PEB charge scheduling algorithm and discharging model** are formulated and analysed simultaneously using mixed-integer linear programming (MILP) in the CPLEX model and their charging impact on a real distribution system in New Zealand is also analysed.

v) **Both the proposed algorithms are tested for all four seasons;** in the pantograph, worst case, charging all the PEBs at the same time causes heavy overloading of the distribution transformer. However, in depot charging due to charging the PEBs during the night-time, the distribution transformer is not overloaded.

Chapter 6 Conclusion and Future Work

The work carried out in this thesis is summarised in this chapter, the role of each chapter in accomplishing the key objective of the thesis is discussed. The overall conclusion is then drawn, and the scope and possible future work of this thesis is also presented.

6.1 Summary

The key objective of this thesis was firstly to develop an Energy Management System (EMS) model with an efficient control scheme and smart optimisation for the Plug-In Electric Bus (PEB) eco-system (consisting of PV and ESS, electrical grid, and chargers). The proposed EMS model is based on a double-sided auction mechanism and not only reduces the carbon emission but also maximises the Bus Depot Operator's (BDO) profit. Secondly, it focused on the development of charge scheduling algorithms for the depot, and pantograph-based PEB charging. These charging algorithms not only overcome the bus driver range anxiety issue but also develop the depot charge scheduling algorithm which reduces the PEB charging impact on the LV feeder.

Chapter 1 outlines the background and motivation of this thesis focusing on the feasibility study for green and resilient transportation considering the i) government policy framework ii) low emission bus roadmap iii) PEB and charging infrastructure economic iv) greenhouse gas emission, and v) current and future power generation to increase the uptake of PEB eco charging infrastructure. The challenges and issues e.g., charging demand, PEB operating economy, grid security, geographical and social ecology for the allocation of the PEB Depot Charging (PEBDC) ecosystem are also presented. Consequently, to accomplish a coherent piece of research the detailed mathematical modeling of depot charging ecosystem components including energy storage system, solar PV, charge controller, and the inverter have been discussed in this chapter.

To familiarise the reader with basic EV characteristics and its charging impact on the LV feeder, Chapter 2 highlights the literature review on i) the State-of-the-Art Microgrid, ii) EV technologies, iii) EV Charing Methods iv) EV charging configuration, standards, ports, and connectors, v) PEBDC ecosystem opportunities and challenges, and vi) PEB charging impact on LV feeder.

To evaluate the charging impact of PEBs on LV feeder, the Particle Swarm Optimization (PSO) algorithm was used in Chapter 3 to find optimal distributed generation (DG) size and location for the PEBDC ecosystem integrated with an LV feeder to reduce costs such as i) DG deployment, ii) voltage limit violation and, iii) active power loss. The PEBs penetration was increased from 0 % to 100 % and the size and location for two IEEE test systems and one real distribution system were calculated.

Chapter 4 discusses the comprehensive mathematical model used to maximise the BDO profit by performing the energy trading among the participants such as grid PV, ESS, and PEBs in the bus depot charging ecosystem. The double-sided auction-based EMS model is proposed and used for energy trading and the model is tested for all four seasons (summer, autumn, winter, and spring).

Chapter 5 discusses the two proposed PEB charge scheduling algorithms i.e., i) Overnight Depot and ii) Pantograph. Simulations have been performed and the results show that the PEBDC ecosystem (consisting of the grid and solar PV system integrated with ESS) can significantly reduce the load on the grid while pantograph charging (consisting of the grid only) immensely increased the load on the grid and this causes the distribution transformer to be heavily overloaded.

6.2 Scope for Future Work

Even though a conclusive body of the thesis work has been summarised, there is an area where this thesis can further contribute. The charge scheduling algorithms and EMS model presented in this thesis can be utilised in other EV charge scheduling and controlling areas. The scope of the future work which can lead from this thesis is summarised below.

- The proposed PEB charge scheduling algorithms can be applied to the charging scheduling of private EVs and Electric Ferries where the arrival and departure schedules are known.

- The proposed charging ecosystem consists of PV, ESS, and the electrical grid. However, mixing the other renewable DGs such as wind energy and Biomass energy can make the ecosystem more robust and sustainable and can conquer the intermittency issue caused by PV and wind.
- Consideration of the power generated by the regenerative braking system of PEBs in the proposed charging and discharging model can lead to a more precise SOC estimation of PEBs.
- Chapter 4 analysed the energy trading among the entities (PV, ESS, building, grid, and PEBs) in the ecosystem. However, generating power in multiple depots by using renewable energy resources and performing the energy trading between them can reduce the overloading of the grid.
- Performing the energy trading between Vehicle to Vehicle (V2V) and Vehicle to Grid (V2G) can avoid the peak load on the grid and encourage the participation of the depot owner in the energy reserve market.
- The investigation of the risk of charging PEBs on the distribution grid, such as over-current and under-voltage, power losses, and the stress on the distribution transformer can be done.
- The battery capacity optimisation for a given route can also be evaluated to minimise the vehicle cost.

References

[1] E. S. Mills and B.-N. Song, *Urbanization and urban problems*. Brill, 2020.

[2] F. Pan, "Industrialization," *International Encyclopedia of Geography: People, the Earth, Environment and Technology: People, the Earth, Environment and Technology*, pp. 1-6, 2016.

[3] P. Nejat, F. Jomehzadeh, M. M. Taheri, M. Gohari, and M. Z. Abd. Majid, "A global review of energy consumption, CO_2 emissions and policy in the residential sector.," *Renew and Sustain Energy Rev*, vol. 43, pp. 843-862, 2015, doi: 10.1016/j.rser.2014.11.066.

[4] Y. Yoldaş, A. Önen, S. Muyeen, A. V. Vasilakos, and İ. Alan, "Enhancing smart grid with microgrids: Challenges and opportunities," *Renewable and Sustainable Energy Reviews*, vol. 72, pp. 205-214, 2017.

[5] L. P. Fernandez, T. G. San Román, R. Cossent, C. M. Domingo, and P. Frias, "Assessment of the impact of plug-in electric vehicles on distribution networks," *IEEE transactions on power systems*, vol. 26, no. 1, pp. 206-213, 2010.

[6] H. Farzin, M. Fotuhi-Firuzabad, and M. Moeini-Aghtaie, "Reliability studies of modern distribution systems integrated with renewable generation and parking lots," *IEEE Transactions on Sustainable Energy*, vol. 8, no. 1, pp. 431-440, 2016.

[7] Z. Liu, F. Wen, and G. Ledwich, "Optimal planning of electric-vehicle charging stations in distribution systems," *IEEE Transactions on Power Delivery*, vol. 28, no. 1, pp. 102-110, 2012.

[8] *Electric Mobility & Development. Available online : http://documents1.worldbank.org/curated/pt/193791543856434540/pdf/132636-EMADv4-web.pdf (accessed on 20 January 2020).*

[9] *Auckland's Low Emission Bus Roadmap. Available online https://at.govt.nz/media/1980070/low-emissions-bus-roadmap-dec-2018.pdf (accessed on 15 March 2020).*

[10] *Vehicles exempt from paying road user charge. Avaiable online : https://www.transport.govt.nz/land/road-user-charges-ruc-and-petrol-excise-duty-*

ped/roaduserchargeslegislationchanges/vehiclesexemptfrompayingrucqandas/ (accessed on 15 March 2020).

[11] *Electric Vehicles Programme. Avialable online : https://www.transport.govt.nz/multi-modal/climatechange/electric-vehicles (accessed on 21 August 2020).*

[12] *New Zealand's emissions reduction targets. Available online : https://www.mfe.govt.nz/climate-change/climate-change-and-government/emissions-reduction-targets/about-our-emissions (accessed on 21 August 2020).*

[13] *Uptake of battery electric buses countries. Avaiable online: https://www.bloomberg.com/news/articles/2019-05-15/in-shift-to-electric-bus-it-s-china-ahead-of-u-s-421-000-to-300 (accessed on 21 August 2020).*

[14] *Waiheke bus network gets electrified. Avaiable online: https://ourauckland.aucklandcouncil.govt.nz/articles/news/2019/07/waiheke-bus-network-gets-electrified/ (accessed on 22 September 2020).*

[15] *Tranzit Coachlines Commitment to New Zealand. Avaiable online: https://tranzit.co.nz/environmental-promise (accessed on 21 August 2020).*

[16] *Powering ahead towards a better city. Avaiable online : https://www.redbus.co.nz/about/electric-buses/ (accessed on 21 August 2020).*

[17] S. Yang, R. Li, and J. Li, "“Separation of Vehicle and Battery” of Private Electric Vehicles and Customer Delivered Value: Based on the Attempt of 2 Chinese EV Companies," *Sustainability*, vol. 12, no. 5, p. 2042, 2020.

[18] Battery Pack Prices Fall As Market Ramps Up. Avaiable online: https://about.bnef.com/blog/battery-pack-prices-fall-as-market-ramps-up-with-market-average-at-156-kwh-in-2019/ (accessed on 21 August 2020).

[19] *Auckland's Greenhouse Gas Inventory to 2016. Avaiable online: https://knowledgeauckland.org.nz/media/1057/tr2019-002-aucklands-greenhouse-gas-inventory-to-2016.pdf (accessed on 21 July 2020).*

[20] *Transpower: Power System Live Data. Avaiable online: https://www.transpower.co.nz/power-system-live-data (Accessed on 21 July 2020).*

[21] NZ embracing renewable electricity future. Avaiable online: https://www.beehive.govt.nz/release/nz-embracing-renewable-electricity-future (acccessed on 21 July 2020).

[22] H. Wu and D. Niu, "Study on influence factors of electric vehicles charging station location based on ISM and FMICMAC," *Sustainability,* vol. 9, no. 4, p. 484, 2017.

[23] H. Zhang, Z. Hu, Z. Xu, and Y. Song, "An integrated planning framework for different types of PEV charging facilities in urban area," *IEEE Transactions on Smart Grid,* vol. 7, no. 5, pp. 2273-2284, 2015.

[24] A. Jahic, M. Eskander, and D. Schulz, "Charging schedule for load peak minimization on large-scale electric bus depots," *Applied Sciences,* vol. 9, no. 9, p. 1748, 2019.

[25] S. M. Arif, T. T. Lie, B. C. Seet, S. M. Ahsan, and H. A. Khan, "Plug-In Electric Bus Depot Charging with PV and ESS and Their Impact on LV Feeder," *Energies,* vol. 13, no. 9, p. 2139, 2020.

[26] L. P. Fernandez, T. G. San Roman, R. Cossent, C. M. Domingo, and P. Frias, "Assessment of the impact of plug-in electric vehicles on distribution networks," *IEEE transactions on power systems,* vol. 26, no. 1, pp. 206-213, 2010.

[27] E-buses today in operation. Available online : https://www.sustainable-bus.com/news/electric-vehicle-outlook-2020-bnef-electric-buses/ (accessed on 24 August 2020).

[28] S. Khan, A. Ahmad, F. Ahmad, M. Shafaati Shemami, M. Saad Alam, and S. Khateeb, "A comprehensive review on solar powered electric vehicle charging system," *Smart Science,* vol. 6, no. 1, pp. 54-79, 2018.

[29] V. Hassija, V. Chamola, S. Garg, N. G. K. Dara, G. Kaddoum, and D. N. K. Jayakody, "A blockchain-based framework for lightweight data sharing and energy trading in V2G network," *IEEE Transactions on Vehicular Technology,* 2020.

[30] A. Tchagang and Y. Yoo, "V2B/V2G on Energy Cost and Battery Degradation under Different Driving Scenarios, Peak Shaving, and Frequency Regulations," *World Electric Vehicle Journal,* vol. 11, no. 1, p. 14, 2020.

[31] R. Baharom, N. Hakim, and N. Rahman, "Wireless Vehicle to Vehicle (V2V) Power Transmission using SPMC," in *2020 IEEE 10th Symposium on Computer Applications & Industrial Electronics (ISCAIE)*, 2020: IEEE, pp. 125-130.

[32] Z. Qiao and J. Yang, "Comparison of centralised and distributed battery energy storage systems in LV distribution networks on operational optimisation and financial benefits," *The Journal of Engineering,* vol. 2017, no. 13, pp. 1671-1675, 2017.

[33] L. Noel, G. Z. de Rubens, B. K. Sovacool, and J. Kester, "Fear and loathing of electric vehicles: the reactionary rhetoric of range anxiety," *Energy research & social science,* vol. 48, pp. 96-107, 2019.

[34] R. A. Messenger and A. Abtahi, *Photovoltaic systems engineering*. CRC press, 2017.

[35] I. Alsaidan, A. Alanazi, W. Gao, H. Wu, and A. Khodaei, "State-of-the-art in microgrid-integrated distributed energy storage sizing," *Energies,* vol. 10, no. 9, p. 1421, 2017.

[36] M. Nouni, S. Mullick, and T. Kandpal, "Photovoltaic projects for decentralized power supply in India: A financial evaluation," *Energy policy,* vol. 34, no. 18, pp. 3727-3738, 2006.

[37] L. He and K. G. Shin, "How Long Will My Phone Battery Last?," *arXiv preprint arXiv:1711.03651,* 2017.

[38] J. Fellner, G. Loeber, S. Vukson, and C. Riepenhoff, "Lithium-ion testing for spacecraft applications," *Journal of Power Sources,* vol. 119, pp. 911-913, 2003.

[39] A. Gupta, R. Saini, and M. Sharma, "Modelling of hybrid energy system—Part I: Problem formulation and model development," *Renewable Energy,* vol. 36, no. 2, pp. 459-465, 2011.

[40] Å. G. Tveten, T. F. Bolkesjø, T. Martinsen, and H. Hvarnes, "Solar feed-in tariffs and the merit order effect: A study of the German electricity market," *Energy Policy,* vol. 61, pp. 761-770, 2013.

[41] R. H. Lasseter, "Microgrids," in *2002 IEEE Power Engineering Society Winter Meeting. Conference Proceedings (Cat. No. 02CH37309),* 2002, vol. 1: IEEE, pp. 305-308.

[42] N. Pearre and L. Swan, "Reimagining renewable electricity grid management with dispatchable generation to stabilize energy storage," *Energy,* p. 117917, 2020.

[43] L. Shi and M. Y. L. Chew, "A review on sustainable design of renewable energy systems," *Renewable and Sustainable Energy Reviews,* vol. 16, no. 1, pp. 192-207, 2012.

[44] F. Ahmad and M. S. Alam, "Optimal sizing and analysis of solar PV, wind, and energy storage hybrid system for campus microgrid," *Smart Science,* vol. 6, no. 2, pp. 150-157, 2018.

[45] S. Parhizi, H. Lotfi, A. Khodaei, and S. Bahramirad, "State of the art in research on microgrids: A review," *Ieee Access,* vol. 3, pp. 890-925, 2015.

[46] A. M. l. MIT, "New Zealand import Crude Petroleum " https://atlas.media.mit.edu/en/profile/country/deu/, 2016.

[47] M. F. M. Sabri, K. A. Danapalasingam, and M. F. Rahmat, "A review on hybrid electric vehicles architecture and energy management strategies," *Renew and Sustain Energy Rev,* vol. 53, pp. 1433-1442, 2016, doi: 10.1016/j.rser.2015.09.036.

[48] N. Shaukat *et al.*, "A survey on electric vehicle transportation within smart grid system," *Renew and Sustain Energy Rev,* vol. 81, pp. 1329-1349, 2018, doi: 10.1016/j.rser.2017.05.092.

[49] Y. G. M. Ehsani, S. E. Gay, and A. Emadi,, "Modern Electric, Hybrid Electric, and Fuel Cell Vehicles: Fundamentals, Theory, and Design," *CRC press*, 2018.

[50] K. T. Chau and Y. S. Wong, "Overview of power management in hybrid electric vehicles," *Energy Conversion and Management* vol. 43, pp. 1953–1968, 2002.

[51] S. Miller, "Hybrid-Electric Vehicle Model in Simulink," https://au.mathworks.com/matlabcentral/fileexchange/28441-hybrid-electric-vehicle-model-in-simulink, 2014.

[52] Q. Dai, T. Cai, S. Duan, W. Zhang, and J. Zhao, "A smart energy management system for electric city bus battery swap station," in *2014 IEEE Conference and Expo Transportation Electrification Asia-Pacific (ITEC Asia-Pacific),* 2014: IEEE, pp. 1-4.

[53] C. Yang, W. Lou, J. Yao, and S. Xie, "On charging scheduling optimization for a wirelessly charged electric bus system," *IEEE Transactions on Intelligent Transportation Systems,* vol. 19, no. 6, pp. 1814-1826, 2017.

[54] S. M. Arif, T. T. Lie, and B. C. Seet, "A Novel Simulation Model for analyzing the State of Charge of Electric Vehicle," *IEEE PES, Innovative Smart Grid Technologies Asia, Singapore* pp. 1–5, 2018.

[55] H. S. Das, C. W. Tan, and A. Yatim, "Fuel cell hybrid electric vehicles: A review on power conditioning units and topologies," *Renewable and Sustainable Energy Reviews,* vol. 76, pp. 268-291, 2017.

[56] Q. Jiang, O. Béthoux, F. Ossart, E. Berthelot, and C. Marchand, "A comparison of real-time energy management strategies of FC/SC hybrid power source: Statistical analysis using random cycles," *International Journal of Hydrogen Energy,* 2020.

[57] A. Emadi, S. S. Williamson, and A. Khaligh, "Power electronics intensive solutions for advanced electric, hybrid electric, and fuel cell vehicular power systems," *IEEE Transactions on power electronics,* vol. 21, no. 3, pp. 567-577, 2006.

[58] A. Ahmad, Z. A. Khan, M. Saad Alam, and S. Khateeb, "A Review of the Electric Vehicle Charging Techniques, Standards, Progression and Evolution of EV Technologies in Germany," *Smart Science,* vol. 6, no. 1, pp. 36-53, 2017, doi: 10.1080/23080477.2017.1420132.

[59] Q. Dai, T. Cai, S. Duan, and F. Zhao, "Stochastic Modeling and Forecasting of Load Demand for Electric Bus Battery-Swap Station," *IEEE Trans Power Del,* vol. 29, no. 4, pp. 1909-1917, 2014, doi: 10.1109/tpwrd.2014.2308990.

[60] J. Martínez-Lao, F. G. Montoya, M. G. Montoya, and F. Manzano-Agugliaro, "Electric vehicles in Spain: An overview of charging systems," *Renew and Sustain Energy Rev,* vol. 77, pp. 970-983, 2017, doi: 10.1016/j.rser.2016.11.239.

[61] B. Sun, X. Tan, and D. Tsang, "Optimal Charging Operation of Battery Swapping and Charging Stations with QoS Guarantee," *IEEE Trans Smart Grid,* pp. 1-1, 2017, doi: 10.1109/tsg.2017.2666815.

[62] T. Zhang, X. Chen, Z. Yu, X. Zhu, and D. Shi, "A Monte-Carlo Simulation Approach to Evaluate Service Capacities of EV Charging and Battery Swapping Stations," *IEEE Trans Ind Informat,* pp. 1-1, 2018, doi: 10.1109/tii.2018.2796498.

[63] D. H. Tran, V. B. Vu, and W. Choi, "Design of a High-Efficiency Wireless Power Transfer System With Intermediate Coils for the On-Board Chargers of Electric Vehicles," *IEEE Trans Power Electron,* vol. 33, no. 1, pp. 175-187, 2018, doi: 10.1109/tpel.2017.2662067.

[64] D. Patil, M. K. McDonough, J. M. Miller, B. Fahimi, and P. T. Balsara, "Wireless Power Transfer for Vehicular Applications: Overview and Challenges," *IEEE Trans Transport Electrific*, vol. 4, no. 1, pp. 3-37, 2018, doi: 10.1109/tte.2017.2780627.

[65] K. M. Tan, V. K. Ramachandaramurthy, and J. Y. Yong, "Integration of electric vehicles in smart grid: A review on vehicle to grid technologies and optimization techniques," *Renew Sustain Energy Rev,* vol. 53, pp. 720-732, 2016.

[66] Y. Yoldaş, A. Önen, S. M. Muyeen, A. V. Vasilakos, and İ. Alan, "Enhancing smart grid with microgrids: Challenges and opportunities," *Renew and Sustain Energy Rev,* vol. 72, pp. 205-214, 2017, doi: 10.1016/j.rser.2017.01.064.

[67] C. H. Dharmakeerthi, N. Mithulananthan, and T. K. Saha, "Impact of electric vehicle fast charging on power system voltage stability," *International Journal of Electrical Power & Energy Systems,* vol. 57, pp. 241-249, 2014, doi: 10.1016/j.ijepes.2013.12.005.

[68] S. Habib, M. M. Khan, F. Abbas, L. Sang, M. U. Shahid, and H. Tang, "A Comprehensive Study of Implemented International Standards, Technical Challenges, Impacts and Prospects for Electric Vehicles," *IEEE Access*, vol. 6, pp. 13866-13890, 2018, doi: 10.1109/access.2018.2812303.

[69] J. Y. Yong, V. K. Ramachandaramurthy, K. M. Tan, and N. Mithulananthan, "A review on the state-of-the-art technologies of electric vehicle, its impacts and prospects," *Renew Sustain Energy Rev,* vol. 49, pp. 365-385, 2015, doi: 10.1016/j.rser.2015.04.130.

[70] M. Yilmaz and P. T. Krein, "Review of the Impact of Vehicle-to-Grid Technologies on Distribution Systems and Utility Interfaces," *IEEE Trans Power Electron,* vol. 28, no. 12, pp. 5673-5689, 2013, doi: 10.1109/tpel.2012.2227500.

[71] F. Meishner, B. Satvat, and D. U. Sauer, "Battery electric buses in european cities: Economic comparison of different technological concepts based on actual demonstrations," in *2017 IEEE Vehicle Power and Propulsion Conference (VPPC),* 2017: IEEE, pp. 1-6.

[72] I. Carrilero, M. González, D. Anseán, J. C. Viera, J. Chacón, and P. G. Pereirinha, "Redesigning European Public Transport: Impact of New Battery Technologies in the Design of Electric Bus Fleets," *Transportation research procedia,* vol. 33, pp. 195-202, 2018.

[73] N. S. Pearre, W. Kempton, R. L. Guensler, and V. V. Elango, "Electric vehicles: How much range is required for a day's driving?," *Transportation Research Part C: Emerging Technologies*, vol. 19, no. 6, pp. 1171-1184, 2011, doi: 10.1016/j.trc.2010.12.010.

[74] F. Mwasilu, J. J. Justo, E.-K. Kim, T. D. Do, and J.-W. Jung, "Electric vehicles and smart grid interaction: A review on vehicle to grid and renewable energy sources integration," *Renewable and sustainable energy reviews,* vol. 34, pp. 501-516, 2014.

[75] K. K. Saeid Haghbin, Sonja Lundmark, Mats Alaküla, Ola Carlson, Mats Leksell and Oskar Wallmark, "Integrated Chargers for EV's and PHEV's:Examples and New Solutions," *ICEM* 2010

[76] M. Grenier, MG Hosseini Aghdam, and Torbjörn Thiringer. , "Design of on-board charger for plug-in hybrid electric vehicle," *IET Gener. Transm. Distrib,* pp. 152-152., 2010.

[77] F. Mwasilu, J. J. Justo, E.-K. Kim, T. D. Do, and J.-W. Jung, "Electric vehicles and smart grid interaction: A review on vehicle to grid and renewable energy sources integration," *Renew Sustainable Energy Rev,* vol. 34, pp. 501-516, 2014, doi: 10.1016/j.rser.2014.03.031.

[78] H. Shareef, M. M. Islam, and A. Mohamed, "A review of the stage-of-the-art charging technologies, placement methodologies, and impacts of electric vehicles," *Renewable and Sustainable Energy Reviews,* vol. 64, pp. 403-420, 2016.

[79] H. Das, M. Rahman, S. Li, and C. Tan, "Electric vehicles standards, charging infrastructure, and impact on grid integration: A technological review," *Renewable and Sustainable Energy Reviews,* vol. 120, p. 109618, 2020.

[80] "Budhiraja N. EV charging standards in China and Japan Online Avaiable: https://ihsmarkit.com/research-analysis/ev-charging-standards-in-china-and-japan.html (accessed on 21 July 2020).".

[81] www.at.govt.nz/bus-train-ferry/bus-services/ Available Online : (access on 20 Aug 2020)

[82] W. Kempton and S. E. Letendre, "Electric vehicles as a new power source for electric utilities," *Transportation Research Part D: Transport and Environment*, vol. 2, no. 3, pp. 157-175, 1997.

[83] W. Khan, A. Ahmad, F. Ahmad, and M. Saad Alam, "A comprehensive review of fast charging infrastructure for electric vehicles," *Smart Science*, vol. 6, no. 3, pp. 256-270, 2018.

[84] B. K. Sovacool, J. Kester, L. Noel, and G. Z. de Rubens, "Actors, business models, and innovation activity systems for vehicle-to-grid (V2G) technology: A comprehensive review," *Renewable and Sustainable Energy Reviews*, vol. 131, p. 109963, 2020.

[85] J. D. Bishop, C. J. Axon, D. Bonilla, M. Tran, D. Banister, and M. D. McCulloch, "Evaluating the impact of V2G services on the degradation of batteries in PHEV and EV," *Applied energy*, vol. 111, pp. 206-218, 2013.

[86] J. Hu, H. Morais, T. Sousa, and M. Lind, "Electric vehicle fleet management in smart grids: A review of services, optimization and control aspects," *Renewable and Sustainable Energy Reviews*, vol. 56, pp. 1207-1226, 2016.

[87] Y. Yang, W. Zhang, L. Niu, and J. Jiang, "Coordinated charging strategy for electric taxis in temporal and spatial scale," *Energies*, vol. 8, no. 2, pp. 1256-1272, 2015.

[88] A. R. Abul'Wafa and W. A. F. Mohamed, "Uncoordinated vs Coordinated Charging of Electric Vehicles in Distribution Systems Performance," 2017.

[89] S. Deb, K. Tammi, K. Kalita, and P. Mahanta, "Impact of electric vehicle charging station load on distribution network," *Energies*, vol. 11, no. 1, p. 178, 2018.

[90] M. Mohamed, H. Farag, N. El-Taweel, and M. Ferguson, "Simulation of electric buses on a full transit network: Operational feasibility and grid impact analysis," *Electric Power Systems Research*, vol. 142, pp. 163-175, 2017.

[91] T. Thiringer and S. Haghbin, "Power quality issues of a battery fast charging station for a fully-electric public transport system in Gothenburg city," *Batteries*, vol. 1, no. 1, pp. 22-33, 2015.

[92] M. Schumann, M. Meyer, M. Dietmannsberger, and S. Detlef, "Demands on the Electrical Grid due to Electromobility in Hamburg," in *Proceedings of the 1st E-Mobility Power System Integration Symposium, Berlin, Germany*, 2017, vol. 23.

[93] Z. Chao and C. Xiaohong, "Optimizing battery electric bus transit vehicle scheduling with battery exchanging: Model and case study," *Procedia-Social and Behavioral Sciences*, vol. 96, pp. 2725-2736, 2013.

[94] D. Zhou, Z. Ren, K. Sun, and H. Dai, "Optimization Method of Fast Charging Buses Charging Strategy for Complex Operating Environment," in *2018 2nd IEEE Conference on Energy Internet and Energy System Integration (EI2)*, 2018: IEEE, pp. 1-6.

[95] R.-C. Leou and J.-J. Hung, "Optimal charging schedule planning and economic analysis for electric bus charging stations," *Energies*, vol. 10, no. 4, p. 483, 2017.

[96] D. Singh, D. Singh, and K. Verma, "Multiobjective optimization for DG planning with load models," *IEEE transactions on power systems*, vol. 24, no. 1, pp. 427-436, 2009.

[97] M. H. Moradi and M. Abedini, "A combination of genetic algorithm and particle swarm optimization for optimal DG location and sizing in distribution systems," *International Journal of Electrical Power & Energy Systems*, vol. 34, no. 1, pp. 66-74, 2012.

[98] A. Crossland, D. Jones, and N. Wade, "Planning the location and rating of distributed energy storage in LV networks using a genetic algorithm with simulated annealing," *International Journal of Electrical Power & Energy Systems*, vol. 59, pp. 103-110, 2014.

[99] A. Hassan, M. Saadawi, M. Kandil, and M. Saeed, "Modified particle swarm optimisation technique for optimal design of small renewable energy system supplying a specific load at Mansoura University," *IET Renewable Power Generation*, vol. 9, no. 5, pp. 474-483, 2015.

[100] A. Ameli, S. Bahrami, F. Khazaeli, and M.-R. Haghifam, "A multiobjective particle swarm optimization for sizing and placement of DGs from DG owner's and distribution company's viewpoints," *IEEE Transactions on power delivery*, vol. 29, no. 4, pp. 1831-1840, 2014.

[101] A. El-Zonkoly, "Optimal placement of multi-distributed generation units including different load models using particle swarm optimisation," *IET generation, transmission & distribution*, vol. 5, no. 7, pp. 760-771, 2011.

[102] W. S. Tan, M. Y. Hassan, H. A. Rahman, M. P. Abdullah, and F. Hussin, "Multi-distributed generation planning using hybrid particle swarm optimisation-gravitational search algorithm including voltage rise issue," *IET Generation, Transmission & Distribution,* vol. 7, no. 9, pp. 929-942, 2013.

[103] T. Niknam, M. Narimani, J. Aghaei, and R. Azizipanah-Abarghooee, "Improved particle swarm optimisation for multi-objective optimal power flow considering the cost, loss, emission and voltage stability index," *IET generation, transmission & distribution,* vol. 6, no. 6, pp. 515-527, 2012.

[104] A. H. Syed Muhammad Arif, Tek Tjing Lie, Syed Muhammad Ahsan, and Hassan Abbas Khan, "Analytical Hybrid Particle Swarm Optimization Algorithm for Optimal DG Siting and Sizing in Smart Grid," 2020.

[105] O. I. Elgerd, *Electrical energy systems theory: an introduction*. McGraw-Hill, 1971.

[106] J. Brownlee and J. Kennedy, "Particle swarm optimization," *Encyclopedia of Machine Learning,* vol. 1, no. CA-TR-20101114b-1, pp. 760-766, 2010.

[107] A. A. Esmin, R. A. Coelho, and S. Matwin, "A review on particle swarm optimization algorithm and its variants to clustering high-dimensional data," *Artificial Intelligence Review,* vol. 44, no. 1, pp. 23-45, 2015.

[108] V. Vita, "Development of a decision-making algorithm for the optimum size and placement of distributed generation units in distribution networks," *Energies,* vol. 10, no. 9, p. 1433, 2017.

[109] N. Acharya, P. Mahat, and N. Mithulananthan, "An analytical approach for DG allocation in primary distribution network," *International Journal of Electrical Power & Energy Systems,* vol. 28, no. 10, pp. 669-678, 2006.

[110] J.-C. Kim, S.-M. Cho, and H.-S. Shin, "Advanced power distribution system configuration for smart grid," *IEEE transactions on smart grid,* vol. 4, no. 1, pp. 353-358, 2013.

[111] M. D. Galus and G. Andersson, "Demand management of grid connected plug-in hybrid electric vehicles (PHEV)," in *2008 IEEE energy 2030 conference*, 2008: IEEE, pp. 1-8.

[112] B. Lin and J. Li, "Analyzing cost of grid-connection of renewable energy development in China," *Renewable and Sustainable Energy Reviews,* vol. 50, pp. 1373-1382, 2015.

[113] G. Celli *et al.*, "A comparison of distribution network planning solutions: Traditional reinforcement versus integration of distributed energy storage," in *2013 IEEE Grenoble Conference*, 2013: IEEE, pp. 1-6.

[114] ETEL Transformers Cost. Available online : http://www.eteltransformers.co.nz/ (accessed on 25 August 2020)

[115] D. Stahleder, D. Reihs, S. Ledinger, and F. Lehfuss, "Impact Assessment of High Power Electric Bus Charging on Urban Distribution Grids," in *IECON 2019-45th Annual Conference of the IEEE Industrial Electronics Society*, 2019, vol. 1: IEEE, pp. 4304-4309.

[116] O. Krishan and S. Suhag, "Grid-independent PV system hybridization with fuel cell-battery/supercapacitor: Optimum sizing and comparative techno-economic analysis," *Sustainable Energy Technologies and Assessments,* vol. 37, p. 100625, 2020.

[117] Y. Fan and X. Xia, "A multi-objective optimization model for energy-efficiency building envelope retrofitting plan with rooftop PV system installation and maintenance," *Applied energy,* vol. 189, pp. 327-335, 2017.

[118] P. G. V. Sampaio and M. O. A. González, "Photovoltaic solar energy: Conceptual framework," *Renewable and Sustainable Energy Reviews,* vol. 74, pp. 590-601, 2017.

[119] W. Cole, B. Frew, P. Gagnon, A. Reimers, J. Zuboy, and R. Margolis, "Envisioning a low-cost solar future: Exploring the potential impact of Achieving the SunShot 2030 targets for photovoltaics," *Energy,* vol. 155, pp. 690-704, 2018.

[120] Q. Dai, J. Liu, and Q. Wei, "Optimal photovoltaic/battery energy storage/electric vehicle charging station design based on multi-agent particle swarm optimization algorithm," *Sustainability,* vol. 11, no. 7, p. 1973, 2019.

[121] W. Khan, F. Ahmad, and M. S. Alam, "Fast EV charging station integration with grid ensuring optimal and quality power exchange," *Engineering Science and Technology, an International Journal,* vol. 22, no. 1, pp. 143-152, 2019.

[122] A. Zahedmanesh, K. M. Muttaqi, and D. Sutanto, "A Consecutive Energy Management Approach for a VPP Comprising Commercial Loads and Electric Vehicle Parking Lots Integrated with Solar PV Units and Energy Storage Systems," in *2019 1st Global Power, Energy and Communication Conference (GPECOM)*, 2019: IEEE, pp. 242-247.

[123] M. N. Faqiry and S. Das, "Double-Sided Energy Auction Equilibrium Under Price Anticipation," *arXiv preprint arXiv:1605.06564*, 2016.

[124] W. El-Baz, P. Tzscheutschler, and U. Wagner, "Integration of energy markets in microgrids: A double-sided auction with device-oriented bidding strategies," *Applied energy*, vol. 241, pp. 625-639, 2019.

[125] *Genesis Energy. Avaiable onile : https://www.genesisenergy.co.nz/solar (accessed on 20 August 2020).*

[126] *National Renewable Energy Laboratory, " Solar Resource Data". Available online :https://www.nrel.gov/grid/solar-resource/renewable-resource-data.html (accessed on 26 April 2020).*

[127] H. Lee and A. Clark, "Charging the Future: Challenges and Opportunities for Electric Vehicle Adoption," 2018.

[128] "Electra Electricity Distribution Pricing. Avaiable online : https://electra.co.nz/ (accessed on 5 September 2020) ".

[129] K. Kim, T. Yoon, G. Byeon, H. Jung, H. Kim, and G. Jang, "Power demand and power quality analysis of EV charging station using BESS in MicroGrid," in *2012 IEEE Vehicle Power and Propulsion Conference*, 2012: IEEE, pp. 996-1001.

[130] *General depreciation rates. Available online : https://www.ird.govt.nz/-/media/Project/IR/Documents/Forms-and-Guides/IR200---IR299/IR265/IR265-20 (accessed on 15 September 2020).*

[131] S. Ayyadi, H. Bilil, and M. Maaroufi, "Optimal charging of Electric Vehicles in residential area," *Sustainable Energy, Grids and Networks*, vol. 19, p. 100240, 2019.

[132] S. Ayyadi, Maaroufi, Mohamed Arif, Syed Muhammad, "EVs charging and discharging model consisted of EV users behaviour," in *2020 5th International Conference on Renewable Energies for Developing Countries (REDEC)*, 2020: IEEE, pp. 1-4.

[133] Yutong. Yutong Electric Bus Real Time Energy Management Software [Online] Available: https://yutongev.vehicleplus.net/#/batterySOCManagement

[134] "Skybus, Auckland City Express timetable. Available online : https://www.skybus.co.nz/auckland-city-express/timetable (accessed on 20 September 2020)."

[135] M. T. Sebastiani, R. Lüders, and K. V. O. Fonseca, "Evaluating electric bus operation for a real-world BRT public transportation using simulation optimization," *IEEE Transactions on Intelligent Transportation Systems,* vol. 17, no. 10, pp. 2777-2786, 2016.

[136] O. Teichert, F. Chang, A. Ongel, and M. Lienkamp, "Joint Optimization of Vehicle Battery Pack Capacity and Charging Infrastructure for Electrified Public Bus Systems," *IEEE Transactions on Transportation Electrification,* vol. 5, no. 3, pp. 672-682, 2019.

[137] O. A. h. m. c. l.-c.-a.-d.-v.-y.-o.-m.-e.-v. The five buses developed by Vectia already operate in electric mode in Valladolid.

[138] *Irizar. Available online: http://www.irizar.com/en/autobuses-y-autocares/autobuses/irizar-ie-tram/ (accessed on 20 January 2020).*

[139] "RAPT. Available online: https://www.ratp.fr/en/groupe-ratp/newsroom/bus/ile-de-france-mobilitesand-ratp-launch-biggest-tender-europe-buy-electric.(accessed on 20 January 2020)."

[140] Z. Wu, F. Guo, J. Polak, and G. Strbac, "Evaluating grid-interactive electric bus operation and demand response with load management tariff," *Applied Energy,* vol. 255, p. 113798, 2019.

[141] B. Marmiroli, G. Dotelli, and E. Spessa, "Life cycle assessment of an on-road dynamic charging infrastructure," *Applied Sciences,* vol. 9, no. 15, p. 3117, 2019.

[142] *Ecotricity. Wind Farm Group (Airtricity) and Pioneer Generation. Available online: https://ecotricity.co.nz/electricvehicles/ (accessed on 29 August 2020).*

[143] N. Sadeghianpourhamami, J. Deleu, and C. Develder, "Definition and evaluation of model-free coordination of electrical vehicle charging with reinforcement learning," *IEEE Transactions on Smart Grid,* 2019.

[144] M. O. Badawy *et al.*, "Design and implementation of a 75-kW mobile charging system for electric vehicles," *IEEE Transactions on Industry Applications,* vol. 52, no. 1, pp. 369-377, 2015.

[145] L. Nurhadi, S. Borén, and H. Ny, "A sensitivity analysis of total cost of ownership for electric public bus transport systems in Swedish medium sized cities," *Transportation Research Procedia*, vol. 3, pp. 818-827, 2014.

[146] N. Baharin and T. A. R. T. Abdullah, "Challenges of PHEV penetration to the residential network in Malaysia," *Procedia Technology*, vol. 11, pp. 359-365, 2013.

[147] "Electric Bus arrive on Time: Marketplace, economic, technology, environmental and policy perspectives for fully electric buses in the EU," November 2018. [Online]. Available: Online Available : https://www.transportenvironment.org/sites/te/files/publications/Electric%20buses%20arrive%20on%20time.pdf

[148] D. Göhlich, T.-A. Fay, and S. Park, "Conceptual Design of Urban E-Bus Systems with Special Focus on Battery Technology," in *Proceedings of the Design Society: International Conference on Engineering Design*, 2019, vol. 1, no. 1: Cambridge University Press, pp. 2823-2832.

[149] A. Houbbadi, R. Trigui, S. Pelissier, E. Redondo-Iglesias, and T. Bouton, "Optimal scheduling to manage an electric bus fleet overnight charging," *Energies*, vol. 12, no. 14, p. 2727, 2019.

[150] A. Randhahn and T. Knote, "Deployment of Charging Infrastructure for Battery Electric Buses," in *Towards User-Centric Transport in Europe 2*: Springer, 2020, pp. 169-183.

[151] N. Hooftman, M. Messagie, and T. Coosemans, "Analysis of the potential for electric buses."

[152] P. Dicke, B. Meyer, and M. Pruckner, "Analysis of Various Charging Strategies for Electrified Public Bus Transport Utilizing a Lightweight Simulation Model."

[153] E. Lauth, A. F. Raab, P. Teske, D. Göhlich, and K. Strunz, "Smart Grid Integration of Electric Buses: Implementation of a Uni-and Bidirectional Charging Infrastructure," in *2018 International Electric Vehicle Symposium and Exhibition (EVS31)*, 2018.